การดูดซับและการนำกลับของสารประกอบเพอร์ฟลูออรีเนทในน้ำเสียสังเคราะห์โดย
เมโซพอรัสซิลิเกต

นางสาวกุลธิดา สุขสมบูรณ์

วิทยานิพนธ์นี้เป็นส่วนหนึ่งของการศึกษาตามหลักสูตรปริญญาวิทยาศาสตรมหาบัณฑิต
สาขาวิชาการจัดการสิ่งแวดล้อม (สหสาขาวิชา)
บัณฑิตวิทยาลัย จุฬาลงกรณ์มหาวิทยาลัย
ปีการศึกษา 2551
ลิขสิทธิ์ของจุฬาลงกรณ์มหาวิทยาลัย

ADSORPTION AND RECOVERY OF PERFLUORINATED COMPOUNDS FROM SYNTHETIC WASTEWATER USING MESOPOROUS SILICATES

Miss Kuntida Suksomboon

A Thesis Submitted in Partial Fulfillment of the Requirements

for the Degree of Master of Science Program in Environmental Management

(Interdisciplinary Program)

Graduate School

Chulalongkorn University

Academic Year 2008

Thesis Title	ADSORPTION AND RECOVERY OF PERFLUORINATED COMPOUNDS FROM SYNTHETIC WASTEWATER USING MESOPOROUS SILICATES
By	Miss Kuntida Suksomboon
Field of Study	Environmental Management
Advisor	Patiparn Punyapalakul,Ph.D.

Accepted by the Graduate School, Chulalongkorn University in Partial Fulfillment of the Requirements for the Master's Degree

.... Dean of the Graduate School

(Associate Professor Pornpote Piumsomboon,Ph.D.)

THESIS COMMITTEE

.... Chairman

(Chantra Tongcumpou,Ph.D.)

.... Advisor

(Patiparn Punyapalakul,Ph.D.)

.... Examiner

(Associate Professor Jin Anotai,Ph.D.)

.... Examiner

(Assistant Professor Chakkaphan Sutthirat,Ph.D.)

.... External Examiner

(Punjaporn Weschayanwiwat,Ph.D.)

iv

กุลธิดา สุขสมบูรณ์ : การดูดซับและการนำกลับของสารประกอบเพอร์ฟลูออรีเนทในน้ำ
เสียสังเคราะห์โดยเมโซพอรัสซิลิเกต. (ADSORPTION AND RECOVERY OF
PERFLUORINATED COMPOUNDS FROM SYNTHETIC WASTEWATER USING
MESOPOROUS SILICATES) อ. ที่ปรึกษาวิทยานิพนธ์หลัก : อ. ดร. ปฏิภาณ
ปัญญาพลกุล, 177หน้า.

การวิจัยนี้ได้ทำการศึกษาการดูดซับและการนำกลับของสารประกอบเพอร์ฟลูออรีเนท
(PFCs) ซึ่งจัดเป็นสารพิษตกค้างยาวนานในน้ำเสียสังเคราะห์โดยใช้ตัวกลางดูดซับสังเคราะห์ชนิด
เมโซพอรัสซิลิเกต (HMS) และเปรียบเทียบกับซีโอไลต์ (NaY และ HY) และถ่านกัมมันต์ชนิดผง
(PAC) นอกจากนี้ยังได้ทำการศึกษาถึงผลของการต่อติดหมู่ฟังก์ชันต่างๆ (หมู่ซิลานอล หมู่อะมิโน
หมู่เมอร์แคปโต และหมู่อัลคิล) บนพื้นผิวของ HMS และ HMS ที่ถูกแทนที่ด้วยโลหะไททาเนียมใน
โครงสร้างต่อประสิทธิภาพการดูดซับสาร PFCs พบว่าการดูดซับสาร PFOS มีประสิทธิภาพ
มากกว่าสาร PFOA และ PAC มีประสิทธิภาพในการดูดซับสาร PFCs สูงสุดเนื่องจากมีความ
หลากหลายของหมู่ฟังก์ชันและพื้นที่ผิวสูง ตัวกลางดูดซับชนิด HMS ที่ต่อติดด้วยหมู่อะมิโนให้
ประสิทธิภาพการดูดซับมากกว่าตัวกลางดูดซับชนิดอื่น เว้นแต่สาร PFOA พบว่าการลดค่า pH ไม่
มีผลต่อประสิทธิภาพการดูดซับสาร PFOS ยกเว้นตัวกลางดูดซับชนิด HMS ที่ต่อติดด้วยหมู่อะมิ
โน พันธะไฮโดรเจนและแรงประจุทางไฟฟ้าเป็นปัจจัยสำคัญในการดูดซับสาร PFCs บนตัวกลาง
ดูดซับชนิดซิลิเกต และการดูดซับสาร PFOS ของ HMS นั้นสามารถสกัดสาร PFOS กลับมาใช้
ใหม่โดยใช้แอลกอฮอลล์ได้มากที่สุดที่อัตราส่วนน้ำ:แอลกอฮอลล์ที่ 5:5 ซึ่งมีประสิทธิภาพมากกว่า
การนำกลับสารของ PAC การสกัดซ้ำโดยใช้ตัวทำละลายนั้นพบว่าไม่ได้ส่งผลต่อประสิทธิภาพ
การดูดซับสาร PFOS ในตัวกลางดูดซับชนิด HMS ที่ต่อติดด้วยหมู่ฟังก์ชันที่ไม่ชอบน้ำอย่างมี
นัยสำคัญ ปฏิกิริยา hydrolysis ในกระบวนการสกัดด้วยตัวทำละลายส่งผลให้ประสิทธิภาพการ
ดูดซับสาร PFOS ของ HMS มีค่าลดลงถึง 30% ประสิทธิภาพการดูดซับของ PAC ที่นำกลับมาใช้
ใหม่พบว่ามีประสิทธิภาพลดลงถึง 21% เมื่อเปรียบเทียบกับ PAC ที่ไม่ได้ผ่านการดูดซับ

คำสำคัญ : สารประกอบเพอร์ฟลูออรีเนท; เมโซพอรัสซิลิเกต; หมู่ฟังก์ชันบนพื้นผิว; การดูดซับ

สาขาวิชา การจัดการสิ่งแวดล้อม   ลายมือชื่อนิสิต นส กุลธิดา สุขสมบูรณ์
ปีการศึกษา 2551   ลายมือชื่ออ.ที่ปรึกษาวิทยานิพนธ์หลัก

5087557020 : MAJOR ENVIRONMENTAL MANAGEMENT

KEYWORDS : PERFLUORINATED COMPOUNDS / MESOPOROUS SILICATES / SURFACE FUNCTIONAL GROUPS / ADSORPTION

KUNTIDA SUKSOMBOON : ADSORPTION AND RECOVERY OF PERFLUORINATED COMPOUNDS FROM SYNTHETIC WASTEWATER USING MESOPOROUS SILICATES. ADVISOR : PATIPARN PUNYAPALAKUL,Ph.D., 177 pp.

In this study, adsorption and recovery of Perfluorinated Compounds (PFCs), priority persistent chemical, from synthetic wastewater by using Hexagonal Mesoporous Silicate (HMSs) was investigated, comparing with microporous zeolite (NaY and HY) and powdered activated carbon (PAC). Moreover, effects of surface functional groups (silanol groups, 3-aminopropyltriethoxy-, 3-mercaptopropyl-, and Octyldichloroethoxy-) including titanium substitution on PFCs adsorption and recovery efficiency were evaluated. Adsorption of Perfluorooctane Sulfonate (PFOS) was higher than Perfluorooctane Acid (PFOA). PAC showed the highest adsorption affinity of PFCs because of complexity of surface functional groups and large surface area. 3-aminopropyltriethoxy- grafted HMS gave higher adsorption capacity compared with other silicate adsorbents. Unless PFOA, adsorption capacities of PFOS on all adsorbents were not affected by decreasing of pH, except 3-aminopropyltriethoxy- grafted HMS. Hydrogen bonding and electrostatic interaction might play the important role for PFCs adsorption on silicate adsorbents. PFOS adsorbed on HMSs can be completely recovered by a mixture of alcohol and water at 5:5 ratios, which is more effective than PAC. Repeating of regeneration by solvent extraction did not affect the PFOS adsorption capacities of hydrophobic functional groups grafted HMS, significantly. Effect of hydrolysis by solvent-extraction process might decrease PFOS adsorption capacities of pristine HMS up to 30%. Adsorption capacity of reused PAC was decreased up to 21% compared with the virgin one.

Field of Study : Environmental Management Student's Signature _Kuntida Suksomboon_

Academic Year : 2008 Advisor's Signature _P. DL_

Acknowledgements

First of all, I would like to express my thankfulness to my advisor, Dr. Patiparn Punyapalakul, for his supervision and helpful suggestion throughout this thesis. I would like to take this opportunity to thank Dr. Juntra Tongcumpou, chairman of the committee, Dr. Punjaporn Weschayanwiwat, Dr. Chakkaphan Sutthirat and Dr. Jin Anotai, my committee members, for their useful and valuable comments.

I express my gratitude to the National Center of Excellence for Environmental and Hazardous Waste Management (NCE-EHWM), Graduate School Chulalongkorn University for providing my tuition and thesis grants.

I also express my gratitude to the THE 90TH ANNIVERSARY OF CHULALONGKORN UNIVERSITY FUND (Ratchadaphiseksomphot Endowment Fund) for providing my tuition and research grants.

My cordial thanks should be given to all the NCE-EHWM staffs and laboratory staffs for their kind cooperation and help. Moreover, I would like to thank Department of environmental Engineering, Faculty of engineering, Chulalongkorn University for laboratory facilities.

Finally, I would like to express my sincere gratitude to my beloved family and friends for their love, understanding and heartfelt support.

CONTENTS

ศูนย์วิทยทรัพยากร
จุฬาลงกรณ์มหาวิทยาลัย

LIST OF TABLES

Table		Page

LIST OF FIGURES

LIST OF ABBREVIATIONS

PFCs	=	Perfluorinated Compounds
POPs	=	Persisted Organic Pollutants
USEPA	=	United State Environmental Protection Agency
PFASs	=	Perfluoroalkyl Sulfonates
PFACs	=	Perfluoroalkyl Carboxylates
PFOS	=	Perfluorooctane Sulfonic acid
PFOA	=	Perfluorooctanoic Acid
AOPs	=	Advanced Oxidation Processes
UV	=	Ultraviolet
OECD	=	Organization for Economic and Co-operation Development
GAC	=	Granular Activated Carbon
PAC	=	Powder Activated Carbon
HMS	=	Hexagonal Mesoporous Silicates
APTES	=	Aminopropyltriethoxysilane
MPTMS	=	Mercaptopropyltrimethoxysilane
A-HMS or AM-HMS	=	Amino functionalized Hexagonal Mesoporous Silicates
M-HMS or MP-HMS	=	Mercapto functionalized Hexagonal Mesoporous Silicates
OD-HMS	=	Dimethyloctylchlorosilane functionalized Hexagonal Mesoporous Silicates
TEOS	=	Tetraethylorthosilicate or Tetraethoxysilane
DDA	=	Dodecylamine
MCM-41	=	Mobil Catalytic Material, Number 41
CMC	=	Critical Micelle Concentration
XRD	=	X-ray Diffraction
BET	=	Brunauer-Emmett-Teller
BJH	=	Barrett-Joyner-Halenda
FT-IR	=	Fourier Transform Infrared
TN	=	Total Nitrogen content

ICP-AES	=	Inductively Coupled Plasma Atomic Emission
TOC	=	Total Organic Carbon
MSDS	=	Material Safety Data Sheet
PBT	=	Persistent, Bioaccumulated and Toxic
COD	=	Chemical Oxygen Demand
PTFE	=	Polytetrafluoroethylene
BAFs	=	Bioaccumulation Factors
PFBuS	=	Perfluorobutane Sulfonic Acid
PFHxS	=	Perfluorohexansulfonate
PFDA	=	Perfluoro-n-decanoic Acid
PFOSA	=	Perfluorooctanesulfonic Acid
ECF	=	Electro-chemical Fluorination
HF	=	Hydrogen Fluoride
UNEP	=	United Nations Environment Programme
WV DEP	=	West Virginia Department of Environmental Protection
CRG	=	Corporate Remediation Group
MDH	=	Minnesota Department of Health
FTOH	=	Fluorotelomer Alcohols
US	=	United State
AFFF	=	Aqueous Fire Fighting Foam
WWTP	=	Waste Water Treatment
TFA	=	Trifuoroacetate
MMS	=	Mesoporous Molecular Sieves
LCT	=	Liquid Crystal Templating
IR	=	Infrared
BTEX	=	Benzene, Toluene, Ethylbenzene, and Xylenes
pH_{zpc}	=	pH of zero point of charge
OMSs	=	Ordered Mesoporous Silicas
MPS	=	Mesoporous Silica
DCAA	=	Dichloroacetic Acid

ApnEOs	=	Alkylphenol polyethoxylates
AC	=	Activated Carbon
SBUs	=	Secondary building units
TIPOT	=	Tetraisopropyl orthotitanate
SEM	=	Scanning Electron Microscope

CHAPTER I

INTRODUCTION

1.1 Research Background

Persisted organic pollutants (POPs) have been concerned for decades and recently Perfluorinated compounds (PFCs) appeared in the list of POPs. Because of their extraordinary thermal and chemical stability, PFCs are used in a variety of products such as surface protectants, surfactants, fire-fighting foams to the production of Teflon, lubricants, and insecticides for about fifty years. However, they are now considered as persistent, bioaccumulated and toxic (PBT) chemicals and found ubiquitously distributed in the environment and biota. Unlike other organohalogen chemicals, PFCs have unique structures and properties and their behavior in the environment is still unclear due to limited studies. Current studies roughly revealed global distributions and the environmental behavior of PFCs and related chemicals. Developed countries and industrializing areas were highly polluted by PFCs, such as America, Japan, Europe and coastal China. Major source of PFCs in the environment was supposed to be direct discharge from global fluoropolymer manufacturers (Armitage *et al.*, 2006). Ionic PFCs have been detected in municipal effluents, surface and ground water in various countries at concentrations ranging from below detection level to the ng I^{-1} range (Skutlarek *et al.*, 2006). Elevated concentrations of PFCs have been detected near sites impacted by manufacturing plants or accidental emissions of PFCs. Sum concentrations of PFCs as high as 43,348 ng I^{-1} have been detected in a river of a highly industrialized area in Germany, with the major components being PFOA (33,900 ng I^{-1}) and PFOS (3,160 ng I^{-1}) (Skutlarek *et al.*, 2006). Unfortunately, current water and wastewater treatment processes seemed not effective to remove PFCs in trace levels. Therefore, regulatory actions, scientific studies and engineering solutions are of urgent necessities to control PFCs in this area.

PFCs have been detected not only in the physical environment, but also in humans and wildlife (Yamashita et al., 2005). Several studies have reported the presence of perfluorinated chemicals in a variety of wildlife species, including freshwater and marine mammals (Kannan et al., 2001). The described concentrations of PFCs may not be acutely toxic, but these compounds can be enriched in humans (blood and liver), which raises the concern of long-term metabolic effects of these cellular recognized xenobiotics (Harada et al., 2004). There are several kinds of individual PFCs occurred in environment. But, two groups of PFCs, namely Perfluoroalkyl sulfonates (PFASs) and Perfluoroalkyl carboxylates (PFACs) as well-known as Perfluorooctane sulfonic acid (PFOS) and Perfluorooctanoic acid (PFOA) are of particular concern from environmental and public health significance. Because of the multiple toxicities of these compounds (coupled with bioaccumulation and biomagnifications in the food web), different risk assessments on PFOS and PFOA have been undertaken in the last years (OECD 2002). Moreover, they are most persistent in the environment and have been discovered as global pollutants of air, water and soil. The high-energy carbon–fluorine bond renders PFCs resistant to hydrolysis, photolysis, microbial degradation, and metabolism by vertebrates, and makes them environmentally persistent (Giesy and Kannan, 2002).

According to PFCs especially PFOA and PFOS are a possible health treat, many options have increasing concerned to control PFCs concentration that contaminated in wastewater, groundwater, and drinking water. Advanced oxidation processes (AOPs) are effective to specific wastewater. However, removal of PFOS by AOPs was identified unable to decompose PFOS in normal state (Schröder and Meesters, 2005). Ultraviolet (UV) is usually applied in water treatment process for disinfection. PFCAs were proposed to decompose by UV photolysis in stepwise degradation mechanism. This technique one research found that no removal of PFOA was observed under either direct or indirect photolysis (Hatfield, 2001b). Few studies have been conducted to investigate the biodegradability of perfluorinated or partially fluorinated surfactants. PFOS was not degraded under aerobic or anaerobic conditions in wastewater treatment

(Remde and Debus, 1996). Including to PFOS was found not degradable by activated sludge (Schröder, 2003). Furthermore, during microbial degradation, perfluorochemicals tend to be slowly converted to more bioaccumulative and more toxic products (Dimitrov et al., 2004). For the reason that the application of conventional treatments for removing anionic PFCs from aqueous streams containing elevated concentrations of these contaminants is restricted by technical and/or economical constraints. These treatment technologies present some drawbacks and limitations, mainly due to their high-energy demand and/or interference by other compounds present in the wastewater. Although, there are several technologies for degradation or removal of PFCs contaminated in environment. However, in many cases, these methods have proven to be ineffective, expensive, unreliable, and often required an extended time periods for adequate removal. Therefore, some physical technologies including membrane separation and adsorption were investigated. Tang and co-worker (2006) reported that reverse osmosis membrane could efficiently separate PFOS from semiconductor wastewater. Adsorption of anionic PFCs onto granular activated carbon (GAC) could offer a viable alternative for the removal from aqueous streams. The discharge levels of PFOS dropped from the levels of 103 ng l^{-1} to 6.6 ng l^{-1} as 94% reduction and PFOA 83 ng l^{-1} to 45 ng l^{-1} as 46% reduction. However, the activated carbon system is working well to remove PFOA and PFOS but it is not removed as efficiently on a consistent basis. It appears that the activated carbon treatment system may not be as effective in removal of carboxylic acid PFCs (Minnesota Department of Health, 2007).

According to their limitations and among inherent disadvantages of activated carbon are their wide distribution of pore size, heterogeneous pore structure, and low selectivity for adsorption. The recent discovery of mesoporous molecular sieves has simulated a renewed interest in adsorbent and catalyst design (Lee et al., 2001). Hexagonal mesoporous silicates (HMS) having been studied extensively in adsorption and catalytic fields, has mesoscale pore and silanol as surface functional group. Silanol group on HMS surface is expected to have high affinity to high hydrophilic molecules of PFOA and PFOS. Moreover, HMS can be modified by organic-ligand modification or

metal substitution in crystalline structure, to render specific characteristics. However, effects of crystalline structure, surface functional groups as well as pH on PFCs removal from aqueous phase by adsorption have not been studied. Hence, adsorption of PFCs on two types of crystalline structure (mesoporous and microporous structures) and five different types of surface functional groups (3-aminopropyltriethoxysilane, 3-mercaptopropyltrimethoxysilane and dimethyloctthylchlorosilane) grafted onto Hexagonal Mesoporous Silicate (HMS) were investigated comparing with powdered activated carbon (PAC). Furthermore, PFCs recovery efficiency of used adsorbents by solvent and water extraction was studied including re-use efficiency and effect of regeneration methods on physico-chemical characteristic of adsorbents.

1.2 Hypotheses

The hypotheses for this study are: *i)* Perfluorinated compounds (PFCs) adsorption efficiency of HMS at high-level concentration can be increased by positively charge and hydrophilicity of grafted surface functional groups. *ii)* Adsorption capacities of PFCs in aqueous phase can be increased by decreasing pH lower than pH_{zpc}. *iii)* Surface characteristics and crystalline structures, for example, pore structure, surface charge and surface area and pore size, etc. might affect PFCs adsorption capacities. *iiii)* PFCs adsorbed on HMSs can be recovered by solvent extraction easier than PAC. *iiiii)* Grafted organic functional groups can be prevented collapse of silicate crystalline structures.

1.3 Objectives

The two main objectives of this study are to investigate the effect of surface functional groups and crystalline structures of silica-based adsorbents on Perfluorinated compounds (PFCs) adsorption capacity and to investigate regeneration methods in order to study the possibility of using reused HMSs for PFCs removal. The specific objectives are as follow:

1. To study adsorption mechanisms of PFCs on silicate porous material comparing with powdered activated carbon.
2. To determine effects of surface functional groups and crystalline structures on PFCs adsorption efficiency at high-level concentration.
3. To study effects of pH on PFCs adsorption capacities.
4. To investigate regeneration efficiencies of PFCs by solvent extraction methods and effect on porous structure of HMSs.
5. To compare adsorption efficiencies of fresh and reused adsorbents on PFCs adsorption efficiencies.

1.4 Scopes of Study

The physical adsorption process formed by synthesis of mesoporous silicate materials is utilized to remove PFCs from synthesis wastewater. Perfluorooctanoic acid (PFOA) and Perfluorooctane sulfonic acid (PFOS) were used as PFCs models in this study. Pristine HMS, functionalized HMSs, PAC, NaY and HY zeolite are used as adsorbents in this study.

The scope of this study:

Part 1: Synthesis, functionalization with organic-ligand and metal substitution of Hexagonal Mesoporous Silicates (HMSs)

A direct co-condensation method was performed for organic functionalization of mesoporous materials by using dodecylamine as a template and tetraethoxysilane (TEOS) as a silica precursor. Aminopropyltriethoxysilane (APTES), Mercaptopropyltrimethoxysilane (MPTMS) and Dimethyloctylchlorosilane were used for surface functionalized modification on HMS. Including, Titanium was used for metal substitution modification on HMS.

Part 2: Physico-chemical Characterization of synthesis Hexagonal Mesoporous Silicates (HMSs)

The physico-chemical characteristics of adsorbents including surface area and pore size, pore structure, surface charge, elemental components, and surface functional groups were investigated by measure of nitrogen adsorption-desorption measurement, X-ray diffraction, acid-base titration, elemental analysis (Total Nitrogen and Sulfur) and FT-IR spectroscopy, respectively.

Part 3: Adsorption Kinetic

The equilibrium contact times for PFOA and PFOS adsorption were performed by varying contact time from 0 to 48 hrs and varying initial pH solution at 5, 7 and 9 under batch conditions with a solution concentration of PFOA or PFOS 100 mg/l. Except, PAC used solution concentration of 300 mg/l and the amount ratio of adsorbent to PFOA or PFOS solution were set at 0.067 g: 200 ml. To analyze the adsorption rate of PFOA and PFOS onto PAC, NaY-zeolite, HY-zeolite, HMS, Ti-substituted HMS and functionalized HMSs, by using the pseudo-first-order equation of Lagergren and the pseudo-second-order kinetic model.

Part 4: Adsorption Isotherms and Adsorption Mechanisms

Adsorption isotherms and adsorption mechanisms for PFOA and PFOS were performed by varying concentration of PFOA and PFOS solution (25-300 mg/l), initial pH under batch conditions (pH 5, 7 and 9) and the amount ratio of adsorbent to PFOA and PFOS solution were set at 0.01 g: 30 ml. The adsorption isotherm models considered in this experiment were Langmuir and Freundlich types.

Part 5: Analytical method

To compare PFCs adsorption capacity between HMSs and PAC. The concentrations of PFOA and PFOS will be determined by using Total Organic Carbon (TOC) Analyzer (TOC-VCPH).

Part 6: Regeneration Study

Pristine HMS, PAC and functionalized HMSs were used to study the efficiency of regeneration methods by using solvent extraction methods. In solvent extraction, ethanol was chosen as representative solvent to extract PFOS. The solvent extraction method was performed by mixing used adsorbents with varied ratio of Milli-Q water and ethanol. Moreover, effect of amount of mixture on extraction efficiency was also investigated. Regenerated HMS, PAC and functionalized HMSs were re-testing for their adsorption capacities again and compared with virgin adsorbents. Physico-chemical characteristics of regenerated adsorbents such as crystalline structure, surface structure and surface area and pore structure were investigated. Solvent extraction method was repeated 3 times and adsorption efficiencies of regenerated adsorbents were investigated. Moreover, efficiency of regenerated functionalized HMSs was compared with non-grafted HMS to study effects of grafted organic functional groups.

Scope of Study

The physical adsorption process formed by synthesis of mesoporous silicate materials is utilized to remove PFCs from synthetic wastewater.

1. Study of synthesis HMS and modified-HMSs by direct co-condensation method and post-grafting method by grafted with
- 3-aminopropyltriethoxysilane
- 3-mercaptopropyltrimethoxysilane
- n-dimethyloctylchlorosilane
- Metal (Titanium)

2. Physico-chemical characterization of synthesis HMSs such as
- Surface area and pore size
- Pore structure
- Surface charge
- Surface functional groups

3. Adsorption Kinetic
- To analyze the adsorption rate of PFOA and PFOS onto all adsorbents by using the pseudo first-order and the pseudo-second-order model.

4. Adsorption Isotherms and Adsorption Mechanisms
- The adsorption isotherm models considered in this experiment were Langmuir and Freundlich types.

Figure 1.1 Study frameworks of all experiment

5. Analytical method

• The concentrations of PFOA and PFOS will be determined by using Total Organic Carbon (TOC) Analyzer

6. Regeneration Study (solvent extraction)

• PFOS adsorbed pristine HMS

• PFOS adsorbed PAC

• PFOS adsorbed functionalized HMSs

Solvent extraction method

• PFOS recover efficiency

■ Ratio of solvent and water

■ Amount of solvent mixture

PFOS adsorption efficiencies of regenerated adsorbents were investigated by using PFOS adsorption isotherms

Physico-chemical characteristics of regenerated adsorbents on their adsorption capacities

Compare efficiency of regenerated functionalized HMSs with non-grafted HMSs to study effects of grafted organic functional groups

Figure 1.1 (cont.) Study frameworks of all experiment

CHAPTER II

THEORETICAL BACKGROUNDS

2.1 Introduction of Perfluorinated compounds (PFCs)

Science of fluorochemistry begins with fluorine, which is most abundant in halogen family and most reactive to all elements. Because of the highest electro negativity of fluorine in all halogens and even all elements in periodic table (the polar carbon-fluorine bond ~110 kcal/mol), carbon-fluorine bond (C-F) shows stronger polarity and highest strength in nature. This stability confers a variety of unique properties to fluorochemicals (3M, 1999).

Perfluorinated compounds (PFCs) are a group of emerging chemicals of concern in the 21st century. PFCs were produced by industries and consumed "safely" as surfactants, repellents, additives, fire-fighting foams, polymer emulsifiers and insecticides for almost fifty years. PFCs have emerged as priority environmental contaminants due to recent reports of their detection in environmental and biological matrices as well as concerns regarding their persistence and toxicity. Organofluorine molecules have unique physical, chemical, and biological properties; the high-energy carbon–fluorine bond renders PFCs resistant to hydrolysis, photolysis, microbial degradation and metabolism by vertebrates. Although some efforts were contributed to reduce PFCs in environment, such as development of alternatives and recycling processes, huge amount of persisted PFCs have already been discharged in environment and accumulated in biota including humans.
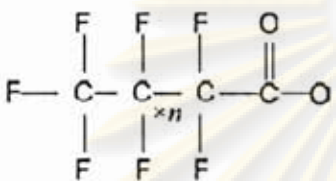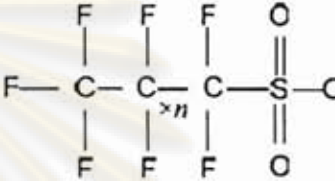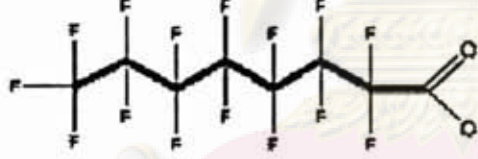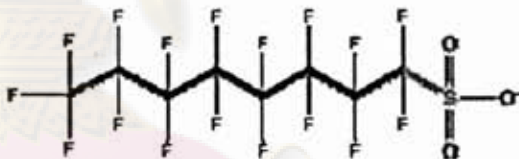
2.1.1 Basic properties of PFCs

2.1.1.1 Physiochemical properties

As shown in Table 2.1, two groups of PFCs dominant occurred in environment. Perfluorocarboxylate (PFCA) and Perfluoroalkyl sulfonate (PFAS) are the

typical chemicals for PFCs, which have eight carbons and the common name as "C8". Their chemical structures are shown in Table 2.1

Table 2.1 Structures of PFCA and PFAS (3M, 1999).

Perfluorocarboxylate (PFCA)	Perfluoroalkyl sulfonate (PFAS)
$CF_3(CF_2)_n COO^-$	$CF_3(CF_2)_n SO_3^-$
PFOA	PFOS

PFCA and PFAS molecules consist of one perfluorinated carbon chain and one special functional group. The functional group, such as carboxylic or sulfonic group, can affiliate with water and make PFCs hydrophilic. Different hydrophilic moiety showed diverse behavior in aqueous environment. The perfluorinated tail is covered by strongest C-F bonds and surrounded by fluorine atoms, which have similar size with carbon atom. This kind of structure protects PFCs molecules from breaking down by oxidants such as OH radicals. The longer is carbon chain length, the more strongly hydrophobic is PFCs molecule. Combination of hydrophobic and hydrophilic moieties, and high stability under extremely thermal and oxidative conditions, make PFCs perfect surfactants which can be applied in extremely critical conditions. Among the PFCs, Perfluorooctanoic acid (PFOA) and Perfluorooctane sulfonate (PFOS)

regarded as the terminal degradation end-products, are the two chemicals that have frequently been detected in environmental samples, and very often occur at the highest concentrations (Poulsen *et al.*, 2005; Prevedouros *et al.*, 2006). They are widely employed in different industrial processes. such as in protective coatings for carpets, textiles, leather, paper, paints, adhesives, grease repellents in popcorn bags and food-wrapper coatings, wiring insulation for telecommunications, in fire-fighting foams, as specialty surfactants in cosmetics, aerospace, electronics (semiconductors), and medical use (Martin *et al.*, 2004b). In particular, PFOA is used as adjuvant in the production of fluoropolymers such as PTFE, Teflon or similar products, and occurs in these applications as aqueous and gaseous process emission. Quantitatively, PFOS and PFOA are the most important anionic PFCs detected in the environment. In addition. these two chemicals are the final degradation products of a variety of precursor perfluorinated chemicals including fluorotelomer alcohols and fluorinated polymers (Dimitrov *et al.*, 2004; Wang *et al.*, 2005).

Considerably higher concentrations of PFCs can be found in effluents from chemical plants manufacturing fluorochemicals and from other industrial activities that utilize ionic PFCs. As an example, PFOS concentrations of 1,650 mg/l have been reported in effluents generated from semiconductor manufacturing (Tang *et al.*, 2006). The semiconductor manufacturing industry has secured a temporary exemption to utilize PFOS in wafer photolithography (Anonymous, 2002). Nowadays, the department of environmental and public health all of the world including, America, Europe and Canada raises the concern of toxicology of perfluorinated surfactants especially PFOA and PFOS and other perfluorinated compounds. They also announced that it intended to cease production in recognition of increasing evidence and concern relating to its environmental distribution by use chemistry based around another PFCs, Perfluorobutane sulfonate (PFBS). This substance (like all PFCs) is persistent but it appears that short chain sulfonates do not bioaccumulate and exhibit relatively low toxicity. However, it is remain persist organic substance persists in the environment. Furthermore, some technologies were performed to use for recovery PFCs in order to

reduce these substances in production process. However, in the semiconductor and photographic industries, chromium plating operations, aviation hydraulics and fire-fighting foams will be permitted to continue indefinitely. Hence, the limitation and reduction procedure including research study of PFCs will be performing to continue reduction of PFCs do not wide spread into environment. The global historical industry-wide emissions of total PFCs from direct (manufacture, use, consumer products) and indirect (PFCA impurities and/or precursors) sources were estimated to be 4,400-8,000 tones (in 1951-2004). It was estimated that the majority 3,200-3,700 tones of PFCs (~80%) have been released to the environment from fluoropolymer manufacture and use (Prevedouros, 2006). Emissions of PFAS-related chemicals were estimated to be 4,650 tons per year in 1990~2000 (Footitt et al., 2004).

Table 2.2 Basic physiochemical properties of several kinds of PFCs occurred in environment (Goss K-U. 2007)

Abbreviation name	Compound name	Molecular Structure	M. W. (g/mol)	CAS No.
PFBA	Perfluorobutyric Acid	$CF_3(CF_2)_2COOH$	214.0	375-22-4
PFPeA	Perfluoropentanoic Acid	$CF_3(CF_2)_3COOH$	264.1	2706-90-3
PFHxA	Perfluorohexanoic Acid	$CF_3(CF_2)_4COOH$	314.1	307-24-4
PFHpA	Perfluoroheptanoic Acid	$CF_3(CF_2)_5COOH$	364.1	375-85-9
PFOA	Perfluorooctane Acid	$CF_3(CF_2)_6COOH$	414.1	335-67-1

Table 2.2 (cont.) Basic physiochemical properties of several kinds of PFCs occurred in environment (Goss K-U. 2007)

Abbreviation name	Compound name	Molecular Structure	M. W. (g/mol)	CAS No.
PFNA	Perfluorononanoic Acid	$CF_3(CF_2)_7COOH$	464.1	375-95-1
PFDA	Perfluorodecanoic Acid	$CF_3(CF_2)_8COOH$	514.1	335-76-2
PFUnA	Perfluoroundecanoic Acid	$CF_3(CF_2)_9COOH$	564.1	2058-94-8
PFDoA	Perfluorododecanoic Acid	$CF_3(CF_2)_{10}COOH$	614.1	307-55-1
PFTeDA	Perfluorotetradecanoic Acid	$CF_3(CF_2)_{12}COOH$	714.1	376-06-7
PFHxDA	Perfluorohexadecanoic Acid	$CF_3(CF_2)_{14}COOH$	814.1	67905-19-5
PFOcDA	Perfluorooctadecanoic Acid	$CF_3(CF_2)_{16}COOH$	914.1	16517-11-6
PFBS	Perfluorobutane Sulfonate	$CF_3(CF_2)_3SO_3K$	338.2	29420-49-3
PFHxS	Perfluorohexane Sulfonate	$CF_3(CF_2)_5SO_3K$	438.2	3871-99-6
PFOS	Perfluorooctane Sulfonate	$CF_3(CF_2)_7SO_3K$	538.2	2795-39-3

2.1.1.2 Persistence, bioaccumulation and toxicity (PBT)

Although PFCs have been produced and consumed "safely" for about fifty years, they were considered as persistent, bioaccumulated and toxic (PBT) chemicals in scientific studies and government reports recently (Renner, 2001; OECD, 2002; US EPA, 2002).

Persistence

3M Company published its reports on hydrolysis (Hatfield, 2001a) and aqueous photolytic degradation (Hatfield, 2001b) of PFOA, which showed rather long half-life times in natural environment. PFOS also showed its resistance to advanced oxidation processes including ozone, ozone/UV, ozone/H_2O_2 and Fenton reagent (Schröder and Meesters, 2005). In this study, COD of each PFCs was analyzed and all PFCs had no response to oxidation by chromium potassium oxide ($Cr_2O_7^{2-}$) or potassium permanganate acid (MnO^{4+}), which confirmed their stabilities in critic environment.

Bioaccumulation

Preliminary study showed dietary Bioaccumulation factors (BAFs) of PFOS were 2,796 in bluegill sunfish and 720 in carp (OECD, 2002) respectively. BAFs of PFOA were about 2 in fathead minnow and 3~8 in carp (US EPA, 2002), which are quite lower than PFOS. Dietary BAFs of PFCAs were ranged from 0.038 to 1.0, while BAFs of PFASs were ranged from 4 to 23,000 both increased with length of carbon chain (Martin et al., 2003a; 2003b). Furthermore, BAFs of PFASs were greater than PFCAs in equivalent carbon chain length, which indicated that acid function groups also played important role to determine accumulation potentials.

<u>Toxicity</u>

Because PFCs are different to normal lipophile toxic substances, their toxicology is still unknown in mechanism and need more studies to elucidate the profile. Although many researches have been conducted for the toxicity of PFCs, the results were in diverse qualities and difficult to summarize in systematically. Nowadays, levels would continue to increase in the environment for many years to come. Researchers are finding serious health concerns about PFCs, including increased risk of cancer (3M Company, 1999).

Generally, medium- and long-chained PFCs may be more toxic than short-chained ones by their longer half-life times in rodents. Review on PFOS toxicity showed that subchronic exposure led to significant weight loss accompanied by hepatotoxicity, and reductions of serum cholesterol and thyroid hormones (OECD, 2002). The United States Environmental Protection Agency's scientific advisory board found in 2005 that Perfluorooctanoic acid (PFOA), a chemical compound used to make Teflon, is a "likely carcinogen".

2.1.2 Production of PFCs

PFCs used in industries were mainly derived from two major classes named Perfluoroalkyl sulfonates (PFASs) and Perlfuorocarboxylate acid (PFCAs), which were produced in processes of electro-chemical fluorination (ECF) and telomerization, respectively. The chemical interaction as shown in Equation 2.1 and 2.2 (3M Company, 1999).

$$C_8H_{17}SO_2F + 17HF \xrightarrow{4.5\text{-}7V} C_8F_{17}SO_2F + 17H_2 \qquad ...(2.1)$$

$$C_8H_{17}COF + 17HF \longrightarrow C_8F_{17}COF + 17H_2 \qquad ...(2.2)$$

2.1.3 Discharge criteria of PFCs

Minnesota Department of Health recommended 7 µg/L in drinking water as the safe level of PFOA for human health in 2002, and then revised it to be 0.5 µg/L in 2007. Other PFCs were also included in the criteria as 0.3 µg/L for PFOS, 1 µg/L for PFCA, and 0.6 µg/L for PFAS, because all of them have been detected in local surface water and drinking water (MDH, 2007).

2.1.4 Environmental behavior of PFCs

2.1.4.1 Source, sink and fate of PFCs

Sources of PFCs were considered mainly from industrial discharge, as well as degradation of PFCs derivatives. Major industrial emissions were suspected from fluoropolymer manufacturing and aqueous fire-fighting foam production. Global emission of total PFCAs was estimated to be 3,200~7,300 tons to environment (Prevedouros et al., 2006) and those of PFASs was 4,650 tons per year in last decade (Footitt et al., 2004). Sink of PFCs was expected to be deep ocean transfer for PFCAs (Yamashita et al., 2005) and biota accumulation and sorption for PFASs, as well as combustion and thermolysis degradation.

2.1.4.2 PFCs contaminations in water environment

Surface water in developed countries and industrialized areas were usually highly polluted by PFCs, such as US (Hansen et al., 2002), Japan (Saito et al., 2003), Germany (Skutlarek et al., 2006) and coastal China (So et al., 2004). Direct discharge from industries and consumption of aqueous fire fighting foam (AFFF) were considered as main sources of PFCs in surface water. Drinking water in these areas was also polluted by PFCs. Investigation of surface water in East Asia demonstrated very high pollution of PFOA in Japan (Yamashita et al., 2005) and PFOS in Korea and China (So et al., 2004). These contaminants caused further pollution in biota, such as marine

mammal and seafood. Groundwater was very easy to be polluted by PFCs because most PFCs could strongly adsorb to particles.

2.1.4.3 PFCs contaminations in biota sphere

Globally distribution of PFCs was firstly reported in wildlife, including PFCs distribution in Arctic animals (Martin *et al.*, 2004b). Contaminations of PFCs in wildlife were in different patterns and caused by multiple sources. PFCs were detected in marine mammals everywhere (Kannan *et al.*, 2002a; 2002b), including South Pacific Ocean and polar bear in Arctic Ocean (Smithwick *et al.*, 2005). PFASs, mainly PFOS, were found dominant in most species because of its rather high BAFs. Studies on temporal trends of PFCs in human, fish, bird and marine mammal samples indicated that exposure of PFCs increased significantly over the past 15-25 years (Holmström *et al.*, 2005).

2.1.4.4 PFCs contaminations in humans

PFCs were often detected in human blood, serum and plasma as well as in tissues especially PFOA and PFOS approximately 3-35 µg/l and 7-82 µg/l, respectively. PFCs in human serum seemed directly correlated with contaminations in surface water or drinking water, which were highly suspected to be caused by local industrial emissions. Control and reduction of PFCs in industries and environment are in great need for purpose of human health and environmental safety.

2.1.5 Removal methods for PFCs

2.1.5.1 Advanced oxidation processes (AOPs)

Advanced oxidation processes (AOPs) involve the generation of hydroxyl radicals in sufficient quantity to effect water purification. These common processes include O_3/H_2O_2, O_3/UV and UV/H_2O_2. UV/TiO_2 process and Fenton reagent

are also effective to specific wastewater. AOPs such as O_3, O_3/UV, O_3/H_2O_2 and Fenton reagents were identified unable to decompose PFOS in normal state, but able to degrade PFOS precursors and partially fluorinated polymers effectively (Schröder and Meesters, 2005). Some oxidation processes can decompose PFCs completely in critical conditions or coupled with catalysts. PFOS can be completely oxidized by subcritical water oxidation, with catalyst of zerovalent metals like iron. PFOS molecules were observed to be strongly adsorbed on Fe_3O_4 sediments and further decomposed to carbon dioxide and fluorine ions due to oxidation by molecular oxygen in subcritic water (Hori *et al.*, 2006).

2.1.5.2 Photolysis and photo-catalysis processes

PFCAs were proposed to decompose by UV photolysis in stepwise degradation mechanism. Direct photolysis (220-240 nm) was able to completely degrade 560 mg/L PFCAs (Hori *et al.*, 2004a); although one early research claimed that no removal of PFOA was observed under either direct or indirect photolysis (Hatfield, 2001b). Direct UV irradiation at 185 nm mercury lamp or 172 nm xenon quasi-molecular lasers light was found able to degrade some PFCs completely in satisfied speed (Zhang *et al.*, 2005b). Although UV/TiO_2 was found ineffective to decompose PFOS, it was effective to decompose PFCAs. By introduction of 310-400 nm UV irradiation, 45% of about 300 mg/l PFOA dissolved in perchloric acid can be completely degraded in 24 hours by molecular oxygen with catalyst of TiO_2 (Dillert *et al.*, 2007).

2.1.5.3 Incineration

During combustion or incineration, PFCs may completely defluorinated into CO_2 and HF, or into stable state of CaF_2, which is possibly reused as industrial materials. The products of PFCs by incineration were determined by temperature. When papers containing PFOA-related precursors and polymers were incinerated at 600-1,000°C, no emission of PFOA occurred during 2 seconds of

incineration time (Yamada *et al.*, 2005). Under lower temperature at 550°C, thermolysis of fluoropolymers such as polytetrafluoroethylene (PTFE, Teflon) mainly generated trifluoroacetate (TFA). Long-chained PFCA (3-14) were also detected in thermolysis products, which implied floropolymers as one source of PFCs in environment (Ellis *et al.*, 2001).

2.1.5.4 Physical adsorption processes

Granular activated carbon (GAC) filters are often applied to ensure the removal of odor and color from drinking water, as well as trace organics. Laboratory studies showed effective removal of PFOA by carbon adsorption (Schaefer, 2006). Industrial application of GAC column by 3M Company also confirmed the efficiency of adsorption. However, GAC filtration was greatly affected by operation parameters and improper operations would make GAC bed both expensive and ineffective (Ho, 2004). Results of environmental monitoring revealed strong correlations between PFCs concentrations in surface and in drinking water, indicating ineffective removal by current waster treatment process including GAC filters (Skutlarek *et al.*, 2006).

2.1.5.5 Biodegradation processes

PFASs and PFCAs were considered stable and persist in environment without natural degradations (OECD, 2002; US EPA, 2002). PFOS was found not degradable by activated sludge (Schröder, 2003). Behavior of PFCs-related precursors in activated sludge was studied to reveal degradation pathways to PFCs. Perfluorinated carbon bonds of 8:2 FTOH were found to be defluorinated and mineralized by microorganisms under conditions similar to wastewater treatment plant. The biodegradation process was considered to be charged by mechanism of both ß–oxidation and enzyme-catalyzed reaction, which generated short-chained fluorinated carbon metabolites (Wang *et al.*, 2005). Although 60% of 171 kinds of PFCs can be

degraded, persistent metabolites were formed in significant quantities. Furthermore, PFCs seemed to be transformed to more bioaccumulative and toxic products, such as PFOS and PFOA, which occupied 27% and 17% of final products respectively (Dimitrov et al., 2004).

2.1.6 Perfluorooctanoic acid (PFOA) (3M Company, 1999)

Pentadecafluorooctanoic acid is an industrial surfactant. One of the most common uses of PFOA is for processing polytetrafluoroethylene (PTFE), most widely recognized under the brand name Teflon by DuPont. PFOA (known as C8- i.e. 8 carbon atoms) is by far the most extensively studied Perfluorocarboxylic acid (PFCA). Attention has focused primarily on PFOA due to the use of it and its ammonium salt as polymerization aids in the manufacture of polytetrafluoroethylene (PTFE). PFOA is also a by-product of the telomerization process-taking place on industrial scale in Asia, North America, and Europe by several international chemical companies. The telomerization process produces perfluorinated alcohol, which is commonly used in many household surface finishes and indirect contact applications in flexible food packaging. PFOA by-product is also in the fabrication of water- and stain-resistant clothes and other materials. PFOA by-product is also found in aqueous film forming foam (AFFF), a component of fire-fighting foams.

Table 2.3 Basic physiochemical properties of PFOA (3M Company, 1999)

Compound name	Perfluorooctane acid (PFOA)
Formula	$CF_3(CF_2)_6COOH$
Molecular Weight (g/mol)	414.17
Molecular Volume ($cm^3\ mol^{-1}$)	226
pK_a	2.8
Melting Point (°C)	55-56
Boiling Point (°C)	189

Table 2.3 (cont.) Basic physiochemical properties of PFOA (3M Company, 1999)

Compound name	Perfluorooctane acid (PFOA)
Solubility in water (mg/l)	3,400
CMC (mg/l)	15,696 (surface tension measurement)
Chemical Structure	
Appearance	White Powder

2.1.7 Perfluorooctanesulfonic acid (PFOS) (3M Company, 1999)

Perfluorooctanesulfonic acid is an organofluorine compound. Salts of this compound are often used as surfactants. Like other fluorocarbons, the C_8F_{17} subunit in this compound repels water, and the sulfonic acid group makes the anion polar. PFOS was a key ingredient in Scotchgard, a fabric protector made by 3M, and numerous stain repellents. All applications exploit the substances' unique surfactant properties and include:

- Chromium Plating
- Aviation hydraulic fluid
- Photolithography and Semiconductors
- Photographic industry
- Fire-fighting Foams

Table 2.4 Basic physiochemical properties of PFOS (3M Company, 1999)

Compound name	Perfluorooctane sulfonate (PFOS)
Formula	$CF_3(CF_2)_7SO_3H$
Molecular Weight (g/mol)	500.13
Molecular Volume ($cm^3 \, mol^{-1}$)	257

Table 2.4 (cont.) Basic physiochemical properties of PFOS (3M Company, 1999)

Compound name	Perfluorooctane sulfonate (PFOS)
pK_a	-3.27
Melting Point (°C)	>400
Boiling Point (°C)	-
Solubility in water (mg/l)	570
CMC (mg/l)	4,573 (surface tension measurement)
Chemical Structure	
Appearance	Clear liquid

2.2 Surfactant

Surfactant, or surface-active agent, has an amphipathic structure consisting of two dissimilar parts in one molecule, which is a hydrophilic polar head group and a hydrophobic non-polar tail (Rosen, 1989; Rouse, 2001). The hydrophilic head group is attracted to polar environments, such as water, while the hydrophobic tail comprised a long chain hydrocarbon is attracted to nonpolar environments, for example oil. Consequently, the surfactants can dissolve either in water or in oil and have the capability to solubilize water or oil to create homogeneous system. Based on the charge of surfactant head group, surfactants are classified into four categories; anionic, cationic, nonionic and zwitterionic (Hill, 1999).
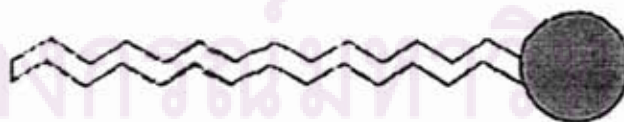
Figure 2.1 Components of a surfactant molecule (Rouse, 2001)

2.3 Mesoporous Silicate

The synthesis of a new family of silicate/aluminosilicate mesoporous materials was disclosed by Mobil scientists in 1992. The synthesis is based on a cooperative liquid crystal templating mechanism, where ionic surfactants and silicate ions from solution coassemble (Thieme and Schüth, 1999). These materials were first described as 'ordered mesoporous molecular sieve' and collectively designated M41S. The M41S family of mesoporous materials was synthesized using silica source and different organic structure directing agents, e.g., cationic surfactants containing long alkyl chain quaternary ammonium compounds containing 10-20 carbons, often followed with addition of co-surfactants. The mesostructure formation depends on the hydrocarbon chain length of the surfactant tail group, the effect of variation of the surfactant concentration and the additional organic swelling agents, such as trimethylbenzene.

Recently, inorganic porous solids have been used technically as adsorbents, catalysts and catalyst supports owing to their high surface areas. Inorganic porous materials are divided into three classes: microporous (<2 nm), mesoporous (2-50 nm) and macroporous materials (>50 nm). However, two classes of materials that are used extensively as heterogeneous catalyst and adsorption media are microporous (such as zeolite) and mesoporous (such as MCM-41, HMS etc.,) inorganic materials. The utility of these materials is manifested in their microstructures, which allow molecules access to large internal surfaces and cavities that enhance catalytic activity and adsorptive capacity (Beck et al., 1992). Furthermore, a study of Hsien and co-worker (1999) has indicated that the adsorption capacity of carbons with similar surface areas and micropore volumes increases with the increasing mesopore volume of the carbons. The idea of using surfactant liquid crystals as templates to generate mesoporous adsorbents and catalysts may be compared to another breakthrough, namely the synthesis of the highly shape selective zeolite ZSM-5 in the 1970s. In both case a rigorous control of pore size and shape was achieved in order to yield solids with molecular sieving properties. In a zeolite micropore the reactants are, however, limited to small molecules

with kinetic diameters lower than 12 Å. Moreover, the kind of functionalizing entities, which may be introduced in the channels to generate catalytic active phases, is also restricted by spatial constraints.

In the 1990's, the silicate and aluminosilicate mesoporous molecular sieves (MMS), which have pore diameters tunable from 15 up to 300 Å was introduced. The large pore size of mesoporous materials, compared to that of zeolites, allows faster diffusion of large organic molecules than zeolitic and aluminum phosphate-based microporous sieves. The spectacular specific surface areas and pore volumes reached by mesoporous molecular sieves constitute another remarkable advantage. Since the walls need not to be made of crystalline material, the restrictions on the chemical nature of the constitutive atoms are much less than in zeolites. These advantages generate the potential for the applications of these materials in catalysis, separation, and sorption for very bulky molecules. Unlike the synthesis of zeolites, which uses a single solvated organic molecule or metal ion as a structure-directing agent that of mesoporous molecular sieves uses a self-assembled surfactant molecular array as a template for the three-dimensional polymerization of silicate species. The pore diameter can be varied by using surfactants with variable chain length, by addition of auxiliary organic compounds, such as trimethylbenzene, and by controlling the synthesis parameters. This property is a direct result of the interplay between organized arrays of the surfactant molecules and silicate species in the aqueous phase.

2.3.1 Porous silicate materials synthesis

The synthesis of inorganic porous materials intensively uses cooperation between organic surfactant as a liquid crystal templating mechanism (LCT) and silicate species in the aqueous phase (silicate-organic complex). The alkyltrimethylammonium surfactants of type $C_nH_{2n+1}(CH_3)_3NBr/Cl$ was found to serve as structure or templates for formations of mesoporous materials (Inagaki et al., 1993), and the sodium silicate is often used as silica source. For production of mesoporous catalyst, the larger alkyl chain

length surfactant is used in LCT for supramolecular templating in low temperature condition (Beck *et al.*, 1994). These proposed synthesis pathways are illustrated in Figures 2.2 and 2.3.
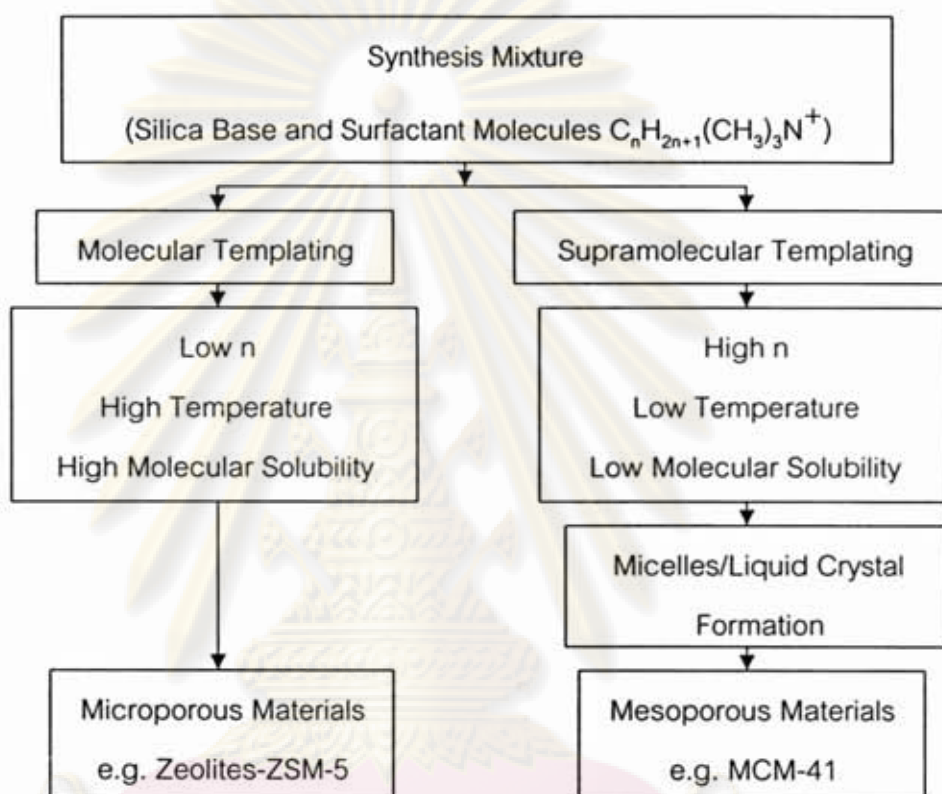
Figure 2.2 Proposed mechanistic pathways for the formation of microporous and mesoporous materials (Beck *et al.*, 1994)

Mesoporous Synthesis pathways

Pathway 1. (S^+I^-)

- cationic surfactant (S^+)

- anionic inorganic species (I^-)

Pathway 2. (S^-I^+)

- anionic surfactant (S^-)

- cationic inorganic species (I^+)

Pathway 3. $(S^+X^-I^-)$

- cationic surfactant (S^+)

- cationic inorganic species (I^-)

- $X^- = Cl^-, Br^-$

Pathway 4. $(S^-M^+I^-)$

- anionic surfactant (S^-)

- anionic inorganic species (I^-)

- $M^+ = Na^+, K^+$

Pathway 5. $(S°I°)$

- neutral surfactant $(S°)$

- neutral inorganic species $(I°)$
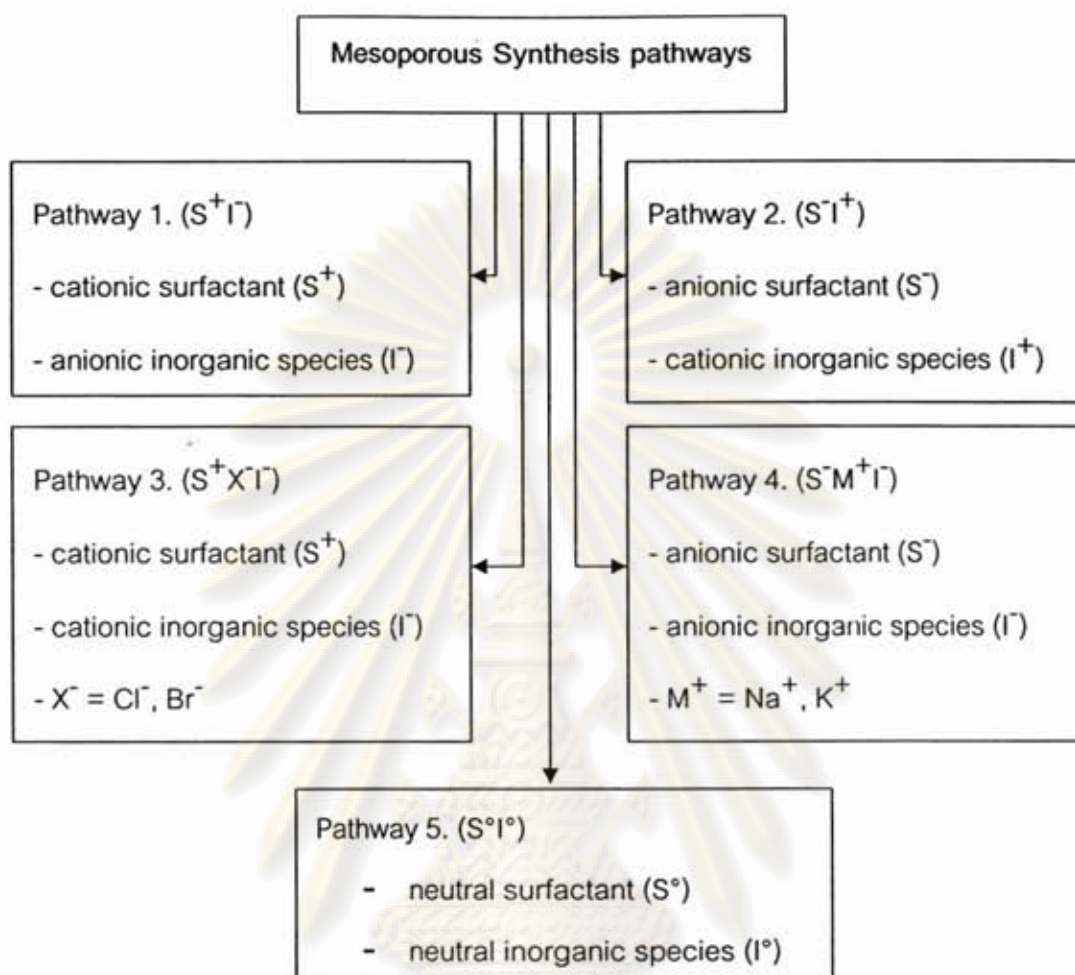
Figure 2.3 Mesoporous synthesis pathways based on charge matching

(Beck *et al.*, 1994)

Recently, synthesis and characterization of different types of mesoporous silicate such as MCM-41, HMS, and FSM-16 have been reported. Synthesis proceeds at normal pressure below 100°C. Moreover, many studies reported that their framework composition might be easily modified by incorporating heteroelement such as aluminum, boron, titanium, vanadium and gallium, which may induce desirable catalytic properties (Yue *et al.*, 1998; Tuel, 1999). At critical micelle concentration (CMC), combination of surfactant molecule (LCT) takes place. The shape of combined molecules also depends on the concentration. At CMC, the cylinder and sphere shape was found, but at higher concentration, the combination becomes more complicated as hexagonal, laminar and cubic shapes. These phenomena bring about the uniformity of

porous structure. Microporous materials are synthesized at lower concentration of template for silicate structure. For this reason, pore size of microporous materials depended on the molecule size of template surfactant.

According to the Mobil report (Beck *et al.*, 1992), characteristics of mesoporous silicate depend on many factors; for example, each crystalline structure (hexagonal, laminar, cubic, etc.) requires the suitable Sur/Si ratio as follow:

- Hexagonal : Sur/Si < 1
- Laminar : Sur/Si = 1.2-2
- Cubic : Sur/Si = 1-1.5

The length of alkyl group of surfactant determines pore size of mesoporous materials. On contrary, the wall thickness of synthesized materials is constant under varying the length of alkyl groups of surfactant.

2.3.2 Synthesis and Formation Mechanism of Mesoporous Silicate

The Mobil researchers proposed synthesis mechanism of mesoporous silicates. In the first way, the $C_nH_{2n+1}(CH_3)_3N^+$ surfactant species organize into lyotropic liquid crystal phase, which can serve as template for the formation of hexagonal MCM-41 structure. Firstly, the surfactant micelle aggregate into a hexagonal array of rods, followed by interaction of silicate or aluminates anions present in the reaction mixture with the surfactant cationic head groups. Thereafter condensation of the silicate species occurs, leading to the formation of an inorganic polymeric species. After combusting of the surfactant template by calcinations, hexagonally arranged inorganic hollow cylinders are produced in the second way, the silicate species added to the reaction mixture influence the ordering of the isotropic rodlike micelles to the desired liquid crystal phase as shown in Figure 2.4.
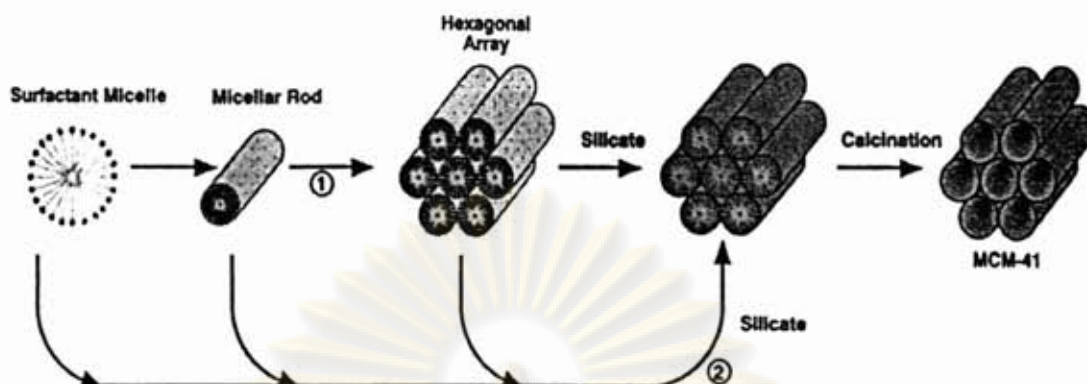
Figure 2.4 Possible mechanistic pathways for the formation of MCM-41

(Beck *et al.*, 1992)

2.3.3 Category and structure of Mesoporous Silicate

Structure of mesoporous silicates were categorized by crystalline structure, shape and size of pores, composition of structure and formation. Table 2.5 shows the category of mesoporous silicate. Crystalline structure was classified as hexagonal, cubic, laminar, etc., depending on the kind of chemical and synthesis condition.

Table 2.5 Categories of uniformity mesoporous materials (Punyapalakul and Takizawa, 2004)

Crystalline Structures	Hexagonal
	Cubic
	Laminar
	Irregularity Structure
Pore size	1.5~10 nm, 3~7 nm, 5~30 nm, 0.4~1.5 nm
Composition of structures	SiO_2, SiO_2-$MO_{n/2}$ (M = Al, Ti, V, B, Mn, Fe, Ga, Zr)
	Al_2O_3, TiO_2, ZrO_2, Ta_2O_5, Nb_2O_5, SnO_2, HfO_2, $AlPO_4$
Formation	Powder, particle, sphere, etc.

a) Hexagonal   b) cubic   c) laminar   d) irregularity structure
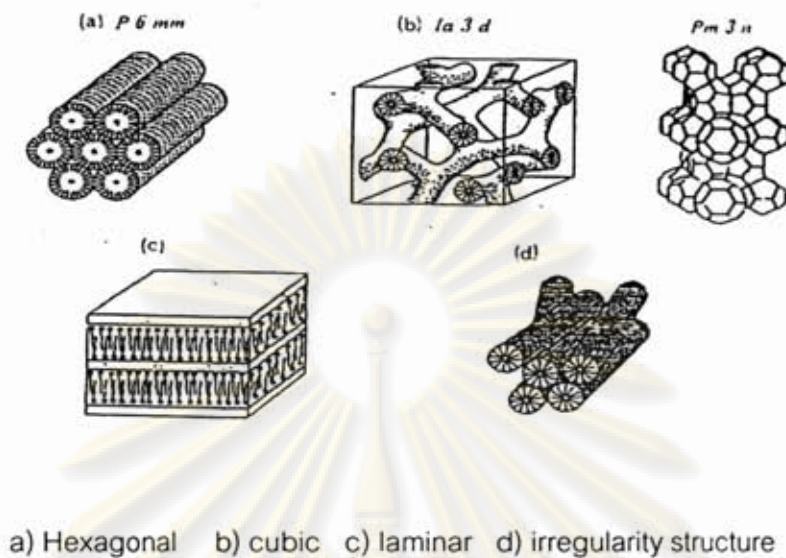
Figure 2.5 Crystalline structures of mesoporous materials

(Punyapalakul and Takizawa, 2004)

2.3.4 Synthesis Methods of Hexagonal Mesoporous Silicate (HMS)

Tanev and Pinnavaia (1996) proposed hexagonal mesoporous silicate (HMS) produced by the neutral synthesis pathway ($S°I°$), which was carried out in the presence of neutral inorganic precursors and uncharged surfactants such as primary amines. In this case, hydrogen bonding rather than electrostatic interaction is a driving force for the cooperative organization of the organic-inorganic mesophase. This neutral $S°I°$ templating route produces mesostructures with larger wall thickness, small scattering domain sizes, and complementary textural mesoporosites relative to materials produced by other pathway (Tanev and Pinnavaia, 1995; Kruk *et al.*, 1997)

Tanev and pinnavaia (1996) proposed hexagonal mesoporous silicas (HMS) having thicker pore walls, high thermal stability and smaller crystallite size but having higher amounts of interparticle mesoporosity and lower degree of long-range ordering of pores than MCM-41 materials. The formation of neutral primary amine surfactant molecule ($S°$) and neutral $Si(OC_2H_5)_{4-x}(OH)_x$ precursor ($I°$) into rodlike

assemblies as shown in Figure 2.6. Hydrogen bonding interactions between the precursor silanol hydrogen and the lone electron pairs on the surfactant head groups changes the head-to-chain volume ratio (i.e., the preferred packing) of the surfactant-inorganic complexes and most likely facilitates the assembly of rodlike micelles. Further hydrolysis and condensation of the silanol groups on the micelle-solution interface afford short-range hexagonal packing of the micelles and framework wall formation.

HMS was prepared by $S^{\circ}I^{\circ}$ assembly pathways in water: ethanol solvent mixtures. In reaction media, tetraethyl orthosilicate (TEOS) intensively served as the neutral silica precursor and dodecylamine (DDA) is the neutral liquid crystal template (LCT). Although many primary amines were studied as the neutral structure, dodecylamine was recommended as the best LCT (Tanev and Pinnavaia, 1995).
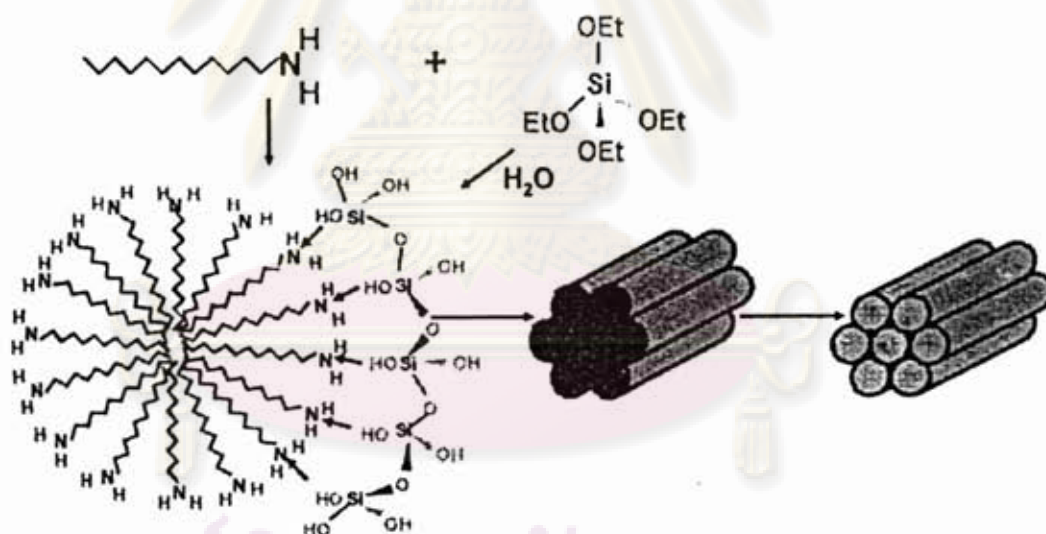
Figure 2.6 Schematic representation of the $S^{\circ}I^{\circ}$ templating mechanism of formation of HMS mesoporous molecular sieves (Tanev and Pinnavaia, 1996)

2.3.5 Organic Functionalization (Tanev and Pinnavaia, 1996)

The application of pure mesoporous silicates or aluminosilicates as

adsorbent is rather limited because of the limitations in the nature of their active sites. To utilize these mesoporous materials for several specific applications including catalysis, sorption, ion exchange, and sensing, it is essential to introduce reactive organic functional groups by modifying the inner surfaces of these materials to form inorganic-organic hybrid. Organically functionalized silica is a subset of a larger class of hybrid organic-inorganic materials. Covalently bonded organic ligands are usually non-hydrolysable and impart partial organic character to an inorganic siloxane network. Organic functionalization can be categorized into two general methods: grafting method and direct co-condensation method.

2.3.5.1 Grafting Method (Tanev and Pinnavaia, 1996)

Grafting refers to post synthesis modification of the inner surface of mesoporous silica, where the organic functional groups are introduced as the terminal groups of an organic monolayer. A large number of surface silanol $[(-Sio)_3 Si-OH]$ groups present in mesoporous silica can be utilized as convenient moieties for anchoring of organic functional groups. The surface modification with organic functional groups is generally carried out by silylation as shown in Figure 2.7
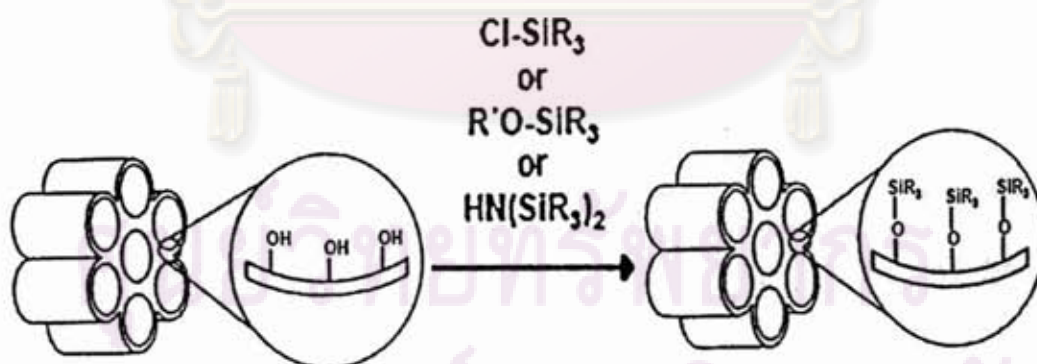
Figure 2.7 Functionalization of inner walls of mesoporous silicates by grafting method

(Tanev and Pinnavaia, 1996)

2.3.5.2 Direct Co-condensation Method (Tanev and Pinnavaia, 1996)

In the grafting methods, organic groups are incorporated by attachment of the organosiloxane precursor with surface Si atoms through Si-O-Si-C covalent bond formation. Then Si-O bond can be cleaved under certain reaction conditions. Therefore, in some cases it would be desirable to have direct formation of a C-Si (surface) covalent bond. Thus, the "one-pot" co-condensation method, where condensation occurs between a tetraalkoxysilane and one or more trialkoxyorganosilanes through sol-gel chemistry (Figure 2.8), seems to have distinct advantages over the grafting methods. A direct co-condensation method is the one-step synthesis of organically functionalized mesoporous silica, which has two different approaches of synthesis (Mercier and Pinnavania, 2000):

(1) Template exchange including the replacement of TEOS as well as alkylamine surfactant with organosilane.

(2) Addition of organosilane by replacing of TEOS with organosilane, maintaining the same alkylamine to TEOS ratio as used to synthesize the non-functionalized HMS materials.

Several research groups have employed this method to prepare inorganic-organic hybrid mesoporous materials under a wide range of synthesis condition. Usually the solvent extraction technique is used to remove the surfactant from the resultant materials.
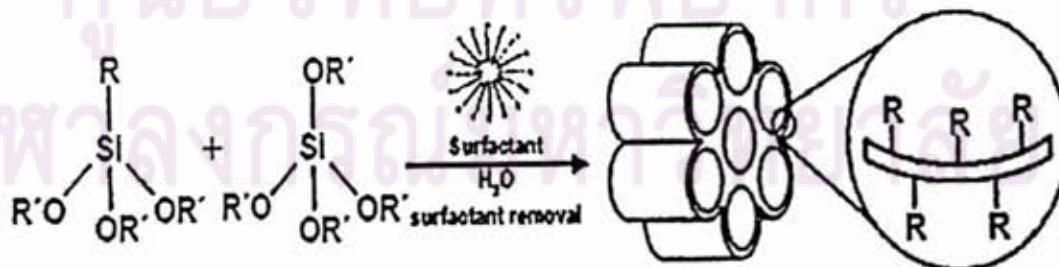
Figure 2.8 Functionalization of inner walls of mesoporous silicates by direct co-condensation method (Tanev and Pinnavaia, 1996)

2.3.6 Properties and Application of Mesoporous

Due to the unique physical properties and higher pore sizes than zeolites, mesoporous materials have been highly desirable for catalytic and adsorption applications. Many researchers have studied their properties and tried to develop surface functional groups for more applications. Functionalization of mesoporous materials has played an important role in various aspects such as immobilization of enzymes (Maria Chong and Zhao, 2004; Yiu and Wright, 2005; Hudson et al., 2005), development of new catalyst (Aprile et al., 2005) and selective adsorbent (Lee et al., 2001; Newalkar et al., 2003; Messina and Schulz, 2006).

Table 2.6 Physico-chemical characteristics of HMS, modified HMSs, PAC and zeolites (Punyapalakul and Takizawa, 2006)

Adsorbents	Surface functional groups	Surface characteristic
HMS	Silanol	Hydrophilic
Ti-HMS	Silanol	Hydrophilic
M-HMS	Mercapto	Hydrophobic
OD-HMS	Octyl	Hydrophobic
A-HMS	Amino	Hydrophilic
PAC	Carboxylic Phenyl Others	Hydrophobic
NaY-zeolite	Na^{+}	Hydrophilic
HY-zeolite	Brönsted acid	Hydrophilic

Many functional groups have been studied depending on purpose. Feng et al., (1997); Mercier and Pinnavaia (1997) and Liu et al., (1998) studied the monolayer of thiol groups grafted on the mesopore walls of ordered mesoporous silicas (OMSs). The results showed that materials have large surface area, insoluble and stable

framework, tunable pore size and relatively high adsorption affinity towards heavy metal ions up to 0.6 g of Hg^{2+} per gram of thiol functionalized OMS.

Kei Inumaru *et al* (2000) studied the molecular selective adsorption of nonylphenol in aqueous solution by octylsilane-grafted mesoporous silica (C$_8$-MPS), dodecylsilane-grafted mesoporous silica (C$_{12}$-MPS) and compare with activated carbon. The results found that MPS was made more hydrophobic by grafting alkyl chains on the inner surface of the mesopores and the octylsilane-grafted hexagonal mesoporous silica showed a high adsorption capacity for nonylphenol, an endocrine disrupter, comparable to that of activated carbon. In addition, The C$_8$-MPS adsorbent showed high molecular selectivity, distinguishing the hydrophobicity of molecules than C$_{12}$-MPS. These results indicate that the introduction of hydrophobic functionalization to inner surface of MPS is an effective strategy to design molecular selective adsorbents.

Robert *et al* (2000) studied remediation of heavy metal using functionalized mesoporous silica. The material, whose mesopores were functionalized with 3-mercaptopropyltrimethoxysilane ligands, can be made into spheres, irregular particles, and truncated cones having diameters from 1 to 15 mm through a one-step emulsion synthesis procedure. The results experiment found that the surface area of these materials determined via the BET method ranged from 864 to 1,184 m^2 g^{-1}. The materials are extremely effective in the removal of mercury and silver ions from aqueous solutions. The amount of mercury adsorbed ranged from 0.24 to 1.26 mmol g^{-1}, depending on the degree of functionalization. Silver is less strongly adsorbed than mercury, with a maximum loading of 0.89 mmol g^{-1}. Functional ligands can be added to the materials to alter the adsorption properties. It was shown that MPTS ligands enable these materials to function as selective adsorbents for the removal of heavy metals from aqueous streams.

Koon Fung Lam *et al* (2004) studied selective ordered mesoporous silica (OMS) adsorbents were prepared by grafting amino, carboxylic and thiol-containing

functional groups onto MCM-41 for the selective removal of dye and metal pollutants from wastewater. The amino containing $OMS-NH_2$ adsorbent has a large adsorption capacity and a strong affinity for the Acid blue 25. It can selectively remove Acid blue 25 from a mixture of dyes. The OMS-COOH is a good adsorbent for methylene blue displaying excellent adsorption capacity and selectivity for the dye. The OMS-SH adsorbent can selectively remove lead from solutions containing Pb^{2+} and Cu^{2+} ions. Moreover, the monolayer of thiol groups on the mesopore walls of ordered mesoporous silicas (OMSs) afforded materials with large surface area, insoluble and stable framework, tunable pore size and relatively high adsorption affinity towards heavy metal ions (Feng et al., 1997; Mercier and Pinnavaia, 1997). Up to 0.6 g of Hg^{2+} per gram of thiol functionalized OMS was reported (Liu et al., 1998).

Yoshitake et al (2005) studied the adsorption of oxylanon and hydrophilic substances by using amino-functional group that having more hydrophilic than activated carbon. The results found that the adsorption capacities for ferric ions on the polyamine-PrM41, amount of ferric ion adsorbed increased monotonously with the number of amino groups in the polyamine chain.

Messina and Schulz (2006) modified silica mesoporous materials by TiO_2 for adsorption of reactive dyes. The presence of TiO_2 augmented the adsorption capacities of reactive dyes. They suggested that this would be due to possible degradation of the dye molecule in contact with the TiO_2 particles in the adsorbent interior.

Jiansheng Li et al (2007) grafted mesoporous silicates material by amino groups, [1-(2-amino-ethyl)-3-aminopropyl]trimethoxysilane (AAPTS) for adsorption of Cr(VI) from aqueous solution. The adsorption experiment results showed that the functionalized mesoporous silica materials show good crystallographic order and large uniform pore size. The maximum Cr(VI) loadings at 25, 35 and 45°C were found to reach 2.28, 2.86 and 3.32 mmol/g, respectively. The functionalized mesoporous silica

materials are promising adsorption materials for reducing toxic chromate pollution. Furthermore, amino-functional group having more hydrophilic than activated carbon has been studied for oxylanon (Yoshitake *et al.*, 2005) and hydrophilic substances adsorption.

Sindia *et al* (2008) functionalized MCM-41 type mesoporous silicates with nickel species via thermal monolayer dispersion and grafting techniques. The experiment result showed the material potential to serve as sorbents for the selective removal of a pharmaceutical drug (Naproxen) from water. In addition, the inclusion of transition metal functionality onto the surface of MCM-41 enhances the material performance during the adsorption of Naproxen from aqueous medium. Furthermore, mesoporous silicates can be grafted on the surface by many organic functional groups to enhance its valuables.

Valeria and Reyes (2008) studied the removal of perfluorinated surfactants by sorption onto granular activated carbon, zeolite and sludge. The results found that among all adsorbents evaluated in this study, activated carbon showed the highest affinity for PFOS at low aqueous equilibrium concentrations, followed by the hydrophobic, high-silica zeolite-NaY, sludge. Moreover, sorption of PFOS onto activated carbon was stronger than PFOA and PFBS, suggesting that the length of the fluorocarbon chain and the nature of the functional group influenced sorption of the anionic surfactants.

Punyapalakul and Takizawa (2004) developed Hexagonal Mesoporous Silica (HMS) by grafted various organic functional group on surface of HMS (e.g., 3-aminopropyltriethoxy, 3-mercaptopropyl, n-octyldimethyl-functional group) and Ti-HMS for adsorbed of dichloroacetic acid (anionic compound) and comparison with PAC. The result showed that pristine HMS and Ti-HMS, which have silanol groups as major functional group on surface was barely, adsorbed DCAA on them. Similarly, hydrophobic HMSs (OD-HMS and MP-HMS) did not adsorb DCAA. Surface

hydrophobicity, coupled with nearly neutral electric charge of MP-HMS and negative surface charge of OD-HMS, resulted in little adsorption of hydrophilic, negatively charged DCAA. On the contrary, AM-HMS had the highest adsorption capacity as powder activated carbon (PAC) at high concentration level because of AM-HMS and PAC has strong positive charge. In the case of AM-HMS, combined effects of hydrophilicity and coulomb interaction force between amino functional group of AM-HMS and DCAA facilitate DCAA adsorption.

Punyapalakul and Takizawa (2004) studied adsorption mechanism of alkylphenon polyethoxylate compound on HMS and modified HMSs (Ti-HMS, OD-HMS and MP-HMS) and also comparison with PAC. The results showed that hydrophilic adsorbents (HMS and Ti-HMS) have higher adsorption capacities of APnEOs than hydrophobic adsorbents (PAC, OD-HMS and MP-HMS). Moreover, hydrophilic surface caused by silanol groups enhance aggregation adsorption on the external surface; on the contrary, hydrophobic surface cause semi-aggregation, which increased adsorption capacities on external surfaces of all adsorbents.

Punyapalakul and Takizawa (2006) also studied selective adsorption of alkylphenol polyethoxylates (APnEOs) from synthetic textile wastewater was investigated using hexagonal mesoporous silicates (HMSs) by grafted with organic surface functional groups, i.e., n-octyldimethyl-, 3-aminopropyltriethoxy-, 3-mercaptopropyl-groups and Ti-HMS. Triton X-100 was used as a model APnEO and either Basic Yellow 1 or Acid Blue 45 was used as cationic or anionic dyes. The results showed that all the HMSs except 3-aminopropyltriethoxy-grafted HMS had higher adsorption capacities of Triton X-100 than powdered activated carbon. FT-IR spectra proved that hydrophilic HMSs adsorbed both Basic Yellow 1 and Acid Blue 45 by hydrogen bonding. Due to negative surface charge, the anionic dye (Acid Blue 45) was not adsorbed on the four HMSs, which proves high selectivity of these HMSs for Triton X-100® over Acid Blue 45. On the contrary, a small amount of cationic dye (Basic Yellow 1) was adsorbed on all HMSs, but 3-

aminopropyltriethoxy-grafted HMS showed the lowest adsorption capacity for Basic Yellow 1 due to positive surface charge.

For regeneration study, Punyapalakul and Takizawa (2004) studied effect of regeneration methods on adsorption capacity and crystalline structure of synthesized HMSs. The results showed that pristine HMS can be regenerated by calcinations method without significantly decreasing adsorption capacity though a little decrease of crystalline structure and surface characteristics. Surface area of calcinations-regenerated HMS and Ti-HMS were decreased by 10% and 23%, respectively. TX-100 adsorbed on HMS and Ti-HMS can be extracted by a mixture of alcohol and water easier than PAC. However, decrease of ApnEOs adsorption capacities of HMS, Ti-HMS and PAC was found at 82%, 61% and 61%, respectively, after alcohol regeneration. Residual ethanol on surface did not cause decrease of organic pollutants adsorption capacities of regenerated HMS and Ti-HMS significantly.

2.4 Activated Carbon (AC) (Soonglerdsongpha, 2006)

Activated carbon is made of tiny clusters of carbon atoms stacked upon one another. It can be made from many substances containing high carbon content such as coal, wood, peanut shells and coconut shells. The raw material has a very large influence on the characteristics and performance activated carbon. The raw carbon source is slowly heated in the absence of air to produce a high carbon material. The carbon is activated by passing oxidizing gases through the material at extremely high temperatures. The activation process produces the pores that result in such high adsorptive properties.

Activated carbon is an adsorbent that is widely used in adsorption processes. Activated carbon consists of a network of interconnected pores of varying sizes which are classified according to their diameter; micropores < 2.0 nm, mesopores 2-50 nm and macropores > 50.0 nm. The pores provide a large internal surface area, typically

ranging from 800 to1,200 m^2/g, which enables activated carbon to adsorb contaminants from water. Activated carbons have been successfully employed as adsorbents, catalyst supports due to their well-developed porous structures, and large internal surface comprised of hydrophobic grapheme layers and hydrophilic surface functional groups. These porous materials can be used for the adsorption of a wide range of species from either gas or liquid phases. An important aspect in the treatment of aqueous systems using active carbons is that it can be used to remove both inorganic and organic species. However, most activated carbons are highly microporous thus; it is effective for some contaminants and not effective for others. It does not remove microbes, sodium, nitrates, fluoride, and hardness.

Figure 2.9 Activated Carbon (Soonglerdsongpha, 2006)

2.5 Zeolites (Soonglerdsongpha, 2006)

Zeolites are microporous crystalline solids with well-defined structures. Generally, they contain silicon, aluminum and oxygen in their framework and cations, water and/or other molecules within their framework and cations, water and/or other molecules within their pores. Many occur naturally as minerals, and are extensively mined in many parts of the world. Others are synthetic, and are made commercially for specific uses, or produced by research scientists trying to understand more about their chemistry. Because of their unique porous properties, zeolites are used in a variety of

applications. Major uses are in petrochemical cracking, ion exchange (water softening and purification), separation and adsorption.

The basic unit of a zeolite structure is the TO_4 tetrahedron, where T is normally a silicon or aluminum atom/ion (or phosphorous in an aluminophosphate). The general formula of the aluminosilicate zeolites is $M_{x/n}$ $[(AlO_2)_x$ $(SiO_2)_y].mH_2O$. The zeolite framework is composed of $[(AlO_2)_x$ $(SiO_2)_y]$ and M is a non-framework, exchangeable cation. The great variety of zeolites is made possible by the different arrangements of linked TO_4 tetrahedral within secondary building units (SBUs), which are linked themselves together in numerous three-dimensional networks. The two simplest SBUs are rings of four and six tetrahedral and others comprise larger single and double ring up to 16 T atoms. The unit cell always contains an integral number of SBUs.
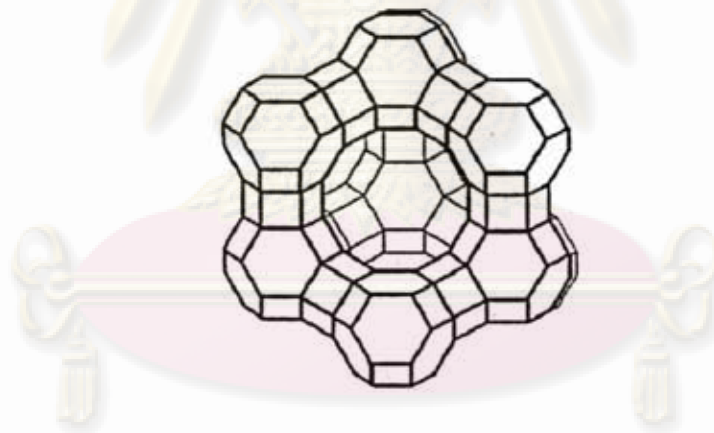
Figure 2.10 Structure of faujasite-type zeolite (Soonglerdsongpha, 2006)

Zeolite Y is the faujasite-type zeolite (Figure 2.10). It has the same framework structure as zeolite X. They crystallize with cubic symmetry. The general composition of the unit cell of faujasite is $(Na, Ca, Mg)_{29}[Al_{58}Si_{134}O_{384}].240H_2O$. The SBUs are double six-rings and FD is 12.7 nm^{-3}. The unit cell contains eight cavities, each of diameters ~ 1.3 nm. The three-dimensional channels have 12-ring windows with free apertures of about 0.74 nm. The difference between zeolites X and Y is in their Si/Al ratios which are 1-1.5 and 1.5-3, respectively.

2.6 Characterization of Hexagonal Mesoporous Silicate

2.6.1 Crystalline Structure Confirmation by X-Ray Powder Diffraction (XRD)

X-ray powder diffraction indicates uniqueness in structure, as the powder diffraction patterns is a fingerprint of individual molecular sieve structures. The powder diffraction pattern can also provide information on the degree of crystallinity as well as phase purity, which is used for quality control in preparing different batches molecular sieve materials.

X-ray diffraction pattern is used for material analysis including characterization by using the pattern as a unique fingerprint for phase. This pattern typically shows a graph of diffraction angle and diffracted line intensity. This X-ray Diffraction instrument makes use of different diffraction pattern of each specimen for identification. In addition, this instrument can determine the approximate pore size. XRD is the first step in characterization of a solid isolated from the synthesis mixture. The following information about the solid is obtained from the diffraction pattern.

*Successful (or unsuccessful) formation of a crystalline material
*Presence of a single phase or mixture of phases
*Structure type or structure types comprising the mixture, identified by
 the presence of peaks.
*If standards are available, the level of crystallinity obtained from that
 synthesis batch.
*Ultimately, with the proper techniques, determination of new structure.

Using an XRD spectrometer, the diffraction pattern created by constructive interference is recorded by a beam detector as the X-ray tube and the detector are rotated around the sample. The relationship between angle at which diffraction peaks occur (2θ (°)) and the inter-atomic spacing of a crystalline lattice (d-spacing) is

spacing) is expressed by Bragg's law: $n\lambda = 2d\sin\theta$. For historical reasons, XRD-traces, or diffractrograms, are expressed in degrees two theta (2θ (°)). Since each crystalline structure is unique, the angles of constructive interference form a unique pattern. By comparing the positions and intensities of the diffraction peaks against a library of known crystalline materials, samples of unknown composition can be identified.

2.6.2 Determination of surface area and pore diameter of the Mesoporous Silicate by nitrogen adsorption isotherms

2.6.2.1 Surface area

There are now exist a number of methods to determine the surface area of porous solid. As a method that is relatively simple to apply, the volumetric adsorption of an inert gas (i.e. nitrogen gas) was used in the present study. The equilibrium distribution of adsorbate molecules between the surface of the adsorbent and the gas phase is dependent upon pressure, temperature, the nature and area of the adsorbent, and the nature of the adsorbate. An adsorption isotherm shows how the amount adsorbed depends upon the equilibrium pressure of the gas at constant temperature.

The Brunauer-Emmett-Teller (BET) method continues to be the most widely used method for the determination of surface area, pore volumes and pore size distributions of porous materials from nitrogen adsorption-desorption isotherm data. The nitrogen adsorption-desorption isotherms (BET) were measured at 77 K on a Surface area and Porosity Analyzer. The BET equation can be represented in Equation 2.3 as below.

$$\frac{p}{v(p_0 - p)} = \frac{1}{v_m c} + \frac{c-1}{v_m c} \frac{p}{p_0}$$

...(2.3)

Where v =   Volume of N_2 adsorbed by the sample under pressure p

               P_0 =   Saturated vapor pressure at the same temperature

               v_m =   Volume of N_2 adsorbed when the surface is covered with a

                       unimolecular layer

And c =   Constant for a given adsorbate

The specific surface areas of samples were calculated

from the adsorption data by Equation 2.4

$$S = \frac{N_0 v_m A}{22414 m}$$

           ...(2.4)

Where S =   Specific surface area

           N_0 =   Avogadro number

           m =   Amount of solid adsorbent

           A =   Cross-section of the gas molecules (16.2 $\text{A}^{\circ 2}$ for N_2)

2.6.2.2 Pore size

In the present study, pore diameter and volume of mesoporous molecular sieve catalysts was calculated following the Barrett-Joyner-Halenda (BJH) method with the corrected Kelvin equation. It was shown that the Kelvin equation for the hemispherical meniscus, corrected for the statistical film thickness, is in quite good agreement with an experiment relation between the pore size and the capillary condensation procedure. With the corrected Kelvin equation, the agreement can be made quantitative in the pore size range from ca. 2 to 6.5 nm.

When the Kelvin equation is to be applied to the N_2 adsorption-desorption isotherm, the pore geometry is assumed to be cylindrical shape filled with condensed liquid nitrogen. Where p_0 is the saturated vapor pressure, p

equilibrium pressure, V_L is the molar volume of the liquid and γ is the surface tension, the Kelvin equation will be describe as follows:

$$\ln \frac{p_0}{p} = \frac{2\gamma V_L}{rRT}$$

...(2.5)

2.6.3 Fourier Transform Infrared (FT-IR) Spectroscopy

The usefulness of infrared (IR) spectroscopy for the study of surface species at the solid/vapor interface is well documented but the development of infrared spectroscopic methods for the study of adsorption from solution has been slow. The addition of a liquid component makes the detection of infrared bands due to the surface more difficult, particularly for liquids which are themselves strong adsorbers of infrared radiation. However, infrared spectroscopy is used widely for the propose of materials surface properties of surfactant modified bentonite, used for BTEX removal, by IR spectra, and they confirmed both of bentonite's surface structure and surfactant modified part. Brunel and co-worker (1995) also presented the characterization of MCM-41 and organic modified MCM-41 (oxidation process) by IR spectra.

For pure silicate mesoporous materials, IR adsorption spectra in the region of 4,000 cm^{-1} were investigated widely for characterization. Table 2.7 shows the adsorption bands that have been assigned for silicate surface investigation. Moreover, IR spectra can be used to further confirm the presence of organics in the mesoporous silicate products, and offers the additional advantage of confirming the integrity of the organic molecules. Table 2.7 presents IR spectra bands reported for confirmation of grafted organic groups.

Table 2.7 Infrared adsorption frequencies for pure silicate and modified porous materials (Punyapalakul and Takizawa, 2004)

Bonding	IR spectra bands (cm^{-1})	Reference
O-Si-O	470	Roy *et al.*, 1996; Carrado *et al.*, 2000; Wang *et al.*, 1999
Si-O	1,100	Roy *et al.*, 1996; Carrado *et al.*, 2000; Wang *et al.*, 1999
Ring structure of SiO_4	800	Roy *et al.*, 1996; Carrado *et al.*, 2000; Wang *et al.*, 1999
Si-OH	973	Roy *et al.*, 1996
H-O-H	3,457	Roy *et al.*, 1996; Decottignies *et al.*, 1978
Deformation mode of H_2O	1,650-1,600	Roy *et al.*, 1996; Decottignies *et al.*, 1978
O-H	3,750	Partiff *et al.*, 1983
CH_3 of ethoxy group	2,970	Brunel *et al.*, 1995
-CH_2-stretching vibration	2,940	Brunel *et al.*, 1995
Si-O-Ti	960	Ahn *et al.*, 1999; Blasco *et al.*, 1995
C-H of alkyl and phenyl groups	1,500-1,300	Wang *et al.*, 1999

2.6.4 Surface charge density

The principle of electroneutrality must hold true for every point on all titration curves, i.e., the sum of all negative charges is equal to the sum of all positive charges (Schulthess et $al.$, 1986; Al-Ghouti et $al.$, 2003).

$$\Sigma \text{ negative charges} = \Sigma \text{ positive charges} \qquad ...(2.6)$$

For example, their titration of an amphoteric oxide surface with HCl or NaOH in the presence of NaCl electrolyte solution, would result in

$$[OH^-] + [Cl^-] + [\text{negative surface}] = [H^+] + [Na^+] + [\text{positive surface}] \quad ...(2.7)$$

Or

$$\sigma_0 = [\text{positive surface}] - [\text{negative surface}]$$

$$= [C_A - C_B] - [H^+ - OH^-] \qquad ...(2.8)$$

Where

σ_0 = surface charge

[negative surface] = the concentration of negative charges on the surface

[positive surface] = the concentration of positive charges on the surface

$[H^+]$ = 10^{-pH}

$[OH^-]$ = 10^{pH-pKw}

$[Cl^-]$ = $[NaCl]_{added} + [HCl]_{added}$

$[Na^+]$ = $[NaCl]_{added} + [NaOH]_{added}$ and

$[C_A-C_B]$ = $[Cl^-] - [Na^+]$

= $[HCl]_{added} - [NaOH]_{added}$

When the surface charge is neutral, the negative and positive charges are equal, (negative surface) = (positive surface), and the surface is said to have zero charge. At the pH of zero point of charge (pH_{zpc}), equation (2.8) simplified to:

$$[C_A - C_B] = [H^+ - OH^-] \qquad ...(2.9)$$

Hydroxyl groups present on the surface of silicate materials can gain or lose a proton, resulting in a surface charge that varies with changing pH. At low pH, surface sites are protonated and the surface becomes positively charged:

$$pH < pH_{zpc} : \quad Si\text{-}OH + H^+ \longrightarrow Si\text{-}OH^{2+} \qquad ...(2.10)$$

While at high pH, the surface hydroxides lose their protons, and the surface becomes anionic.

$$pH > pH_{zpc} : \quad Si\text{-}OH + OH^- \longrightarrow Si\text{-}O^- + H_2O \qquad ...(2.11)$$

pH_{zpc} values of silicate materials were reported by several researchers depending of types of silicate materials.

2.7 Adsorption Theory (Soonglerdsongpha, 2006)

2.7.1 Mechanism of Adsorption onto Porous Adsorbent

Adsorption is a process that occurs when a gas or liquid solute accumulates on the surface or interface of a solid or a liquid (adsorbent), forming a molecular or atomic film (adsorbate). Such a process can occur at an interface of any two phases, such as liquid-liquid, gas-liquid, gas-solid, or liquid-solid interfaces. While there is a preponderance of solute (sorbate) molecules in the solution, there is none in the sorbent particle to start with. This imbalance between the two environments amounts

to a driving force for the solute species. First to create a sorbate layer on the surface and then the sorbate transport into a solid, encompassing the surface by penetration into the solid and condensation within pores. A surface phenomenon in term of adsorption can be divided into the two sub-categories of physical adsorption (physisorption) or Van Der Waals adsorption and chemical adsorption (chemisorptions) and the adsorption process can be determined whether chemical bonds are formed during the process. Physical Adsorption (physisorption) is a dynamic one where an equilibrium state exists with molecules and the interaction between the adsorbate and adsorbent. No chemical bonds are formed during physical adsorption; attraction between the adsorbate and adsorbent exists by the formation of intermolecular electrostatic, such as London dispersion forces, or Van Der Waals forces from induced dipole-dipole interactions, or may be dependent on the physical configuration of the adsorbent such as the porosity of activated carbons. For another thing, chemisorptions involve the transfer of electrons between the adsorbent and the adsorbate with the formation of chemical bonds, by chemical reaction, between the two species causing adhesion of the adsorbate molecules.

Many factors influence the adsorptive capacity for specific organic solutes of a homologous series. First, there are the adsorbate properties of group functionality, branching or geometry, polarity, hydrophobicity, dipole moment, molecular weight and size and aqueous solubility. Second, there are solution conditions such as pH, temperature, adsorbate concentration, ionic strength and competitive solutes. Third, there is the nature of the adsorbent with its surface area, pore size and distribution of functional groups.

2.7.1.1 Properties of Sorbent Materials

The importance of the surface properties (including sorptive properties) of a given weight of material exposed to solution, increase in proportion to the surface area of that material, and its surface charge (or site) density or number of

charged sites per unit area or weight. Surface charge may be permanent and independent of solution composition, or variable, changing with solution composition.

The surface charge of oxides, hydroxide, phosphate, and carbonates is produced chiefly by ionization of surface groups, or surface chemical reactions. For example, the pH-dependent surface charge of silicate might reflect the presence of surface species written symbolically as $SiOH_2^+$, $SiOH$ and SiO^-. The surface species are positively charged at low pH and deprotonate as pH increase to form neutral and negatively charged species at intermediate and higher pH consistent with the amphoteric behavior of the oxide or hydroxide.

2.7.1.2 Properties of Sorbates

The properties and structure of the sorbates most likely to be found in electrostatic attraction are stressed, especially dissociation constant for acid compounds. Acid dissociation constants are commonly reported as pK_a values. Acidity constants of organic compounds depend on the type of functional acid groups. For example, carboxylic acids and sulfonic acids are significant components of most contaminants originating from organic-rich wastes. The high apparent of carboxylate ions occur at higher pH of solution than pK_a, and they will be protonated to form carboxylic acids at lower pH. Moreover, sulfonic acid is considered as to be a strong acid. Thus, from the very low pK_a value, solution relate to the ionized form.

Table 2.8 Acid dissociation constants for some carboxylic acids and sulfonic acids (USEPA, 2002)

Compound Name	Formula	pK_a
Perfluorooctane acid (PFOA)	$CF_3(CF_2)_6COOH$	2.8
Perfluorooctane sulfonate (PFOS)	$CF_3(CF_2)_7SO_3H$	-3.27

2.7.1.3 Temperature Effect

Temperature is a crucial parameter in adsorption reactions. It was noted that the temperature could influence the sorption process. The sorptive removal of copper ions from aqueous solution by tree fern increased with increase in temperature, which is typical for the biosorption of most metal ions from their solution (Ho, 2003). However, the magnitude of such increase continues to decline as temperatures are raised from 30 to 80ºC. The decrease in adsorption with increasing temperature, suggest weak adsorption interaction between biomass surface and the metal ion, which supports physisorption. For physical adsorption, adsorption heat $\Delta H° < 0$, adsorption reaction is exothermic and preferred at lower temperatures. For chemisorptions, $\Delta H° > 0$, adsorption reaction is endothermic and favored at higher temperatures; however, the effect of temperature is small as compared to other influencing factors.

2.7.1.4 Influence of pH

Solution pH not only influences the properties of the sorbent surface, but also affects the sorbate speciation in solution. Therefore, it is an important parameter affecting sorption behaviors in many cases of the ionic adsorption, in which the influence of pH has directly relation with the surface charge of adsorbents. Such pH value that gives zero surface charge is called the zero point of charge (pH_{zpc}). At this pH cationic surface groups and anionic surface groups, posses equal amount of electric charge.

Moreover, the surface of adsorbents can gain or lose protons, which vary the surface charge with changing pH. At low pH, most of the surface sites are protonated and the surface becomes positively charged, while at high pH, the surface sites lose protons, and the surface become anionic. Thus, the electrostatic attraction between adsorbents and adsorbates usually plays a predominant role (Janos et al., 2003; Higgins and Luthy, 2006).

2.7.1.5 Ionic Strength Effect

The influence of ionic strength is significantly affected ion adsorption by the electrostatic attraction. Punyapalakul and Takizawa (2004) studied the effect of ionic strength and ionic species on TX-100 on adsorption capacity of PAC by varied concentration of NaH_2PO_4, $NaCl$, $CaCl_2$ and $CaPO_4$. Initial concentration of TX-100 was set at 75 mg/l. The results showed that ionic strength did not affect adsorption capacities on PAC until ionic strength up to 100 mM caused a slight increasing of TX-100 adsorption capacities on PAC.

2.7.1.6 Presence of Other Anions

Other sorbable ions in the solution may compete with the contaminants of interest for sorption sites. The binding of the primary is then decreased. For anion sorption, the study of anion exchange established that the selectivity of anion exchanger could be enhanced by the counter ion of higher valence, with the smaller (solvated) equivalent volume and greater polarizability, and interacting more strongly with the fixed ionic groups on the matrix and participating least in complex formation with the co-ion. The established affinity is as follows: $SO_4^{2-}>I^->NO_3^->CrO_4^->Br^->SCN^->Cl^->F^-$. Therefore, it would be appropriate to use electrolytic Cl^- salts as background for ionic strength control.

2.7.2 Adsorption Kinetic (Soonglerdsongpha, 2006)

Several models can be used to express the mechanism of solute sorption onto a sorbent. In order to investigate the mechanism of sorption, characteristic constants of sorption were determined using a pseudo-first order equation of Lagergren based on solid capacity, a first order equation of Bhattacharya and Venkobachar based on solution concentration, and a pseudo-second order equation based on solid phase sorption, respectively.

2.7.2.1 The pseudo-first-order-model

A simple kinetic model for sorption analysis is the pseudo-first-order rate expression of Lagergren in the form:

$$\frac{dq_t}{dt} = k_1(q_e - q_t)$$

...(2.12)

Integrating Equation 2.12 for the boundary conditions $t = 0$ to $t = t$ and $q_t = 0$ to $q_t = q_t$, Equation 2.12 may be rearranged for linearized data plotting as shown by Equation 2.13.

$$\log(q_e - q_t) = \log q_e - \frac{k_1}{2.303}t$$

...(2.13)

Where

k_1 = rate constant of first order sorption (1/min)

q_e = amount of solute sorbed at equilibrium (mg/g)

q_t = amount of solute sorbed on the surface of the sorbent at any time t (mg/g)

t = time (min)

2.7.2.2 The pseudo-second-order-model

The pseudo-second-order rate expression is used to describe chemisorptions involving valency forces through the sharing or exchange of electrons between adsorbent and adsorbate as covalent forces. The rate of pseudo-second-order reaction may be dependent on the amount of solute sorbed on the surface of adsorbent and the amount sorbed at equilibrium. The kinetic rate equations can be written as Equation 2.14

$$\ln(q_e - q_t) = \ln q_e - k_1 t$$

...(2.14)

Where k_2 is pseudo-second-order rate constant (g mg^{-1}h^{-1}). Separating the variables in the Equation 2.14 gives integrating this for the boundary conditions $t = 0$ to t and $q_t = 0$ to q_t gives

$$\frac{t}{q_t} = \frac{1}{k_2 q_e^2} + \frac{t}{q_e}$$

...(2.15)

The advantage of using this model is that there is no need to know the equilibrium capacity from the experiments. In addition, the initial adsorption rate can also be obtained from this model as Equation 2.16.

$$h = k_2 q_e^2$$

...(2.16)

Where h is the initial sorption rate (mg/(g min)).

2.7.3 Adsorption Isotherm (Soonglerdsongpha, 2006)

Adsorption isotherm is an equation that describes how the amount of a substance adsorbed onto a surface depends on its pressure (if a gas) or its concentration (if in a solution), at a constant temperature. Sorption isotherms are plot between the equilibrium adsorption capacity (q) and the final equilibrium concentration of the residual sorbate remaining in the solution (C_e). The equilibrium adsorption capacity, q (mg/g), can be calculated with the Equation 2.17.

$$q = \frac{(C_0 - C_e)V}{m}$$

...(2.17)

Where C_0 is the initial concentration (mg/l), C_e is the residual concentration at equilibrium (mg/l), V is the solution volume (l), and m is the adsorbent mass (g).

The adsorption isotherm relationship can also be mathematically expressed. Langmuir and Freundlich isotherm are the most commonly used for describing relationship.

2.7.3.1 Langmuir Isotherm

Langmuir isotherm relates the coverage or adsorption of molecules on a solid surface to gas pressure or concentration of a medium above the solid surface at a fixed temperature. The equation was developed by Irving Langmuir in 1916. The Langmuir equation is expressed here as:

Langmuir isotherm: $\qquad q = \dfrac{q_m b C_e}{1 + b C_e}$ $\qquad$ ...(2.18)

The Langmuir relationship can be linearized by plotting either $(1/q)$ vs $(1/C_e)$ or (C_e/q) vs. C_e. Where q_m is the maximum adsorption capacity, b is a Langmuir coefficient related to the affinity between the sorbent and sorbate.

$$\frac{1}{q} = \frac{1}{q_m} + \frac{1}{b q_m}\frac{1}{C_e} \qquad ...(2.19)$$
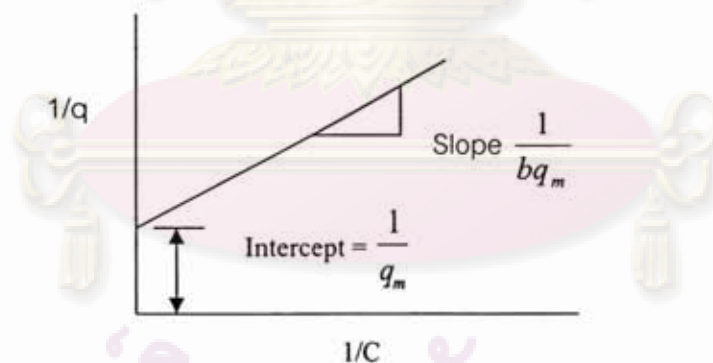
Figure 2.11 The Langmuir isotherm

The Langmuir isotherm considers sorption as a chemical phenomenon. It was first theoretically examined in the adsorption of gases on solid surfaces. Langmuir constant $b = 1/K$ which is related to the energy of adsorption through the Arrhenius equation. The higher b and the smaller K, the higher is the affinity of the sorbent for the sorbate. q_m can also to interpreted as the total number of binding

sites that are available for sorption, and q as the number of binding sites that are in fact occupied by the sorbate at the concentration C_e. Although the Langmuir model sheds no light on the mechanistic aspects of sorption, it provides information on uptake capabilities and is capable of reflecting the usual equilibrium sorption process behavior. Langmuir assumed that the forces that are exerted by chemically unsaturated surface atoms (total number of binding sites) do not extend further than the diameter of one sorbed molecule and therefore sorption is restricted to a monolayer.

In the simplest case, the following hypotheses were made:
  a) The surface of the adsorbent is uniform, that is, all the adsorption sites are equal.
  b) Adsorbed molecules do not interact.
  c) All adsorption occurs through the same mechanism.
  d) At the maximum adsorption, only a monolayer is formed: molecules of adsorbate do not deposit on other, already adsorbed, molecules of adsorbate, only on the free surface of the adsorbent.

Assumption of a value for the surface area covered per molecule then could allow computation of the active specific surface area of the sorbent using Avogadro's number. As long as its restrictions are clearly recognized, the Langmuir equation can be used for describing equilibrium conditions for sorption behavior in different sorbate-sorbent systems, or for varied conditions within any given system.

2.7.3.2 Freundlich Isotherm

The Freundlich Adsorption Isotherm is an adsorption isotherm, which a curve is relating the concentration of a solute on the surface of an adsorbent, to the concentration of the solute in the liquid with which it is in contact.

The Freundlich Adsorption Isotherm is mathematically expressed as shown in equation 2.20:

Freundlich Isotherm: $$q_e = \frac{X}{M} = K_f C_e^{1/n} \qquad \qquad ...(2.20)$$

Where: k = Freundlich coefficient related to the affinity between the sorbent and sorbate

$1/n$ = Freundlich constants related to the concentration dependence

C_e = Equilibrium concentration of adsorbate (mg/l)

M = Weight of adsorbate (g)

q_c = Adsorption capacity (mg/g)

Freundlich model can be easily linearized by plotting it in a (log-log) format.

$$\log\left(\frac{X}{M}\right) = \log K_f + \frac{1}{n} \log C_e \qquad \qquad ...(2.21)$$

$1/n$ = slope of graph

$$K_f = \frac{X}{M} \text{ at } C = 1$$

The Freundlich relationship is an empirical equation. It does not indicate a finite uptake capacity of the sorbent and can thus only be reasonably applied in the low to intermediate concentration ranges. A simple sorption isotherm indicates that the highest fraction of the sorbate species sorbed is observed at the lowest sorbate concentration, corresponding to the steepest past of the isotherm plot. Such behavior is typical of all dissolved species. Stated differently, the lower concentration of a dissolved substance in water, the greater fraction of it will be sorbed on solids. This behavior is typical of trace organic and inorganic substances at µg/l concentrations or lower. However, it is easier to handle mathematically in more complex calculations (e.g. in modeling the dynamic column behavior) where it may appear quite frequently.

2.7.4 Four-region adsorption isotherm of surfactants on the solid–liquid interface (Santanu Paria and Khilar Kartic, 2004)

The typical isotherm of adsorption of surfactants on the solid–liquid interface in a rather wide range of concentration of surfactants going beyond the CMC. In general, a typical isotherm can be subdivided into four regions when plotted on a log–log scale.
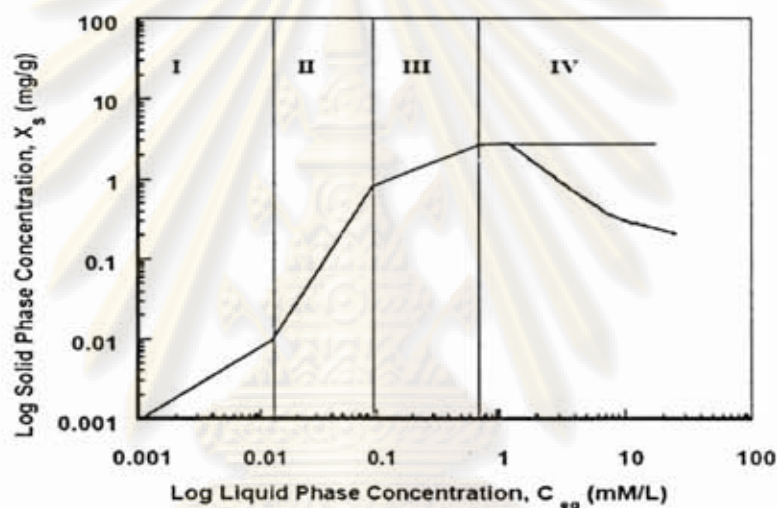
Fig 2.12 Schematic presentation of typical four-regime adsorption isotherm
(Santanu Paria and Khilar Kartic, 2004)

In region I, the adsorption obeys Henry's law, adsorption increases linearly with concentration and the slope of the curve is approximately one. Region I occurs at low concentration of surfactant and monomers are electrostatically adsorbed to the substrate. Region II shows a sudden increase in the adsorption due to lateral interaction between the adsorbed monomer, resulting surface aggregation of the surfactants. Region III shows a slower rate of adsorption than region II. Region IV is the plateau region above the CMC.

2.8 Comparison of sorption Performance (Soonglerdsongpha, 2006)

Performance of sorbing materials often needs to be compared. The simplest case is when there is only one sorbate species in the system. The comparison of single-sorbate sorption performance is best based on a complete single-sorbate sorption isotherm curve. In order for the comparison of two or more sorbents to be 'fair' it must always be done under the same conditions. These may be restricted by the environmental factors under which sorption may have to take place (pH, temperature, ionic strength, etc.). By performance of the sorbent is usually meant its uptake (q). The sorbents can be compared by their respective q_m values which are calculated from fitting the Langmuir isotherm model to the actual experimental data (if it fits). This approach is feasible if there exists the characteristic q_m sorption performance plateau (the maximum sorbent saturation). A 'good' sorbent that one always looks for would feature a high sorption uptake capacity q_m. However, also desirable is a high affinity between the sorbent and sorbate reflected in good uptake values at low concentrations (C_e). This is characterized by a steep rise of the isotherm curve close to its origin. Performance in this region is reflected in the Langmuir coefficient b.

2.9 Regeneration Study

Over the years, a variety of regeneration techniques have been suggested, evaluated and applied. These methods are based either on desorption, induced by increasing temperature or by displacement with a solvent, or on decomposition induced by thermal, chemical, electrochemical or microbial processes. Regeneration of HMSs is also an important issue in HMSs utilization. Because of, synthesized HMSs, which have silicate structure and uniform surface functional group, are suggested to have high affinity for regeneration. Currently, two major regeneration methods have been used, high temperature calcinations for removal of organic and carbon deposits on HMSs and solvent extraction.

CHAPTER III
MATERIALS AND METHODS

3.1 Materials

1. Perfluorooctanoic acid (PFOA) >90% (Solid) (Fluka)
2. Perfluorooctane sulfonate (PFOS) >40% (Solution) (Fluka)
3. Dodecylamine 98% (ACROSS ORGANICS)
4. Tetraethoxysilane 98% (ACROSS ORGANICS)
5. Powder activated carbon (Tosoh Corporation, Japan)
6. 3-aminopropyltriethoxysilane (Fluka)
7. 3-mercaptopropyltrimethoxysilane (Chisso)
8. Dimethyloctylchlorosilane (Fluka)
9. NaY zeolite (Tosoh Corporation, Japan)
10. Ethyl alcohol absolute RPE-ACS (CARLO ERBA)
11. Ammonium nitrate (CARLO ERBA)
12. Potassium persulfate (CARLO ERBA)
13. Potassium nitrate (MERCK)
14. Potassium bromide (MERCK)
15. Sodium hydroxide (LAB SCAN)
16. Sodium chloride (LAB SCAN)
17. Hydrochloric acid 37% (LAB SCAN)
18. Hydrogen peroxide 30% (LAB SCAN)
19. Sulfuric acid 98% (LAB SCAN)
20. Potassium dihydrogenphosphate (Riedel-de-Haen)
21. Dipotassium hydrogenphosphate (Riedel-de-Haen)
22. Potassium hydrogenphthalate (Riedel-de-Haen)
23. Sodium hydrogencarbonate (Riedel-de-Haen)
24. Sodium carbonate (Riedel-de-Haen)

3.2 Instrument

Table 3.1 The entire instruments used in this study

Instrument	Detail
1. Total Organic Carbon (TOC Analysis)	TOC-VCPH, ASI-V SHIMADZU
2. Inductive Couple Plasma (OES)	Perkin Elmer model PLASMA-1000.
3. Microwave digestion and Extraction System	Model : ETHOS SEL, Milestone, Italy
4. Orbital Shaker	PNP, Model NO. : OS-3, Serial NO. : PNP064/48
5. Oven	Model NO. : 400 (E2)
6. Sension 4 pH ISE Meter	Model NO. : 51775-11, Serial NO. : 030700000425, HACH Company
7. Soxhlet Extraction	Model NO. : RE6, Serial NO. : 01501036185, SCIENCETIFIC PROMOTION CO., LTD.
8. Basic Plus Balance (2 Digits)	Model NO. : BP 3100S, Serial NO. : 13006504, Sartorius
9. Basic Plus Balance (4 Digits)	Model NO. : AG204, Serial NO. : 3687-45, Mettler Toledo (Switzerland)
9. UV-Visible Spectrophotometers	Model : Helios Alpha, Serial NO. : UVA 112726
10. Magnetic Stirrer	Model NO. : MSO-3, Serial NO. : 47300, NICKEL ELECTRO LTD.
11. Hotplate	Model NO. : SP131320-33, Serial NO. : 1313041234859
12. Vacuum Pump	Model NO. : NO.26, Serial NO. : 1448740, SCIENCETIFIC PROMOTION CO., LTD.
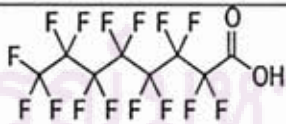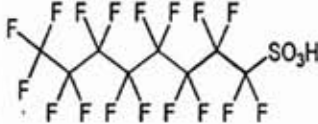
Table 3.1 (cont.) The entire instruments used in this study

Instrument	Detail
13. Incinerator	Model : AAF 11/18/201, SCIENCETIFIC PROMOTION CO., LTD.
14. Water Bath	Model NO. : GFL 1086
15. Distilled Water Distributor	Model : ULTRA ANALYTIC
16. Incubator	Model NO. : BD115
17. Autoclave	Model NO. : HVE-50, HIRAYAMA
18. Hood	Model NO. : MMRI 4230 007 0008 5/1/37
19. Storage Refrigerator	Model NO. : IRI1930A14
20. Incinerator	Model NO. : AAF 11/18/201
21. Scanning Electro Microscope	JSM-6400

3.3 Contaminants

An anionic Perfluorinated compounds (PFCs), Perfluorooctanoic acid (PFOA) and Perfluorooctane sulfonate (PFOS) were chosen as representative compounds. PFOA with a purity of >90% and PFOS with a purity of 40% will be purchased from Fluka Chemica (Switzerland). Their properties are listed in Table 3.2.

Table 3.2 The physical and chemical properties of anionic surfactants (Kissa, 2001)

Surfactant	MW (g/mol)	Chemical Structure	Solubility in water (mg/l)	Appearance	CMC (mg/l)
Perfluorooctanoic acid (PFOA), $CF_3(CF_2)_6COOH$	414.17		3,400	White Powder	15,696
Perfluorooctane sulfonic acid (PFOS), $CF_3(CF_2)_7SO_3H$	500.13		570	Clear liquid	4,573

3.4 Preparation of Adsorbents

3.4.1 HMS Synthesis

Hexagonal Mesoporous Silicate (HMS) was synthesized at an ambient temperature and pressure through the neutral pathway ($S^\circ I^\circ$) (Tanev and Pinnavaia, 1995). This synthesis method makes use of on hydrogen bonding and self-assembles between neutral primary amine self-assembly and neutral inorganic precursors. Dodecylamine (DDA, $CH_3(CH_2)_{11}NH_2$) and tetraethoxysilane (TEOS) were used as the liquid crystal templating (LCT) and silica source, respectively. Moreover, ethanol was used as cosolvent in the following mole ratio.

HMS was prepared by the following method:

1. Mix 29.6 mol of water with 0.27 mol of dodecylamine (DDA) and 9.09 mol of ethanol to form as organic template of HMS.

2. Add 1.0 mol of tetraethoxysilane (TEOS) in the mixture and were then mixed under vigorous stirring.

3. The reaction mixture was aged at an ambient temperature for 18 hrs.

4. The resulting mixture was filtered and air-dried on a glass plate.

5. The product was calcined in air under static condition at 650°C for 4 hrs to remove organic template.

3.4.2 Surface and structure modification methods (Punyapalakul and Takizawa , 2004)

3.4.2.1 Titanium substitution modification

The Ti-substituted HMS, denoted as Ti-HMS, was synthesized following with method reported by Tanev et al., (1994). Synthesis method was prepared following the same protocol as that of HMS, except that adding Ti precursor. In this

study, tetraisopropyl orthotitanate (TIPOT) (TCI-EP, Tokyo, Japan) was selected and mixed with silica precursor (TEOS) with a ratio of TEOS: TIPOT = 100:1. Mixture of silica and titanium precursor was added into mixture of DDA, water and ethanol after stirring for 1 hr.

3.4.2.2 Direct Co-condensation Method of Organic functional groups on HMS

3.4.2.2.1 3-aminopropyltriethoxysilane (APTES)

Silanization with 3-aminopropyltriethoxysilane (APTES), denoted as A-HMS, was prepared by the following method:

1. Mix 50 mol of water with 0.25 mol of dodecylamine and 10.25 mol of ethanol to form as organic template of HMS.

2. Add 1.0 mol of tetraethixysilane (TEOS) in the mixture and were then mixed under vigorous stirring for 30 mins.

3. Then 0.25 mol of 3-aminopropyltriethoxysilane (APTES) was added in the mixture.

4. The reaction mixture was vigorously stirred for 20 hrs at ambient temperature and the resulting were filtered and air-dried on a glass plate for 24 hrs.

5. Residual organosilane and organic template were removed by solvent extraction for 72 hrs with ethanol. Amino functional groups increase hydrophilicity of obtained adsorbent.
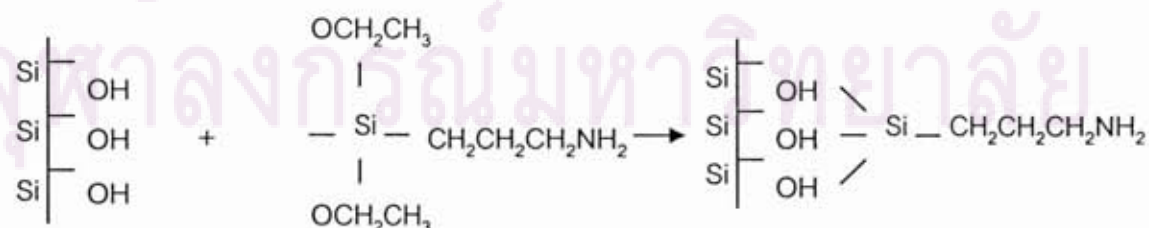
Figure 3.1 Silanization reaction of 3-aminopropyltriethoxysilane (APTES) and HMS (A-HMS)

3.4.2.2.2 3-mercaptopropyltrimethoxysilane (MPTMS)

Silanization with 3-mercaptopropyltrimethoxysilane (MPTMS), denoted as M-HMS, was prepared by the following method:

1. Mix 50 mol of water with 0.25 mol of dodecylamine and 10.25 mol of ethanol to form as organic template of HMS.

2. Add 1.0 mol of tetraethixysilane (TEOS) in the mixture and were then mixed under vigorous stirring for 30 mins.

3. Then 0.25 mol 3-mercaptopropyltrimethoxysilane (MPTMS) was added in the mixture.

4. The reaction mixture was vigorously stirred for 20 hrs at ambient temperature and the resulting were filtered and air-dried on a glass plate for 24 hrs.

5. Residual organosilane and organic template were removed by solvent extraction for 72 hrs with ethanol. Mercapto functional groups increase hydrophobicity of obtained adsorbent.
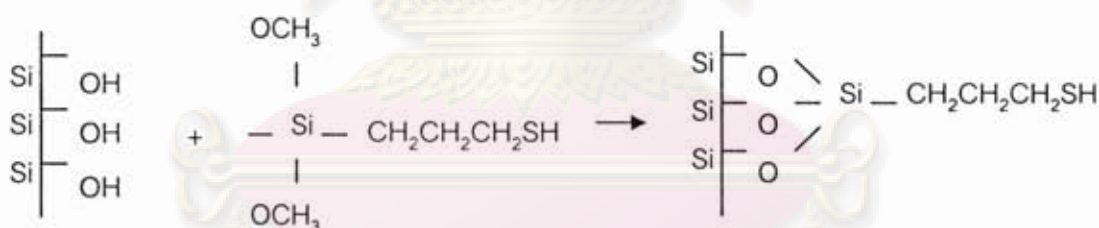
Figure 3.2 Silanization reaction of 3-mercaptopropyltrimethoxysilane (MPTMS) and HMS (M-HMS)

3.4.2.3 Post-grafting method of Organic functional groups on HMS

3.4.2.3.1 Dimethyloctylchlorosilane

Silanization with Dimethyloctylchlorosilane, denoted as OD-HMS, was prepared by the following method:

1. 0.5 g HMS dried in oven at 80°C for 5 hrs and then 120°C for 12 hrs.

2. 0.5 g Dimethyloctylchlorosilane was dissolved in 30 ml toluene.

3. Then 0.5 g HMS after reacting at 80°C for 5 hrs and then 120°C for 12 hrs was added in the mixture.

4. The reaction mixture was vigorously stirred for 24 hrs at room temperature and the resulting were filtered, washed with toluene thoroughly, and dried at 90°C.

5. Dimethyloctylchlorosilane functional groups increase hydrophobicity of obtained adsorbent.
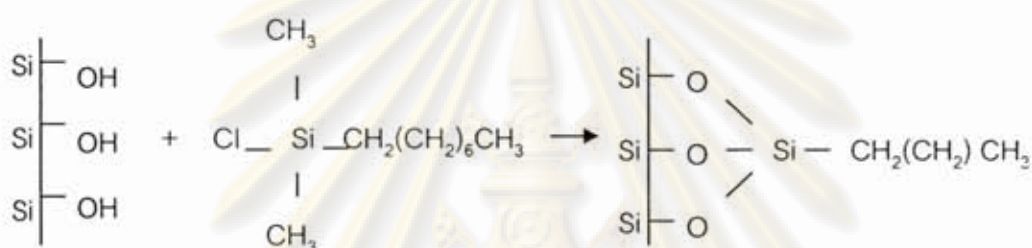
Figure 3.3 Silanization reaction of Dimethyloctylchlorosilane and HMS (OD-HMS)

3.4.3 Preparation of NaY-zeolite and HY-zeolite (Soonglerdsongpha, 2006)

NaY-zeolite was activated by temperature. It was prepared by the following method:

1. Added on evaporating dish and place them into incubator.

2. The temperature of incubator was set at 400°C at a rate of 1°C/min and hold for 3 hrs.

HY-zeolite was prepared by exchanging of sodium ion of NaY zeolite with ammonium ion by the following method:

1. Adding 1 M ammonium nitrate at the solid to liquid ratio of 1:20.

2. The mixture was stirred at 60°C for 2 hrs.

3. Then, the resulting was filtered and washed with Milli-Q water (18.2 MΩ). The experiment was repeated for 2 times.

4. The retentate was dried at 100°C for 12 hrs and calcined at 400°C at a rate of 1°C/min and hold for 3 hrs.

3.5 Physico-Chemical Characterization for Adsorbents

3.5.1 Pore Structure

Crystalline structure of HMS and modified HMSs were determined by Powder X-ray diffraction (XRD) patterns of synthesized adsorbents. XRD patterns were recorded on Powder Diffractometer; Bruker AXS Model D8 Discover equipped with Cu Kα radiation source in the 2θ range 0.35-6°.

3.5.2 Surface Area, Pore volume and Pore Size

Surface area, pore volume and pore size were investigated by nitrogen adsorption isotherm. A sample (ca. 50 mg) was pretreated at 200°C with evacuation at 1.33×10^{-14} Pa for 3 hrs. Nitrogen adsorption-desorption isotherms (BET) were measured at 77 K on a Surface area and Porosity Analyzer Micromeritic model: ASAP 2020 version 1.04H. The BET specific surface areas, S_{BET}, were calculated by using adsorption data in the relative pressure from 0.06 to 0.14. The mesopore volume, V_p, was obtained by using the high-resolution t-plot method. Pore size distributions were calculated from adsorption branches of isotherms using the Barrett-Joyner-Halenda (BJH) formula.

3.5.3 Surface Functional group

Surface functional groups of prepared HMSs were investigated by Fourier Transform Infrared (FT-IR) Spectroscopy Nicolet Impact 410. Before measuring KBr was used as the background and sample mixer (KBr: Sample ratio = 10:1), sample was heated at 110°C for reducing the effect of H_2O at 3,750 and 3,457 cm^{-1}.

3.5.4 Elemental Analysis

3.5.4.1 Analysis of Nitrogen content

The amount of nitrogen in synthesized HMSs was measured by UV adsorption technique. Adsorbents were digested by potassium persulfate ($K_2S_2O_8$) with base condition in autoclave. Chemicals preparations were described as follows:

- Mixture of sodium hydroxide (NaOH) and potassium persulfate was prepared by adding 3 g of potassium persulfate in solution of 4 g NaOH in 100 ml. This solution was newly prepared every time.

- Stock solution (0.1 mg N/ml) for total nitrogen standard curve was prepared by adding 0.722 g of dried potassium nitrate (KNO_3) in Milli-Q water, and made volume to 1,000 ml.

- HCl (1+500) was prepared by mixing of 1 conc.HCl in 500 ml of Milli-Q water, and HCl (1+16) also was prepared by mixing 1 conc.HCl in 16 ml of Milli-Q water.

The experiment method for analysis of nitrogen content was described as follows:

1. Small amount of sample (50mg) was added to autoclave glass bottle, and then 50 ml of Milli-Q water was added.

2. 10 ml of mixture of NaOH and $K_2S_2O_8$ were added into the mixture and autoclaved at 120°C for 30 mins.

3. Then sample was filtered and 25 ml of filtrate was taken.

4. After that, 5 ml of HCL (1+16) were added to adjust pH to 2-3 and filled into 50 ml of colorimetric tube.

5. Sample was diluted to 50 ml by Milli-Q water.

6. All samples were measured by UV spectrophotometer at 220 nm.

7. Blank was prepared by adding 5 ml of HCl (1+500) into Milli-Q water and diluted to 50 ml. Calibration curve was made by following procedure. 10 ml of prepared TN stock solution was taken and diluted ten times to 100 ml. Then 1-15 ml of obtained

solution (0.01 mg N/ml) was added to each colorimetric tube and 5 ml of HCl (1+500) was added to each tube. All of tubes were made volume to 50 ml and measured by UV spectrophotometer with same condition.

8. Amount of TN was plotted against UV-absorbance. TN (mg/g) was calculated by the following equation:

$$TN\ (mg/g) = \{[a \times (60/25)] / b\} \qquad ...(3.1)$$

Where a is amount of TN obtained from calibration curve (mg) and b is amount of synthesized adsorbent (g).

3.5.4.2 Analysis of Sulfur content

The experiment method for analysis of sulfur content was described as follows:

1. Added 0.1 g of sample in Teflon vessel.

2. The synthesized HMSs were digested with 7 ml of HNO_3 65% and 1 ml of H_2O_2 35% in Microwave equipment to analyze the amounts of sulfur.

3. Microwave was temperature-programmed at 240°C in 10 mins and held for 20 mins.

4. After microwave completion, samples were cooled by air until the solution reached room temperature.

5. Filtered and diluted with DI water (18.2 MΩ) in volumetric flask 50 ml.

6. The amounts of sulfur were analyzed by Inductively Coupled Plasma Atomic Emission Spectroscopy (ICP-AES); Perkin Elmer model PLASMA-1000.

3.5.5 Surface Charge

Surface charge of synthesized HMSs and PAC was measured by the acid/base titration method.

1. 10 ml of adsorbents (1 g/l) mixed with a predetermined amount of NaCl for adjustment of initial ionic strength at 0.001 M when diluted to 25 ml.

2. Different amounts of 0.025 M HCl or 0.025 M NaOH were added to HMSs or PAC solutions in order to vary the pH. Intrinsic pH was also measured for each of HMSs or PAC solutions without adding acid or base.

3. Then each sample was diluted to a final volume of 25 ml with Milli-Q water. The ionic strength was adjusted with NaCl solution at 0.01 M when diluted in 25 ml.

4. Then the samples were shaken in shaking water bath at 25±2°C for 24 hrs.

5. Surface charges were calculated from suspension pH of each sample measured after equilibrating from the principle of electro neutrality.

$$\text{Surface charge (C/g)} = \{[HCl]_{add} - [NaOH]_{add} - [H^+] + [OH^-]\} \times 96,500/w \quad ...(3.2)$$

Where $[HCl]_{add}$ = Concentration of HCl were added (mol/l)

$[NaOH]_{add}$ = Concentration of NaCl were added (mol/l)

$[H^+]$ = Concentration of proton (mol/l) calculated from

$pH = -\log[H^+]$

$[OH^-]$ = Concentration of hydroxide ion (mol/l) calculated

from $pOH = -\log[OH^-]$ and $pOH = 14 - pH$

96,500 = Faraday constant (C/mol)

W = Weight of adsorbent (g/l)

3.6 Adsorption Experiments

To study the adsorption experiments, the rest concentration of PFOA and PFOS were analyzed by using Total Organic Carbon (TOC) Analyzer (TOC-VCPH). In order to protect the interference of some organic species dissociate in the solution and cause the stability of obtained TOC value, which come from the reality values of the rest concentration of both PFOA and PFOS in solution. In this step, we also prepared blank

of Milli-Q water and blank of solution by prepared the same way as prepared sample but without addition of solution of PFOA and PFOS. Details of prepared blank method are shown in appendix B.

3.6.1 Adsorption Kinetic

To study the adsorption kinetic of PFOA and PFOS adsorbed onto all adsorbents, the experiment methods were described as follow:

1. The equilibrium contact time for PFOA and PFOS adsorption was performed by varying contact time from 0 to 48 hrs (2 mins, 5 mins, 10 mins, 30 mins, 1 hr, 3 hrs, 5 hrs, 10 hrs, 24 hrs, 30 hrs and 48 hrs) under batch condition at initial PFOA or PFOS concentration of 100 mg/l. Except, on PAC used initial PFOA or PFOS concentration of 300 mg/l and the amount ratio of adsorbent to PFOA or PFOS solution were set at 0.067 g: 200 ml.

2. The initial pH of solution was varied at pH 5, 7 and 9 and fixed ionic strength at 0.01 M by phosphate buffer.

3. Samples were shaken in shaking water bath at 25±2°C, 150 rpm.

4. After that they were filtered by filter paper no.42 and

5. The rest of PFOA and PFOS concentration then were analyzed by using Total Organic Carbon (TOC) Analyzer (TOC-VCPH).

6. The experimental results were fitted to pseudo-first-order and pseudo-second-order kinetic model to evaluate adsorption rate of PFOA and PFOS.

3.6.2 Adsorption Isotherm

To study the adsorption isotherm of PFOA and PFOS adsorbed onto all adsorbents, the experiment methods were described as follow:

1. The PFOA and PFOS adsorption isotherm was performed by varying initial PFOA and PFOS concentration from 25, 50, 75, 100, 200, 300 mg/l under batch condition. Fixed initial pH solution at 7 and ionic strength at 0.01 M by phosphate buffer.

2. The amount ratio of adsorbent to PFOA or PFOS solution was set at 0.01 g: 30 ml. Samples were shaken in shaking water bath at 25±2°C, 150 rpm until equilibrium.

3. After that they were filtered by filter paper no.42

4. The rest of PFOA and PFOS concentration then were analyzed by using Total Organic Carbon (TOC) Analyzer (TOC-VCPH).

5. The experimental results were fitted to Langmuir and Freundlich Equation.

3.6.3 Adsorption mechanism

3.6.3.1 Effect of pH

To study the effect of adsorption mechanism of PFOA and PFOS adsorbed onto all adsorbents, the experiment methods were described as follow:

1. The effect of pH for PFOA and PFOS adsorption was performed by varying initial pH solution at 5, 7 and 9 and the ionic strength was fixed at 0.01 M controlled by phosphate buffer.

2. The PFOA and PFOS adsorption mechanism was performed by varying initial PFOA or PFOS concentration from 25, 50, 75, 100, 200, 300 mg/l under batch condition.

3. The amount ratio of adsorbent to PFOA or PFOS solution was set at 0.01 g: 30 ml.

3. Samples were shaken in shaking water bath at 25±2°C, 150 rpm until equilibrium.

4. Samples were filtered by filter paper no.42.

5. The rest of PFOA and PFOS concentration then were analyzed by using Total Organic Carbon (TOC) Analyzer (TOC-VCPH).

3.7 Analytical Method

A concentration of PFOA and PFOS was determined using Total Organic Carbon (TOC) Analyzer (TOC-VCPH) which is determining the total organic carbon of surfactant. A 20 ml of sample was adding into glass vial for measured. The sample volume injected was 50 µL. The sorption amount was calculated according to the difference of PFOS or PFOA concentrations before and after sorption.

3.8 Regeneration Study (solvent extraction method)

3.8.1 Regenerate efficiency of PFOS

In this study was used the concentration of PFOS adsorbed on HMS, PAC, and hydrophobic functionalized HMSs (M-HMS and OD-HMS) at 300 mg/l. PFOS adsorbed HMS, PAC, M-HMS and OD-HMS were extracted by mixture of solvents and Milli-Q water. Ethanol was chosen for representative solvent for extraction. The recoveries of PFOS adsorbed onto four adsorbents (HMS, PAC, M-HMS and OD-HMS) were described as follow:

1. Ratios of solvents and Milli-Q water were set at 10:0 to 1:9.

2. 0.10 g of PFOS adsorbed onto adsorbents were added in 50 ml of mixtures and stirred at $25\pm2°C$ for 3 hrs.

3. Filtered by filter paper no.42 and air-dried at ambient temperature for 24 hrs.

4. The rest concentration of PFOS were investigated by measured amounts of sulfur which analyzed by Inductively Coupled Plasma Atomic Emission Spectroscopy (ICP-AES).

Extraction efficiency was calculated from:

$$\text{Extraction efficiency (\%)} = 100 \times q / \{W - (10^6 \times W / (S_{max} + 1000))\} \qquad ....(3.3)$$

Where q is extracted PFOS in mg, S_{max} is adsorbed PFOS on adsorbents and W is Weight of used adsorbents.

3.8.2 Effect of ratios of amount of used adsorbents and volume of mixture on PFOS recovery efficiency

To study the effect of ratios of amount of used adsorbents and volume of mixture on PFOS recovery efficiency were described as follow:

1. Suitable ratio of used adsorbents and volume of mixture were varying ratios of amount of used adsorbents and volume of mixture (w/v) from 250 to 8,000.

2. Samples were stirred in water bath at 25±2°C for 3 hrs.

3. Filtered by filter paper no.42 and air-dried at ambient temperature for 24 hrs.

4. The solvent with lowest solvent ratio, which gives highest extraction efficiency, will be chosen for this step.

3.8.3 Reused HMS, functionalized HMSs and PAC efficiencies

PFOS adsorption isotherms of virgin adsorbents and extraction regenerated adsorbents were determined same as previous adsorption isotherm method. Solvents extraction method of all adsorbents was repeated 3 times.

3.8.4 Physico-chemical characteristics of regenerated adsorbents

Physico-chemical characteristics of regenerated adsorbents such as crystalline structure, surface area and pore structure and surface structure were investigated by XRD, nitrogen adsorption isotherms and SEM, respectively.

CHAPTER IV

RESULTS AND DISCUSSION

4.1 Physico-Chemical Characterization

4.1.1 Pore Structure

In this study, HMS and functionalized HMSs with amino-, mercapto- and octyl- functional groups were synthesized by direct co-condensation method and grafting method, respectively. Dodecylamine and TEOS were used as organic template and silica precursor, respectively. APTES, MPTMS and n-Octyl were used for amino-, mercapto- and alkyl groups functionalized HMS. Then organic template was removed by calcinations for HMS and solvent extraction for functionalized HMS. After that, physico-chemical characteristics of synthesized HMSs, zeolites were investigated comparing with PAC. Obtained data were combined with adsorption experiment results for study relationships between physico-chemical characteristics (e.g., crystalline structure, surface characteristics, hydrophilicity, surface charges, etc.) and PFCs adsorption phenomenon.
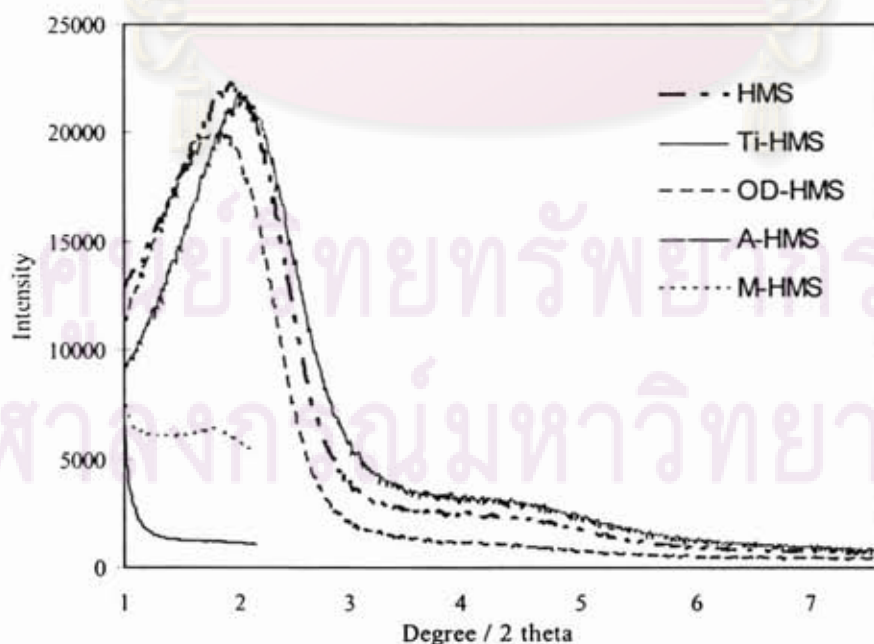
Figure 4.1 XRD patterns of synthesized HMSs

Figure 4.1 presents the X-ray Powder Diffraction (XRD) pattern of all synthesized HMS by showed scale expansion of the 1–8°. Normally, diffraction peak corresponding to the (100) plane at 2θ ~ 2-3°, which is a typical characteristic of HMS materials (Peter *et al.*, 1994; Bagshaw *et al.*, 1995; Tanev and Pinnavaia, 1996; Liu *et al.*, 2006). According to the XRD pattern, synthesized pristine HMS (pure silica HMS) exhibited a strong sharp single diffraction peak corresponding to the (100) plane at 2θ = 2.22° or d-spacing = 4.01 nm and weak diffraction peak corresponding to the (200) plane at 2θ = 4.3° or d-spacing = 2.06 nm as an evidence of the hexagonal crystalline structure which is characteristic of HMS materials (Peter *et al.*, 1994; Bagshaw *et al.*, 1995; Tanev and Pinnavaia, 1996; Liu *et al.*, 2006). Although, crystalline structure of prepared HMS was not complete hexagonal crystalline (comparing with other hexagonal crystalline silicate), which should show an XRD pattern consisting of (100) plane at 2θ ~ 2-3°, (110) plane at 2θ ~ 3.7°, (200) at 2θ ~4.3° and (210) at 2θ ~ 4.6° as diffraction for the hexagonal array of typical HMS material (Peter *et al.*, 1994; Bagshaw *et al.*, 1995; Tanev and Pinnavaia, 1996; Liu *et al.*, 2006). XRD pattern of titanium substituted HMS (Ti-HMS) showed a little bit shifting from XRD pattern of pristine HMS of strong diffraction peak corresponding to the (100) plane at 2.32° or d-spacing = 3.80 nm and weak diffraction peak corresponding to the (200) plane at 4.3° or d-spacing = 2.06 nm. For XRD pattern of organic functional group grafted HMS (OD-HMS) by post-grafting method showed strong diffraction peak corresponding to the (100) plane 2.12° or d-spacing = 4.16 nm and weak diffraction peak corresponding to the (200) plane at 4.3° or d-spacing = 2.06 nm. However, XRD pattern of functionalized HMS (A-HMS and M-HMS) indicated that crystalline structure was lost by co-condensation method compared with pristine HMS result.

4.1.2 Surface Area and Pore Size

The Barrett-Joyner-Halenda (BJH) model was used for calculated of pore size distributions of materials. The BET surface areas, pore volumes, and pore size

distributions of PAC, HMS, functionalized HMSs, NaY and HY zeolite are shown in Table 4.1.

Table 4.1 BET surface area, pore volume, and pore diameter of PAC, HMS, functionalized HMSs, NaY and HY zeolite

Adsorbents	Pore diameter (nm)	BET Surface Area (m^2/g)	Pore volume (mm^3/g)	pH$_{zpc}$	Surface functional groups	Surface characteristic
HMS	2.60	712	773	4.00-6.00	Silanol	Hydrophilic
A-HMS	3.95	262	147	8.80	Amino, Silanol	Hydrophilic
M-HMS	2.48	912	433	3.97-6.14	Mercapto, Silanol	Hydrophobic
OD-HMS	2.36	476	499	4.01	Octyl , Silanol	Hydrophobic
Ti-HMS	3.18	766	1276	7.39	Silanol	Hydrophilic
NaY-zeolite	0.74	653	326	6.57	Na$^+$	Hydrophilic
HY-zeolite	0.74	370	201	4.08	Brönsted acid	Hydrophilic
PAC	1.90	980	276	6.87	Carboxyl, Phenyl and others	Hydrophobic

The BET surface area of PAC, HMS, A-HMS, M-HMS, OD-HMS, Ti-HMS, NaY and HY zeolite were found to be 980, 712, 262, 912, 476, 766, 653 and 370 m^2/g, respectively. The obtained result indicated that the specific surface area of PAC was higher than other adsorbents. Furthermore, the results showed that specific surface areas of organosilane functionalized HMSs were decreased due to pre-grafting of organic functional group affected the structure of mesoporous silicate, which was indicated by decrease of BET surface area, especially amino functional groups. However, titanium substitution modification increased both pore diameter and surface area. Although, specific surface area of M-HMS is larger than HMS, pore volume of M-HMS indicated internal surface of M-HMS was affected and confirmed disorder of mesostructure.

From data in Table 4.1, average pore size of PAC, HMS, A-HMS, M-HMS, OD-HMS, Ti-HMS, NaY and HY zeolite calculated by BJH model was 1.90, 2.60, 3.95, 2.48, 2.36, 3.18 and 0.74 nm, respectively. This result showed that A-HMS had largest pore sized, followed by Ti-HMS, HMS, M-HMS, OD-HMS, PAC, NaY and HY zeolite, respectively. Except NaY and HY zeolite, PAC had smallest pore size including pore volume in microporous structure, which was consistency with many research studies. For HMS and functionalized HMSs, their average pore sizes were in the range of 2-50 nm, which indicated the mesoporous structures. Moreover, presence of organo-functional groups on HMS affected to the average pore size. For example, mercaptopropyl groups on M-HMS exhibited a smaller pore size than pristine HMS. However, A-HMS and Ti-HMS exhibited the larger average pore size than pristine HMS. It can be concluded that presence of amino-functional groups can cause the collapse of hexagonal mesostructure. Average pore size of HY zeolite was in micropore scale as well as NaY.

4.1.3 Surface Functional Groups

Surface functional groups of HMS and functionalized HMSs were investigated by Fourier Transform Infrared (FT-IR) Spectroscopy. It deals with the vibration of chemical bonds in a molecule at various frequencies depending on the elements and types of bonds. In this experiment the FT-IR spectra was used to confirm functional groups on adsorbents surface which loaded during synthesis of functionalized HMSs. The FT-IR spectra of HMS and functionalized HMSs were illustrated in Figures 4.2-4.6.

FT-IR spectra of HMS and functionalized HMSs. HMS exhibit O-H stretching peak at wave number of 3,746 cm^{-1} (Partiff et al., 1983). It indicates that it have silanol groups on surface of materials. Particularly, HMS shows the highest percent transmittance of FT-IR spectra. It might be telling that it has more silanol groups than

others. The presence of silanol groups on HMS surface cause the hydrophilicity characteristic.

FT-IR of A-HMS had very weak peak at around 2,861-2,969 cm^{-1} (Brunel et al., 1995), which evidences the presence of CH$_2$ and CH$_3$ functional group in 3-aminopropyltriethoxy structure. However, broad peak of hydrogen bonded N-H groups at 3,315-3,484 cm^{-1} (Partiff et al., 1983) was detected. The presence of amino functional groups was proved by TN detection method. However, hydrophilicity of A-HMS can be confirmed by presence of peak at 3,315-3,484 cm^{-1} (Partiff et al., 1983), which is due to hydrogen bonding of N-H functional groups.

FT-IR spectrum of Ti-HMS had the same peaks as HMS spectrum, except for higher intensity of peak at 992 cm^{-1} (Ahn et al., 1999; Blasco et al., 1995), due to Ti-O bonding. Unfortunately, the peak of Ti-O bonding at 992 cm^{-1} is close to the peak of Si-OH functional group at 830 cm^{-1} (Roy et al., 1996; Carrado et al., 2000; Wang et al., 1999) and cannot be separated from each other completely. Hence, some previous studies commended that the other method might be suitable for confirmation of the presence and bonding of Ti in the framework such as UV-VIS spectrophotometer and ICP-AES with digestion. A very sharp and high intensity peak at 3,746 cm^{-1} (Partiff et al., 1983) is due to free hydroxyl group of silanol groups on surface, which indicates hydrophilic characteristic of Ti-HMS.

FT-IR spectrum of M-HMS confirmed the presence of grafted organic moieties results by peaks around 2,921 cm^{-1} (Brunel et al., 1995). The peak of S-H functional group in M-HMS is a very weak peak (around 2,560 cm^{-1}), but it can be used for providing the presence of S-H because there are not so many peaks of other functional groups around the peak of S-H functional group. In addition, the peak detected at 3,412 cm^{-1} (Partiff et al., 1983) is due to residual inaccessible silanol groups, which are inaccessible to 3-mercaptopropyl silylation reaction.

OD-HMS has a group of peaks between 2,930-2,965 cm^{-1} due to C-H stretching of CH_2 and CH_3 (Brunel *et al.*, 1995). Furthermore, drastic decreasing of peaks of both free and bonded hydroxyl group at 3,746 and 3,482 cm^{-1} (Partiff *et al.*, 1983) evidences significant increasing of hydrophobic characteristics of OD-HMS, which was caused by grafted organic functional groups. Hence, presence of dimethyloctylchlorosilane functional groups on OD-HMS was confirmed.
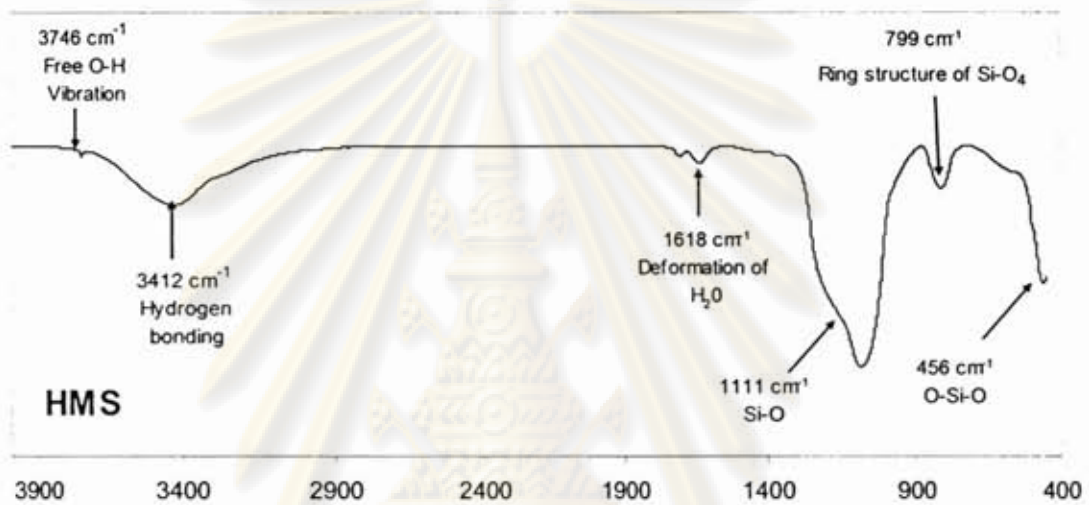
Figure 4.2 FT-IR spectrum of HMS
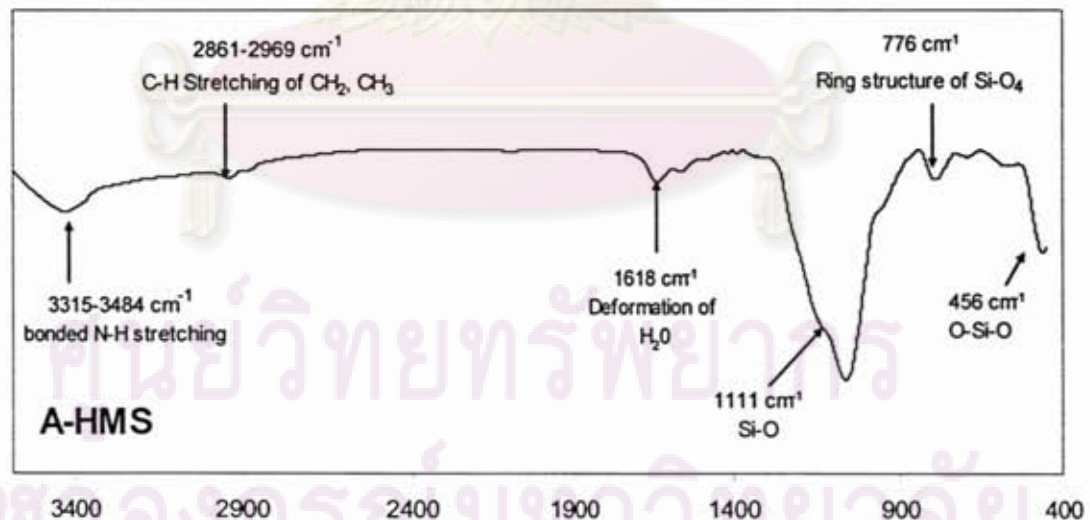
Figure 4.3 FT-IR spectrum of A-HMS
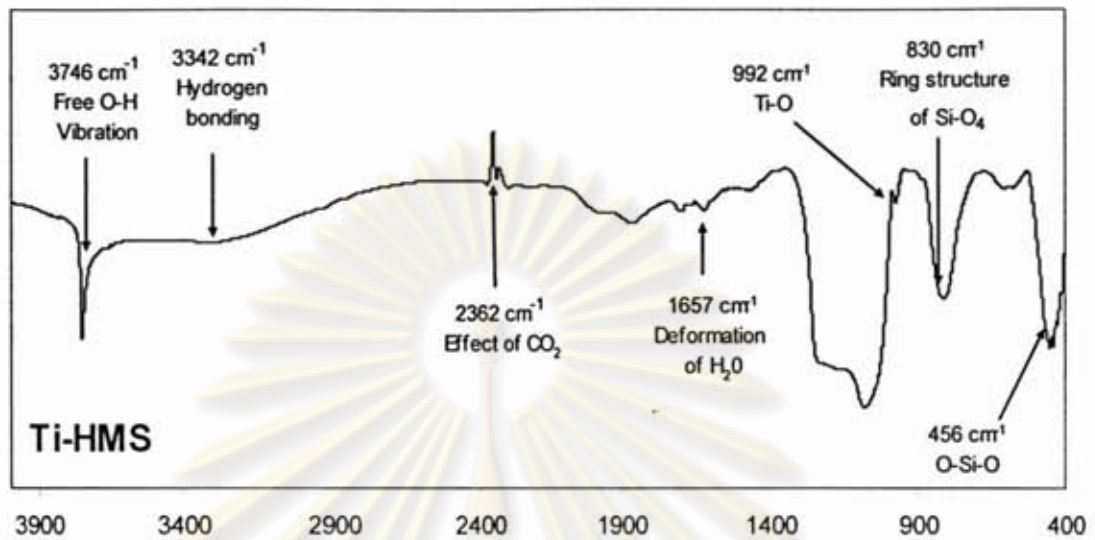
Figure 4.4 FT-IR spectrum of Ti-HMS
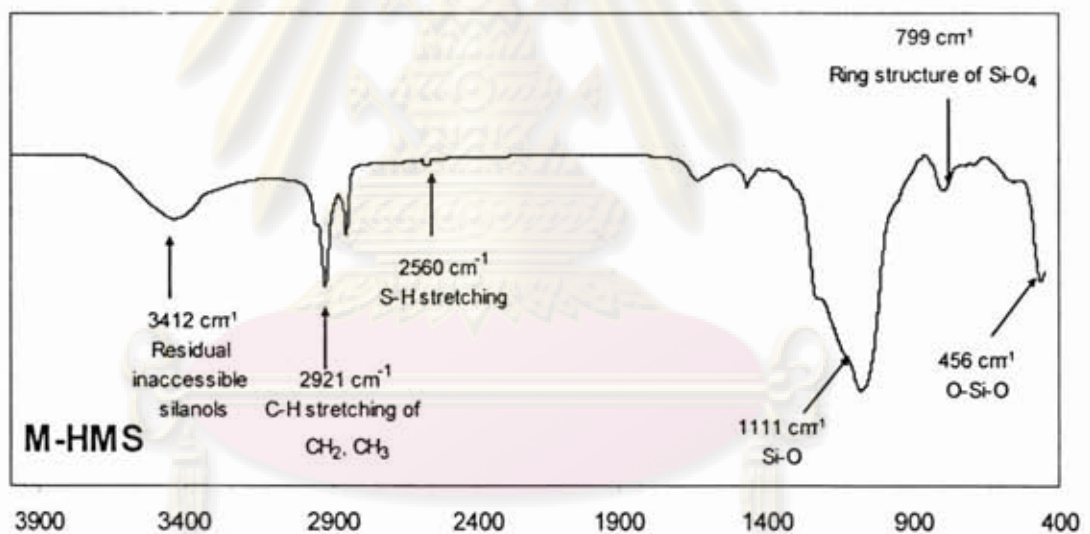
Figure 4.5 FT-IR spectrum of M-HMS
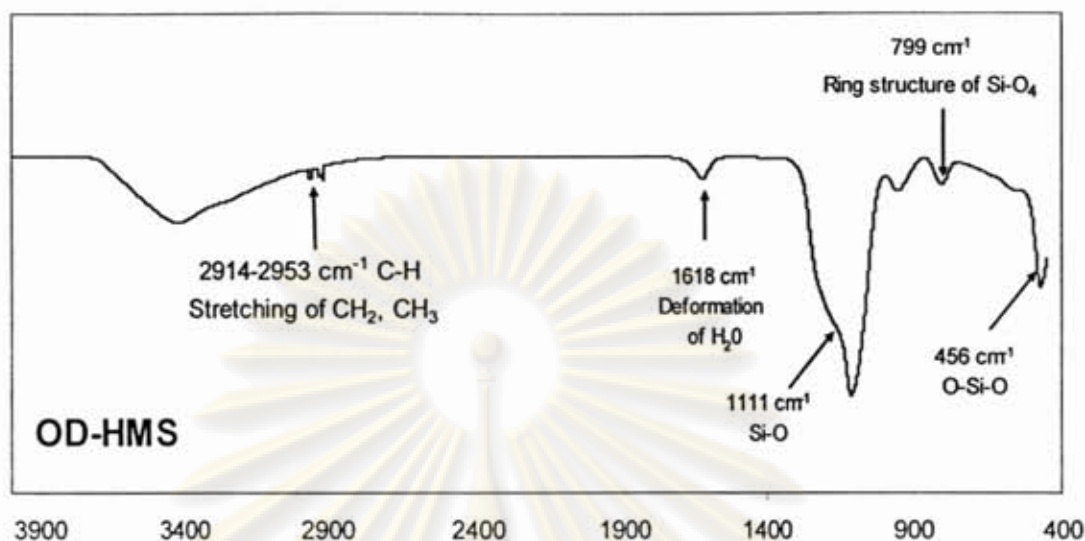
Figure 4.6 FT-IR spectra of OD-HMS

4.1.4 Elemental Analysis

In addition to the evidence given by FT-IR spectra, amount of N and S in A-HMS and M-HMS were investigated for confirming the presence of N and S. Autoclave digestion by potassium persulfate ($K_2S_2O_8$) in alkaline condition was conducted for quantitative nitrogen analysis. Inductively Coupled Plasma Atomic Emission Spectroscopy (ICP-AES) technique was applied for S quantification. Pure silicate HMS was also investigated as a blank sample. Amount of N in A-HMS was quantified as 1.48%. S in M-HMS was detected as 9.92%. Obtained results and combination with FT-IR spectra of A-HMS and M-HMS can confirmed the presence of amino and mercapto functional groups on the surfaces of A-HMS and M-HMS, respectively.
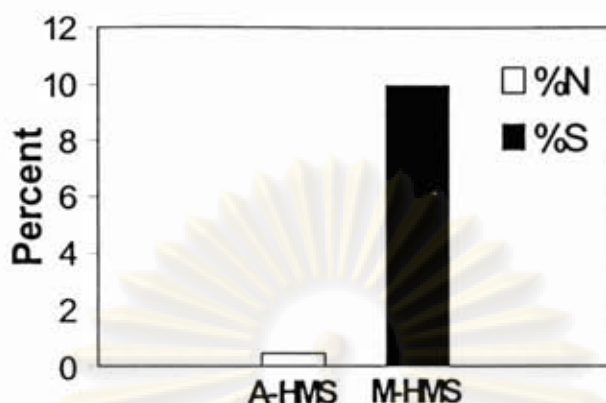
Figure 4.7 Total nitrogen and sulfur content in functionalized HMSs (%w/w)

4.1.5 Surface Charge

Acid/base titration technique was used to determine the surface charge of materials. The ionic strength was fixed at 0.01 M by NaCl solution. After equilibrium, pH of solutions were measured and plotted against surface charges. Surface charges were calculated from the principle of electroneutrality as shown in Equation 4.1.

$$\text{Surface charge (C/g)} = \{[HCl]_{add} - [NaOH]_{add} - [OH^-]\} \times 96,500/W \quad \ldots(4.1)$$

Where $[HCl]_{add}$ = Concentration of HCl were added (mol/l)

$[NaOH]_{add}$ = Concentration of NaCl were added (mol/l)

$[H^+]$ = Concentration of proton (mol/l) calculated from pH = -log[H$^+$]

$[OH^-]$ = Concentration of hydroxide ion (mol/l) calculated from pOH = -log[OH$^-$] and pOH = 14-pH

96,500 = Faraday constant (C/mol)

W = Weight of adsorbent (g/l)

The surface charge density of PAC, HMS, Ti-HMS, A-HMS, M-HMS, OD-HMS, NaY and HY zeolite as function of pH are shown in Figures 4.8-4.9.
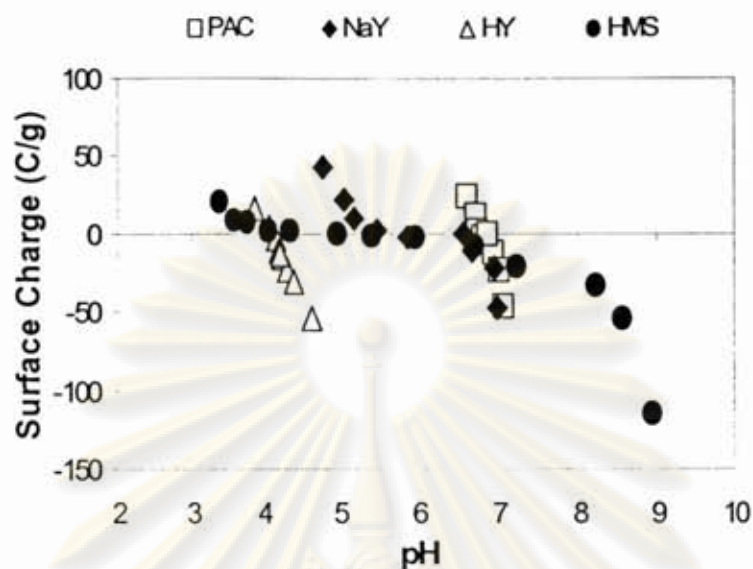
Figure 4.8 Surface charge of PAC, NaY and HY zeolite as a function of pH
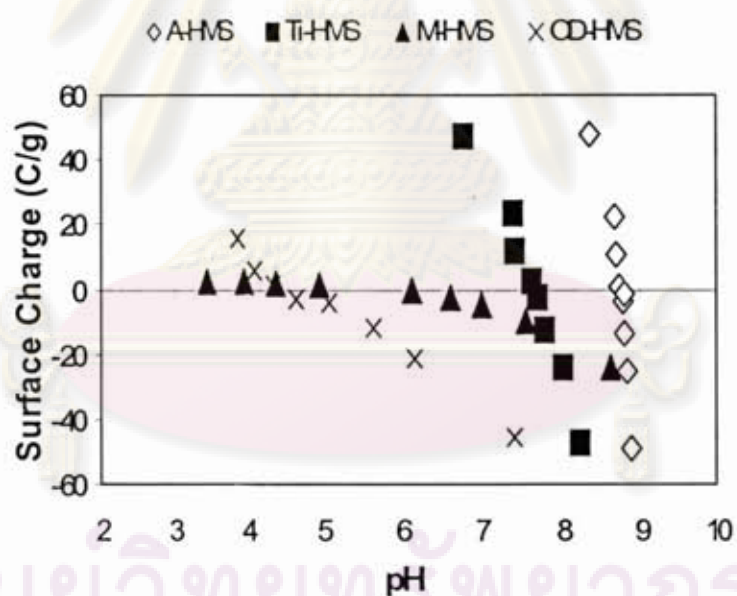
Figure 4.9 Surface charge of functionalized HMS as a function of pH

Figures 4.8-4.9 show the surface charge density of applied adsorbents as function of pH. The pH value that gives zero surface charge is defined as the zero point of charge (pH_{zpc}). pH_{zpc} of all adsorbents was summarized in Table 4.2.

At this pH value, the positive charge of cationic surface groups and the negative charge of anionic surface groups are balanced. As shown in Figures 4.8-4.9, the surface charge density decreases as the pH increase from acidic region to neutral pH. The silanol groups on the surface of HMSs gain or lose protons, resulting in surface charge variation at different pH as shown in the following equation. At low pH, surface sites of HMSs were protonated and the surfaces become positively charged; whereas at a high pH, the surface hydroxides lose their protons, and the surface becomes negatively charged.

1) Silanol group

$pH < pH_{zpc}$: $\equiv Si - OH + H^{+} \longrightarrow \equiv Si - OH_2^{+}$

$pH > pH_{zpc}$: $\equiv Si - OH + OH^{-} \longrightarrow \equiv Si - O^{-} + H_2O$

2) Amino- group

$pH < pH_{zpc}$: $\equiv Si - NH_2 + H^{+} \longrightarrow \equiv Si - NH_3^{+}$

$pH > pH_{zpc}$: $\equiv Si - NH_2 + OH^{-} \longrightarrow \equiv Si - NH_2 + OH^{-}$

3) Mercapto- group

$pH < pH_{zpc}$: $\equiv Si - SH + H^{+} \longrightarrow \equiv Si - SH_2^{+}$

$pH > pH_{zpc}$: $\equiv Si - SH + OH^{-} \longrightarrow \equiv Si - SH + OH^{-}$
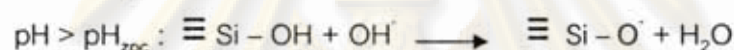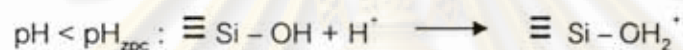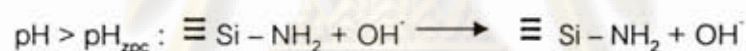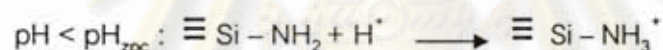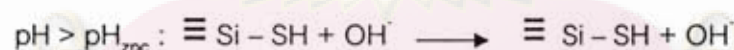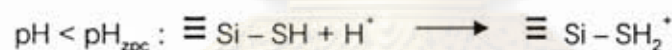
Table 4.2 pH_{zpc} of PAC, HMS, Ti-HMS, A-HMS, M-HMS, OD-HMS, NaY and HY zeolite

Adsorbents	pH_{zpc}
PAC	6.87
HMS	4.00-6.00
Ti-HMS	7.39
A-HMS	8.80
M-HMS	3.97-6.14
OD-HMS	4.36
NaY zeolite	6.57
HY zeolite	4.08

The amino-functional groups presented on HMS gave a higher pH_{zpc} than pristine HMS and M-HMS due to the presence of amino functional group was highly protonated and become positively charges on surface. Furthermore, surface charge of HMS did not change significantly at pH in range of 4.00-6.00. HMS and M-HMS exhibited nearly zero charge (pH_{zpc}) in the range of pH at 3.97-6.14, while PAC showed neutral charge at pH around 7. On the contrary, the surface of OD-HMS had strong negatively charges at the pH solution higher than 4.36. Therefore, it might be indicated that different kinds of grafting organic functional groups grafted on the surface of adsorbents can be also affected to cause differentiation of pH_{zpc} value in each adsorbents.

4.2 Adsorption Kinetic

From Figures 4.10-4.12 showing the adsorption kinetics of PFOA and PFOS on the eight adsorbents including the PAC, HMS, A-HMS, M-HMS, OD-HMS, Ti-HMS, NaY and HY zeolite. The obtained results demonstrated that all the adsorption processes were time dependent. Their kinetic profiles showed quite same by the adsorption of PFOA and PFOS onto all adsorbents and at different pH were achieved equilibrium stage time after at least 10 hrs. The adsorption of PFOA and PFOS onto all adsorbents showed increase dramatically in first 30 minutes and reached equilibrium stage around 10 hrs. However, from the kinetic rates data were indicated that PAC had faster initial adsorption rate comparing with synthesized HMSs and zeolite, which might be caused by surface functional group complexity and its large surface area. However, pH did not affect to contact time for adsorption of PFOA and PFOS on all adsorbents.
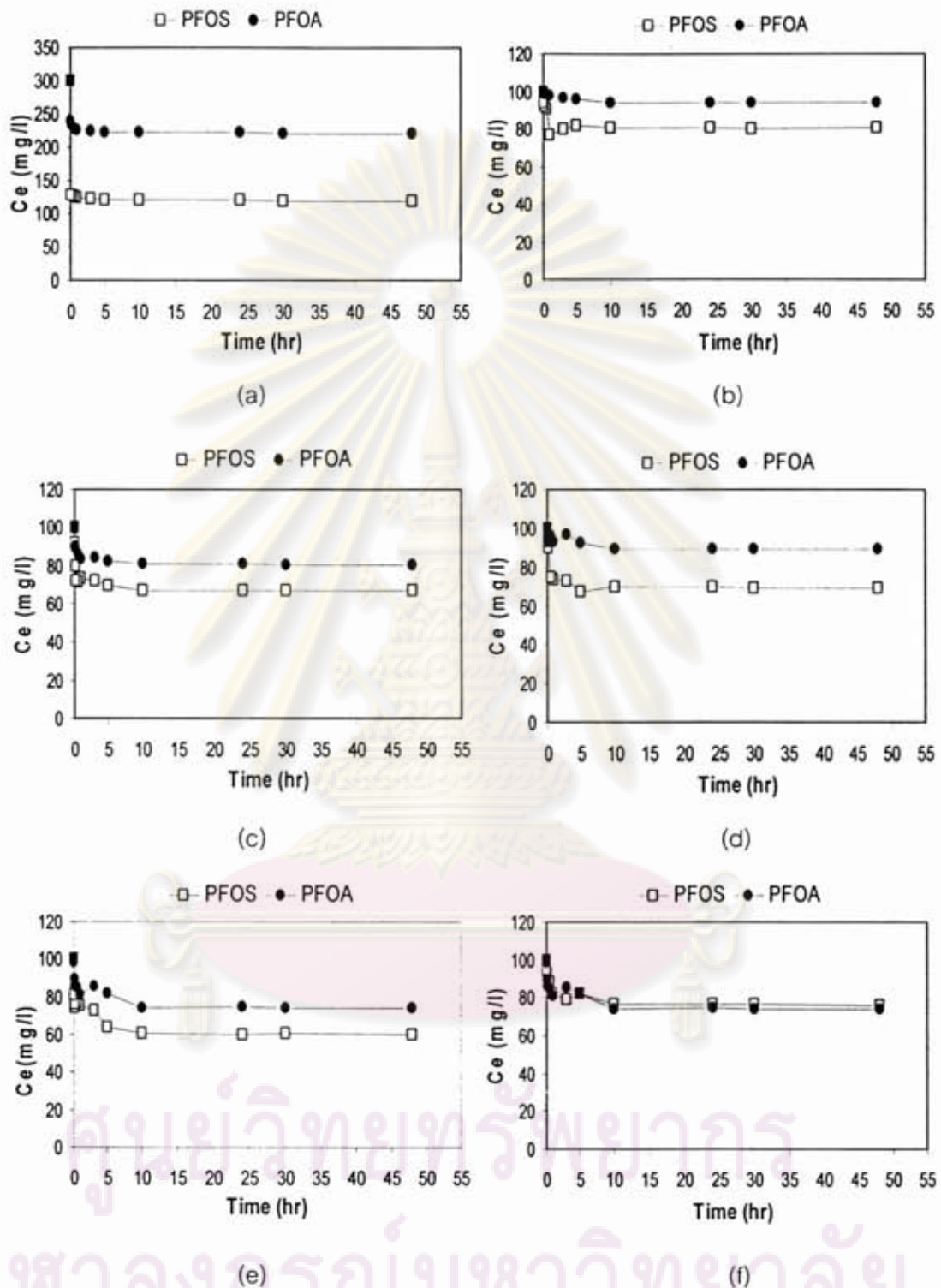
Figure 4.10 Adsorption kinetic of PFOA and PFOS adsorption onto (a) PAC, (b) HMS, (c) A-HMS, (d) M-HMS, (e) OD-HMS, (f) Ti-HMS, (g) NaY and (h) HY zeolite at initial pH solution 5, ionic strength 0.01 M, temperature 25±2 °C
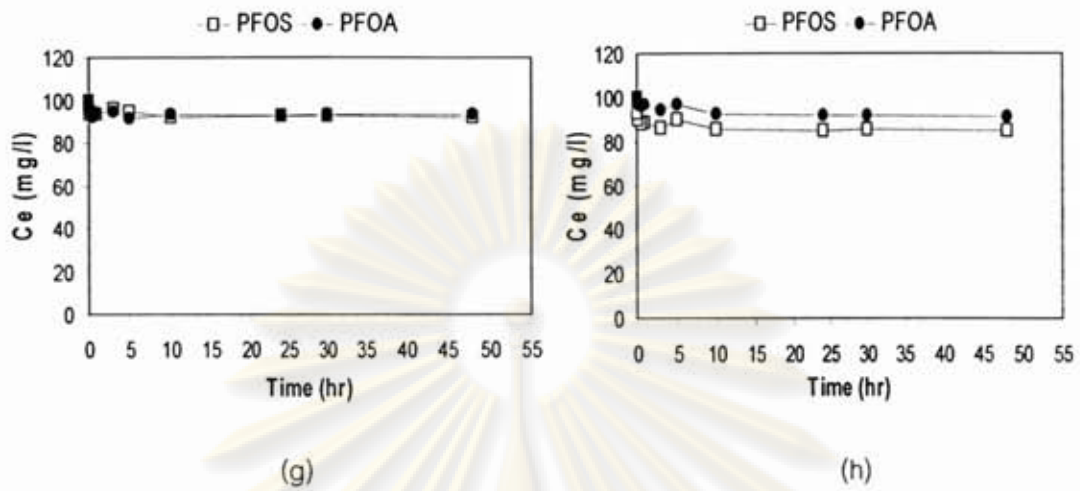
Figure 4.10 (cont.) Adsorption kinetic of PFOA and PFOS adsorption onto (a) PAC, (b) HMS, (c) A-HMS, (d) M-HMS, (e) OD-HMS, (f) Ti-HMS, (g) NaY and (h) HY zeolite at initial pH solution 5, ionic strength 0.01 M, ternperature 25±2 °C
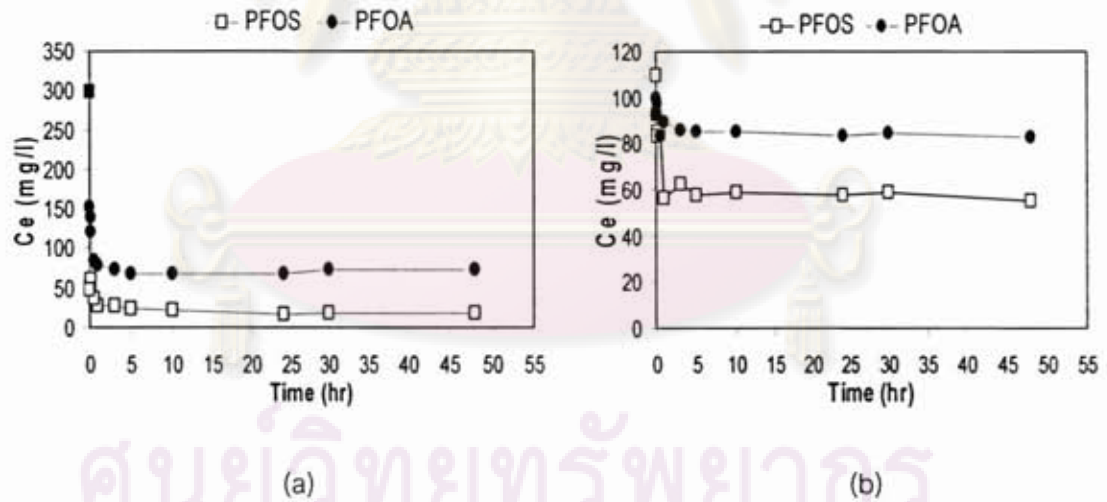
Figure 4.11 Adsorption kinetic of PFOA and PFOS adsorption onto (a) PAC, (b) HMS, (c) A-HMS, (d) M-HMS, (e) OD-HMS, (f) Ti-HMS, (g) NaY and (h) HY zeolite at initial pH solution 7, ionic strength 0.01 M, temperature 25±2 °C
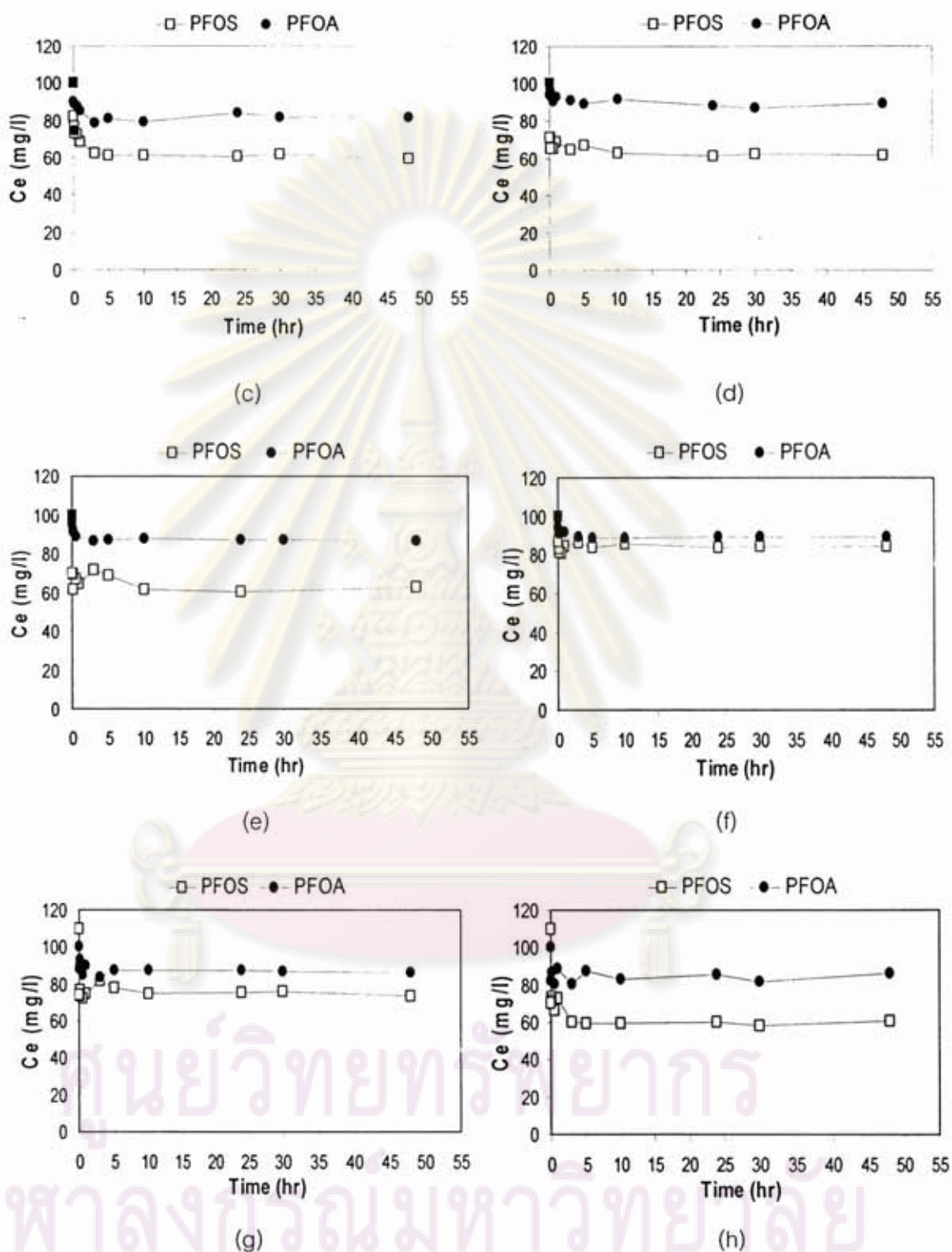
Figure 4.11 (cont.) Adsorption kinetic of PFOA and PFOS adsorption onto (a) PAC, (b) HMS, (c) A-HMS, (d) M-HMS, (e) OD-HMS, (f) Ti-HMS, (g) NaY and (h) HY zeolite at initial pH solution 7, ionic strength 0.01 M, temperature 25±2 °C
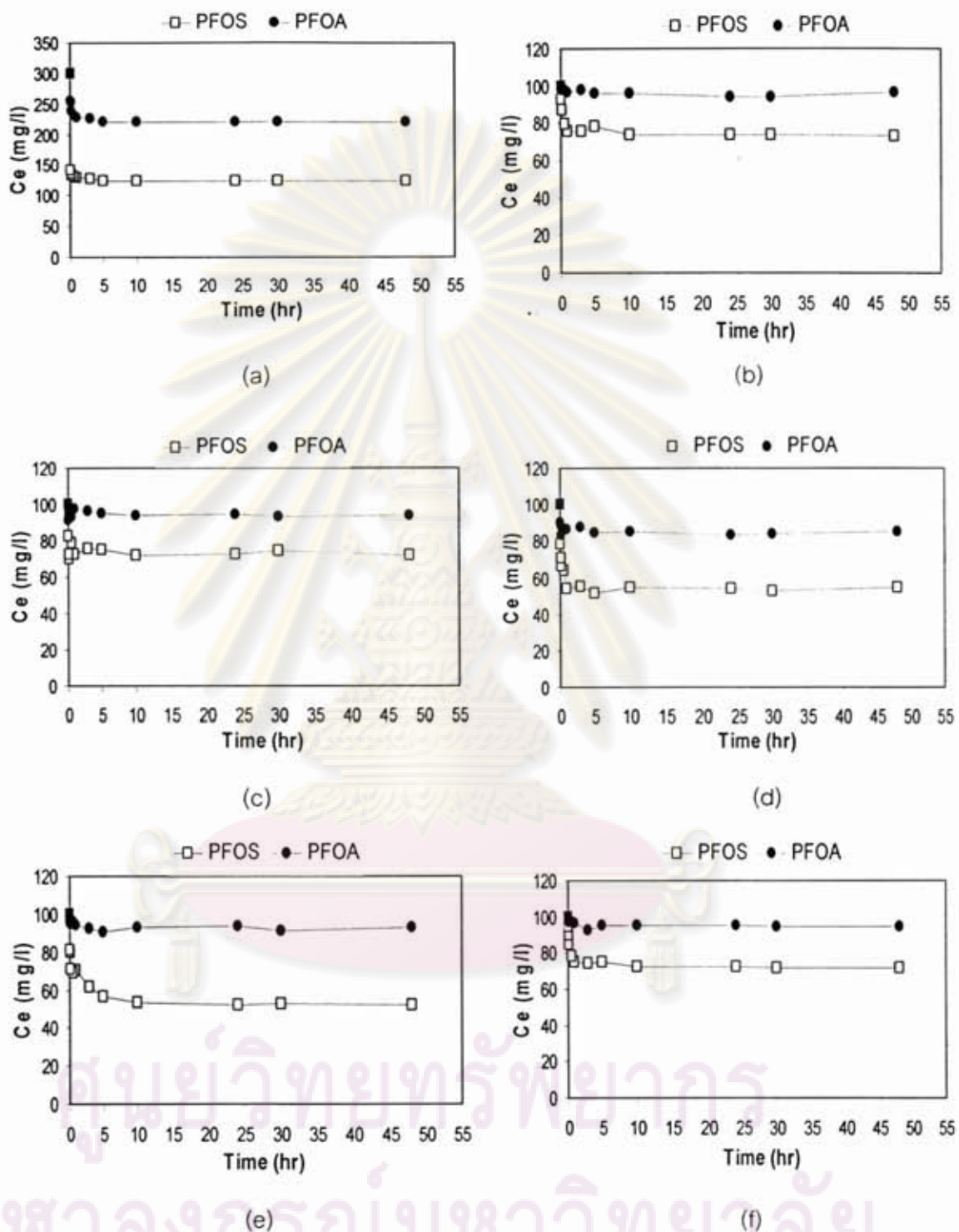
Figure 4.12 Adsorption kinetic of PFOA and PFOS adsorption onto (a) PAC, (b) HMS, (c)

A-HMS, (d) M-HMS, (e) OD-HMS, (f) Ti-HMS, (g) NaY and (h) HY zeolite at initial pH

solution 9, ionic strength 0.01 M, temperature 25±2 °C
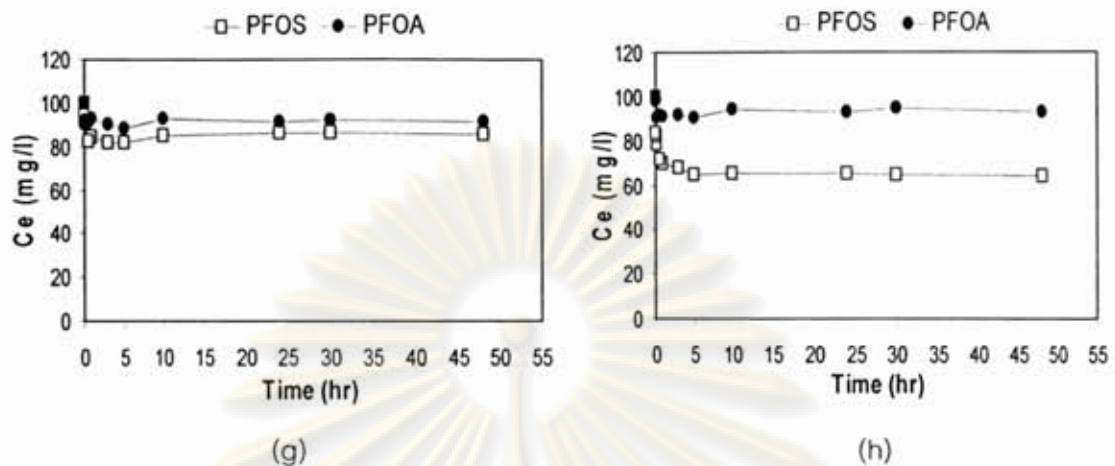
Figure 4.12 (cont.) Adsorption kinetic of PFOA and PFOS adsorption onto (a) PAC, (b) HMS, (c) A-HMS. (d) M-HMS, (e) OD-HMS, (f) Ti-HMS, (g) NaY and (h) HY zeolite at initial pH solution 9, ionic strength 0.01 M, temperature 25±2 °C

To further understand the adsorption kinetics, the pseudo-first-order equation of Lagergren and the pseudo-second-order rate were evaluated base on the experimental data. The pseudo-first-order and pseudo-second-order kinetic model are expressed as Equation 4.2 and Equation 4.3, respectively.

$$\ln(q_e - q_t) = \ln q_e - k_1 t \qquad \ldots(4.2)$$

$$\frac{t}{q_t} = \frac{1}{k_2 q_e^2} + \frac{t}{q_e} \qquad \ldots(4.3)$$

Where k_1 = Lagergren rate constant (min^{-1})

k_2 = Pseudo-second-order rate constant (g mg^{-1} min^{-1})

q_e = Amounts of PFOA and PFOS sorbed at equilibrium (mg/g)

q_t = Amounts of PFOA and PFOS sorbed at time t (mg/g)

t = Time (min)

The experimental data were plotted $\ln(q_e - q_t)$ versus time for first-order-rate and plotted t/q_t versus time for second-order rate. The kinetic constants of adsorbents were

calculated and listed in Tables 4.3 to 4.8. Details of calculation method of pseudo first order model and pseudo second order model are shown in appendix B.

Table 4.3 Kinetics values calculated for PFOA adsorption onto PAC, HMS, functionalized
HMSs, NaY and HY zeolite at initial pH solution 5

Adsorbent	Pseudo First-order				Pseudo Second-order				
	R^2	k_1 (h^{-1})	Calculated q_e (mg/g)	Experimental q_e (mg/g)	R^2	k_2 (g/mg h)	Calculated q_e (mg/g)	Experimental q_e (mg/g)	h (mg/g h)
PAC	0.6378	0.5113	50.83	236.32	1.0000	0.0002	236.12	236.32	12.33
HMS	0.9103	0.2073	14.32	17.93	0.9977	0.0029	18.31	17.93	0.97
A-HMS	0.6045	0.1244	20.83	57.71	0.9995	0.0007	57.97	57.71	2.39
M-HMS	0.7807	0.1105	21.93	32.38	0.9861	0.0081	32.96	32.38	8.84
OD-HMS	0.9022	0.1382	46.04	77.64	0.9973	0.0002	78.70	77.64	1.30
Ti-HMS	0.8233	0.0967	22 63	38.57	0.9985	0.0013	38.51	38.57	1.86
NaY	0.6462	0.0553	15.48	41.71	0.9993	0.1708	20.83	20.82	74.11
HY	0.8740	0.0829	16.71	25.81	0.9976	0.0018	25.60	25.81	1.17

Table 4.4 Kinetics values calculated for PFOS adsorption onto PAC, HMS, functionalized
HMSs, NaY and HY zeolite at initial pH solution 5

Adsorbent	Pseudo First-order				Pseudo Second-order				
	R^2	k_1 (h^{-1})	Calculated q_e (mg/g)	Experimental q_e (mg/g)	R^2	k_2 (g/mg h)	Calculated q_e (mg/g)	Experimental q_e (mg/g)	h (mg/g h)
PAC	0.5342	1.0364	113.82	540.50	1.0000	0.0001	539.78	540.49	38.46
HMS	0.7606	0.1658	30.33	58.74	0.9993	0.0013	58.73	58.74	4.3169
A-HMS	0.8383	0.4836	63.61	98.13	0.9997	0.0006	98.41	98.12	5.5208
M-HMS	0.6612	0.1519	35.92	92.25	0.9996	0.0007	91.83	92.25	5.9468
OD-HMS	0.7344	0.3178	63.67	118.54	0.9985	0.0002	119.43	118.53	2.6051
Ti-HMS	0.8543	0.3455	46.64	71.38	0.9979	0.0004	71.60	71.38	2.1926
NaY	0.8980	0.0829	14.41	22.96	0.9909	0.0041	22.18	22.96	1.9944
HY	0.7052	0.0829	18.90	44.64	0.9938	0.0017	44.04	44.64	3.2329

Table 4.5 Kinetics values calculated for PFOA adsorption onto PAC, HMS, functionalized HMSs, NaY and HY zeolite at initial pH solution 7

Adsorbent	Pseudo First-order				Pseudo Second-order				
	R^2	k_1 (h^{-1})	Calculated q_e (mg/g)	Experimental q_e (mg/g)	R^2	k_2 (g/mg h)	Calculated q_e (mg/g)	Experimental q_e (mg/g)	h (mg/g h)
PAC	0.9557	2.3352	165.38	449.26	0.9999	0.0007	450.46	449.26	144.64
HMS	0.5366	0.0691	6.32	13.83	0.9983	0.0187	12.86	13.83	3.10
A-HMS	0.4843	0.0553	23.21	55.41	0.9985	0.0044	56.00	55.41	13.88
M-HMS	0.5972	0.1520	16.14	32.38	0.9870	0.0017	34.96	32.38	2.07
OD-HMS	0.4001	0.0829	17.03	68.08	0.9977	0.0285	68.26	68.08	133.00
Ti-HMS	0.6995	0.7185	13.37	32.73	0.9996	0.0381	32.35	32.73	39.91
NaY	0.3509	0.0553	3.39	11.17	0.9983	0.2399	10.37	11.17	25.82
HY	0.6615	0.3593	6.15	11.09	0.9941	0.1010	11.76	11.09	13.96

Table 4.6 Kinetics values calculated for PFOS adsorption onto PAC, HMS, functionalized HMSs, NaY and HY zeolite at initial pH solution 7

Adsorbent	Pseudo First-order				Pseudo Second-order				
	R^2	k_1 (h^{-1})	Calculated q_e (mg/g)	Experimental q_e (mg/g)	R^2	k_2 (g/mg h)	Calculated q_e (mg/g)	Experimental q_e (mg/g)	h (mg/g h)
PAC	0.4810	0.2625	62.70	486.33	1.0000	0.0001	486.92	486.33	17.73
HMS	0.3061	0.0691	11.85	43.46	0.9995	0.0043	41.10	43.46	7.21
A-HMS	0.3554	0.0967	40.79	159.25	0.9988	0.0003	157.41	159.25	7.75
M-HMS	0.6941	0.1105	24.07	114.63	0.9999	0.0004	115.27	114.63	4.92
OD-HMS	0.055	0.0553	23.94	111.57	0.9932	0.0002	116.59	111.57	1.98
Ti-HMS	0.4174	0.1520	15.85	46.67	0.9987	0.0050	46.63	46.67	11.09
NaY	0.3062	0.0553	6.05	29.00	0.9991	0.0186	27.03	29.00	13.59
HY	0.6503	0.0829	10.45	38.95	0.9996	0.0052	40.68	38.95	8.57

Table 4.7 Kinetics values calculated for PFOA adsorption onto PAC, HMS,

functionalized HMSs, NaY and HY zeolite at initial pH solution 9

Adsorbent	Pseudo First-order				Pseudo Second-order				
	R^2	k_1 (h^{-1})	Calculated q_e (mg/g)	Experimental q_e (mg/g)	R^2	k_2 (g/mg h)	Calculated q_e (mg/g)	Experimental q_e (mg/g)	h (mg/g h)
PAC	0.8350	0.6771	89.90	238.63	1.0000	0.0002	238.96	238.63	11.68
HMS	0.1573	0.2625	5.43	10.72	0.9829	0.1037	10.24	10.72	10.87
A-HMS	0.4366	0.0553	7.80	18.77	0.9940	0.0112	17.03	18.77	3.24
M-HMS	0.1664	0.3178	12.50	44.00	0.9959	0.0060	44.07	44.00	11.56
OD-HMS	0.5858	0.0967	11.15	21.45	0.9959	0.0064	19.49	21.45	2.44
Ti-HMS	0.8427	0.2487	9.42	15.95	0.9982	0.0192	15.60	15.95	4.67
NaY	0.1809	0.0415	4.97	25.78	0.9966	0.0090	24.05	25.78	5.21
HY	0.6317	0.0553	14.04	20.32	0.9864	0.0229	19.84	20.32	8.99

Table 4.8 Kinetics values calculated for PFOS adsorption onto PAC, HMS,

functionalized HMSs, NaY and HY zeolite at initial pH solution 9

Adsorbent	Pseudo First-order				Pseudo Second-order				
	R^2	k_1 (h^{-1})	Calculated q_e (mg/g)	Experimental q_e (mg/g)	R^2	k_2 (g/mg h)	Calculated q_e (mg/g)	Experimental q_e (mg/g)	h (mg/g h)
PAC	0.6282	0.6633	60.64	526.91	1.0000	0.0002	527.12	526.91	50.33
HMS	0.7552	0.1105	40.52	134.65	0.9997	0.0005	133.42	134.65	8.41
A-HMS	0.5530	0.0829	24.09	83.26	0.9993	0.0014	82.32	83.26	9.44
M-HMS	0.5236	0.4145	48.09	135.93	0.9987	0.0016	136.65	135.93	30.19
OD-HMS	0.7922	0.5942	69.48	128.11	0.9997	0.0004	126.36	128.11	6.58
Ti-HMS	0.8432	0.3869	83.98	148.14	0.9992	0.0001	149.98	148.14	3.03
NaY	0.9456	0.0967	27.43	43.62	0.9982	0.0020	41.27	43.62	3.38
HY	0.5580	0.1105	26.15	106.79	0.9999	0.0007	105.73	106.79	8.09
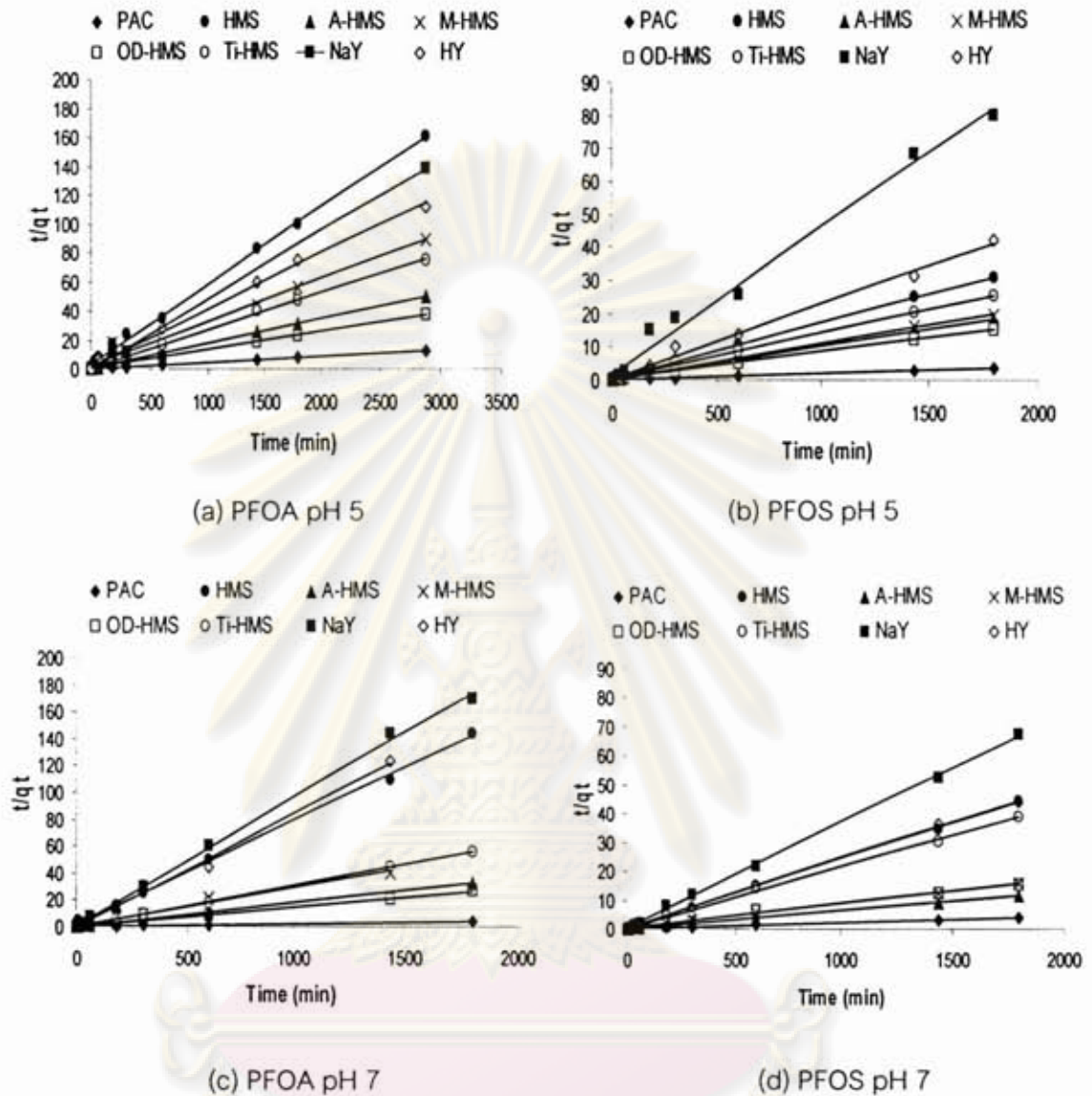
Figure 4.13 The pseudo-second-order model linear plotted of PFOA and PFOS on all
adsorbents at different initial pH solution

ศูนย์วิทยทรัพยากร
จุฬาลงกรณ์มหาวิทยาลัย

(e) PFOA pH 9   (f) PFOS pH 9
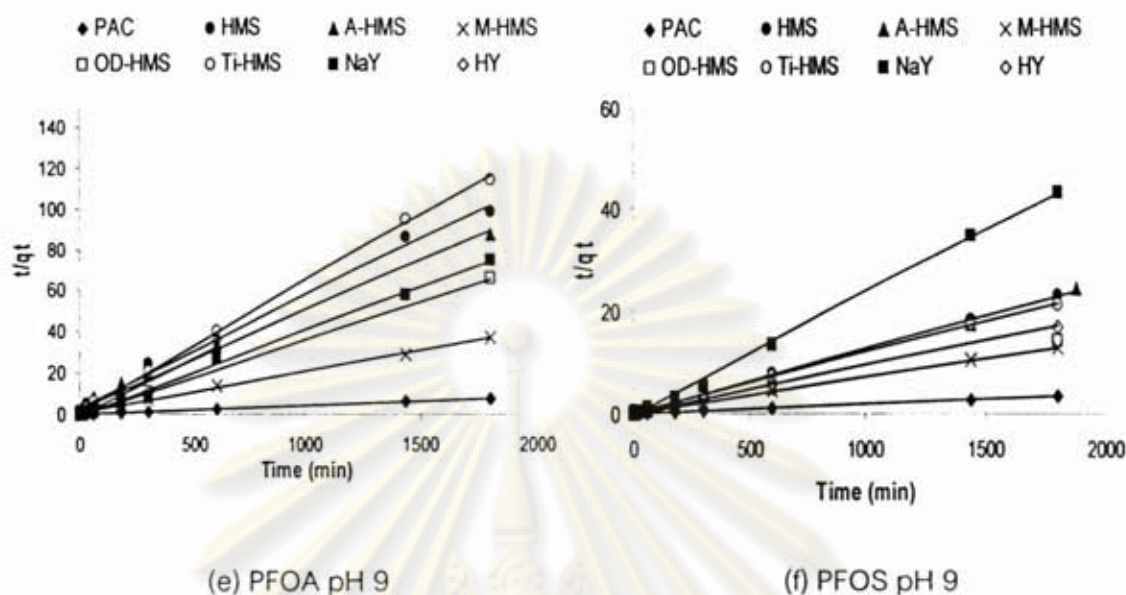
Figure 4.13 (cont.) The pseudo-second-order model linear plotted of PFOA and PFOS
on all adsorbents at different initial pH solution

As shown in Tables 4.3-4.8 and Figure 4.13, the pseudo-second-order model
fitted all the adsorption data well according to the relatively high correlation coefficients
($r^2 > 0.98$), comparing with pseudo first order model. The pseudo-second-order model
linear plotted as shown in Figure 4.13. It was indicated that the pseudo second order
rate models could be described adsorption kinetics for PFOA and PFOS adsorption,
based on the assumption that the adsorption step may involve chemisorptions.
Moreover, the experimental q_e values and the calculated q_e obtained from the linear plot
in Equation 4.5 were compared as shown in Tables 4.3 and 4.8. The result in Tables 4.3
and 4.8 exhibited good consistency between that calculated q_e and experimental q_e in
pseudo-second-order model. Furthermore, the pseudo-second-order rate constant k_2
obtained from the linear plot in Equation 4.5 as shown in Tables 4.3 and 4.8 can be
indicated some characteristic in adsorption kinetic profile. If k_2 value was lower, it might
be told that amount of adsorbent which using in adsorption process of adsorbates was
less while it had same amount of adsorbate in bulk solution. On the other hands, k_2 value
was higher, the amount of adsorbents that using in adsorption process of adsorbates
also was higher while it had same amount of adsorbate in bulk solution. Furthermore, it

might be indicated that the adsorption interaction between adsorbate and adsorbents surface also can be reached to equilibrium stage faster (Qiang Yu *et al.*, 2009). From obtained results in pseudo second order model as shown in Tables 4.3 and 4.8 found that at different initial pH solution, PAC seem to be had k_2 value lower than other adsorbents.

In addition, the initial adsorption rate can also be obtained from this model from Equation 4.4 as shown in Tables 4.3 and 4.8.

$$h = k_2 q_e^2 \qquad \qquad \text{...(4.4)}$$

Where h is the initial adsorption rate (mg/g h)

From calculations, it showed that PAC had the highest initial adsorption rate. The calculated data clearly agree with experimental data observed in Figures 4.10-4.12 that, concentration of PFOA and PFOS adsorbed onto PAC rapidly decrease within 30 mins, and slowly decrease until equilibrium stage at 10 hrs.

4.3 Adsorption Isotherm

Adsorption isotherms were used to evaluate the sorption capacity of adsorbents as well as to understand the adsorbate adsorbent interactions. In this study, adsorption mechanisms of PFOA and PFOS from aqueous solution onto synthesized HMSs and zeolite were investigated. Their adsorption capacities were compared with PAC. Physical characteristics of these adsorbents were investigated and their effects to adsorption mechanisms were discussed. We employed the information from adsorption isotherm together with a theoretical evaluation of the surface properties of adsorbents and adsorbate to elucidate adsorption capacities and mechanisms of synthesized HMSs, zeolite and PAC. Moreover, the experimental results were fitted to Langmuir and Freundlich Equations.

4.3.1 Effect of Surface Functional Groups of adsorbents

In this adsorption experiments, the final equilibrium solution pH of both PFOA and PFOS were measured and final pH solution showed a little bit lower than initial pH that we employed. At initial pH solution equal to 7, final pH solution was in range of 6.5-7.0. According to, both of PFOA and PFOS molecules had low pK_a values at 2.8 and -3.27, respectively, which indicated strong acid (especially PFOS) and can dissociated by carboxylate anion and sulfonate anion into the solution almost 100 percent in this range of pH solution. According to their properties of these pollutants, it might be affected to decrease of initial pH of both PFOA and PFOS solution after interaction.

Figure 4.14 illustrated adsorption isotherms of PFOA and PFOS on pristine HMS, A-HMS, M-HMS, OD-HMS and Ti-HMS at final pH solution in range of 6.5-7.0 and reported by plotted C_e (mg/l) versus q_e (mg/g). Furthermore, adsorption isotherms of PFOA and PFOS on all adsorbents also were reported by plotted C_e (mg/l) versus q_e (mg/m^2). To analyze the results of adsorption isotherms, this experiment was employed initial pH solution at pH 7. Hence, both HMS and M-HMS had weakly negatively charged or nearly neutral charged at pH of 6.5-7.0, but OD-HMS, exhibited strong negative charge. It can be suggested that the electrostatic attraction between positively charge surfaces of adsorbents and negative charge of adsorbates can be neglected for HMS, OD-HMS and M-HMS. On the other hand, HMSs functionalized by amino group (A-HMS) and titanium substitution HMS (Ti-HMS) had positive charge at this pH, hence, negative charged PFOA and PFOS were expected to enhance the adsorption on A-HMS and Ti-HMS due to electrostatic attraction.
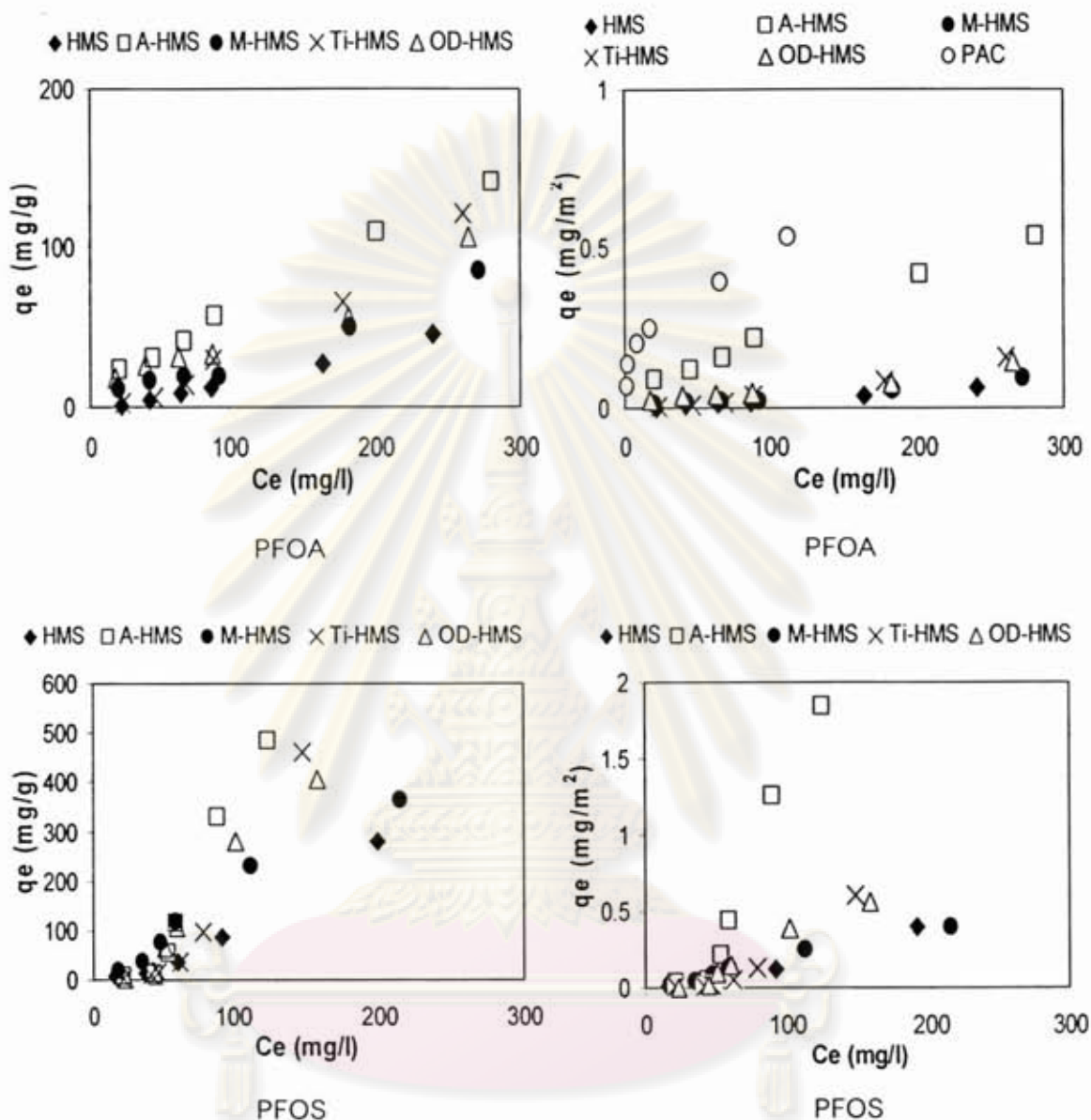
Figure 4.14 Adsorption capacities of PFOA and PFOS on HMS, A-HMS, M-HMS, Ti-HMS

and OD-HMS at initial pH solution 7, ionic strength 0.01 M, temperature 25±2 °C

The obtained results can be seen in Figure 4.14 that the adsorption capacities of PFOA and PFOS on all synthesized HMSs showed the same trend: A-HMS > Ti-HMS > OD-HMS > M-HMS > HMS, respectively. From obtained results, adsorption of both PFOA and PFOS on A-HMS and Ti-HMS, which had both of high hydrophilicity and positively charged on surface, especially A-HMS showed higher adsorption capacities comparing with other synthesized HMSs (HMS, OD-HMS and M-HMS). It

might be suggested that combination between electrostatic interaction and hydrogen bonds of A-HMS and Ti-HMS should play an important role for enhance adsorption of both anionic PFOA and PFOS. However, it found that adsorption of both PFOA and PFOS adsorbed on A-HMS surface showed higher adsorption efficiency while the concentrations of these pollutants in bulk solution were raised up. On the other hands, adsorption of both PFOA and PFOS on pristine HMS had lower comparing with organic-chain-grafted HMSs (A-HMS, Ti-HMS, OD-HMS and M-HMS). Due to, only effect of hydrogen bonds by lacking the promotion force of coulomb interaction on the surface of HMS caused pristine HMS had lower adsorption capacity of both PFOA and PFOS molecule than other hydrophilic positively charged adsorbents (A-HMS and Ti-HMS). Moreover, Ti-HMS showed high adsorption capacity comparing with pristine HMS. Due to as reported by Tanev et al., (1994), titanium silicate is an effective molecular-sieve catalyst which could promote oxidation interaction, but pristine HMS presented low catalyst activities. On the contrary, hydrophobic adsorbents (OD-HMS and M-HMS), the obtained result found that the effect of electrostatic force and hydrogen bonds can be neglected, especially for OD-HMS surface. However, adsorption of both PFOA and PFOS on OD-HMS and M-HMS exhibited higher comparing with hydrophilic adsorbent such as pristine HMS. Hence, it might be indicated that hydrophobic interaction or Van Der Waals force might be the main interaction force for enhance adsorption capacities of hydrophobic M-HMS and OD-HMS. Indeed, given the dual hydrophilic (carboxyl and sulfonyl functional head group) and hydrophobic (perfluoro alkyl tail group) was the nature of PFOA and PFOS; it is unlikely that the adsorption mechanism obeys simple hydrophobic partitioning paradigms, which consistency with other research study (Higgins and Luthy, 2006). They confirmed that the importance of hydrophobic interactions on the adsorption of PFCs by sediments, but they also demonstrated that electrostatic interactions play a role in the adsorption of anionic PFC surfactants. Furthermore, it also found that adsorption capacity of OD-HMS showed higher adsorption capacity than M-HMS. In this case, it might be suggested that increasing hydrophobicity properties of synthesized HMSs could increase adsorption capacities of organic pollutants due to Van Der Waals force between hydrophobic surface and

perfluoro alkyl chain of PFOA and PFOS molecule. This result also was consistent with other research works (Valeria and Reyes, 2008); they found that increasing of hydrophobicity on silicate materials showed the highest adsorption capacity of PFOS. However, adsorption capacities of hydrophobic adsorbents did not high comparing with other hydrophilic and positively charged adsorbents (A-HMS and Ti-HMS). Hence, it also can be suggested that in adsorption of PFOA and PFOS, combined effect of electrostatic force and hydrogen bonds might be more important force could enhance adsorption capacities than Van Der Waals force. Therefore, it might be also suggested that grafted organic functional groups on silicate HMS materials can be directly affected to adsorption capacities of PFCs. Furthermore, adsorption isotherms of PFOA and PFOS results as reported by plotted C_e (mg/l) versus q_e (mg/m^2). It found that the order of affinity still was A-HMS > Ti-HMS > OD-HMS > M-HMS > HMS, respectively. A-HMS had the highest adsorption capacity even the crystalline structure was lost and surface area and pore volume also was collapse comparing other synthesized HMSs as shown in Table 4.1. Due to, the presence of high positively charged and hydrophilic on its surface might be displayed an important role in adsorption phenomenon which could directly affected adsorption capacity of A-HMS more than effect of crystalline structure and surface area. Furthermore, although, crystalline structure of pristine HMS did not lost and its surface area and pore volume values seem to be high comparing other synthesized HMSs. However, the results found that adsorption of PFOA and PFOS on HMS had lowest. Hence, it might be indicated that, in this study, effect of crystalline structure, surface area and pore volume of these synthesized HMSs adsorbents (A-HMS, Ti-HMS, OD-HMS, M-HMS and HMS) did not affected adsorption of PFOA and PFOS.

Moreover, molecular size of PFOS molecule was showed as ~1.3 nm and 1 nm in width and length, respectively. However, the width of PFOA molecule was smaller than PFOS molecule by showed value less than 1.3 nm but, the length of PFOA molecule still was the same as PFOS molecule equal to 1 nm as reported in other research works (Erkoc and Erkoc, 2001; Johnson et al., 2007). According to this data, it

might be indicated that molecular sizes of PFOA and PFOS molecule were smaller than pore size of all mesostructure synthesized HMSs, hence, effect of pore blocking can be neglected in adsorption of PFOA and PFOS on these synthesized HMSs adsorbents (A-HMS, Ti-HMS, OD-HMS, M-HMS and HMS).

4.3.2 Effect of molecular structure of PFCs on adsorption capacity
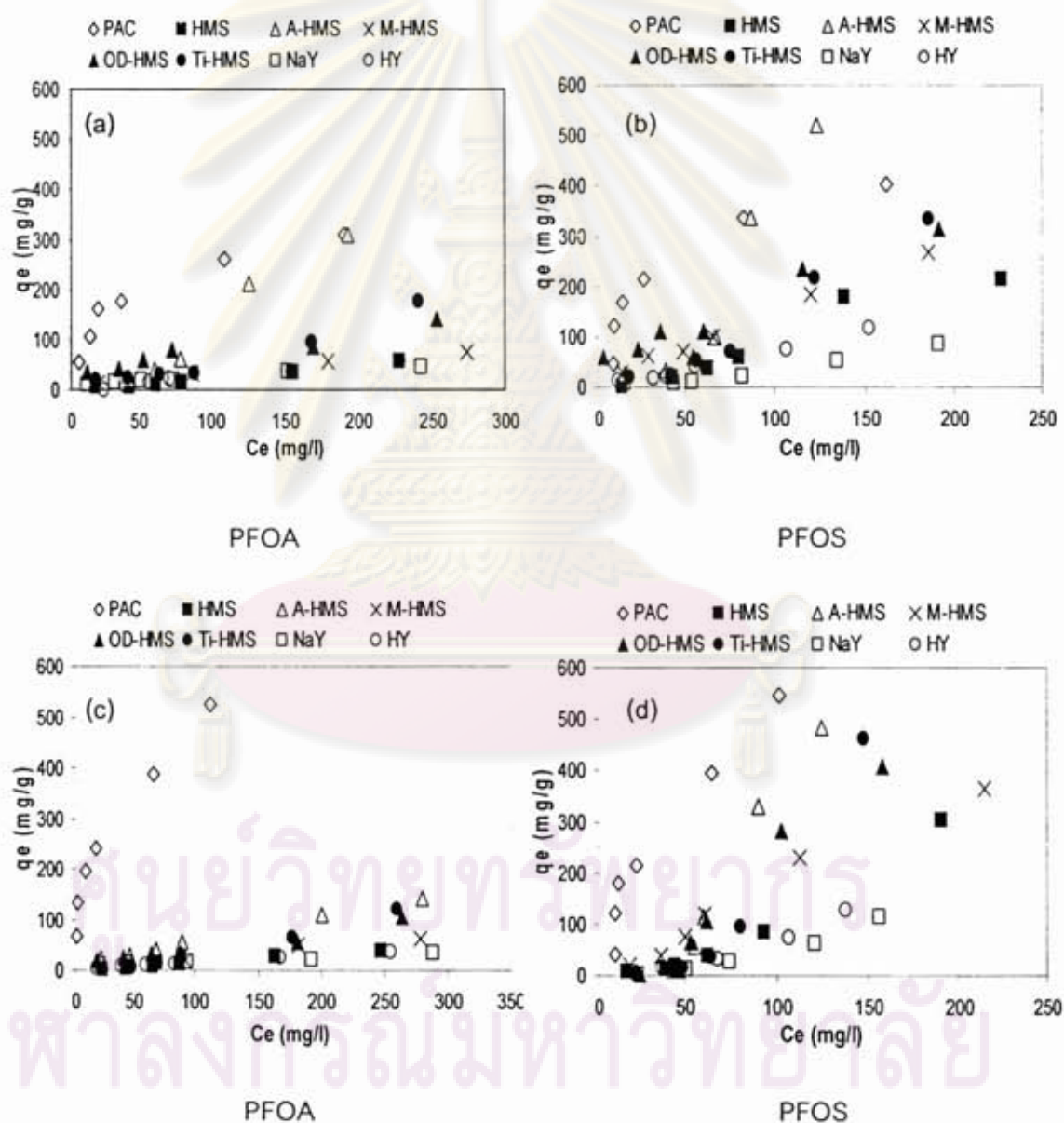
Figure 4.15 Adsorption Isotherms of PFOA and PFOS adsorbed onto all adsorbents: (a) and (b), initial pH solution 5; (c) and (d), initial pH solution 7; (e) and (f), initial pH solution 9, ionic strength 0.01 M, temperature 25±2 °C
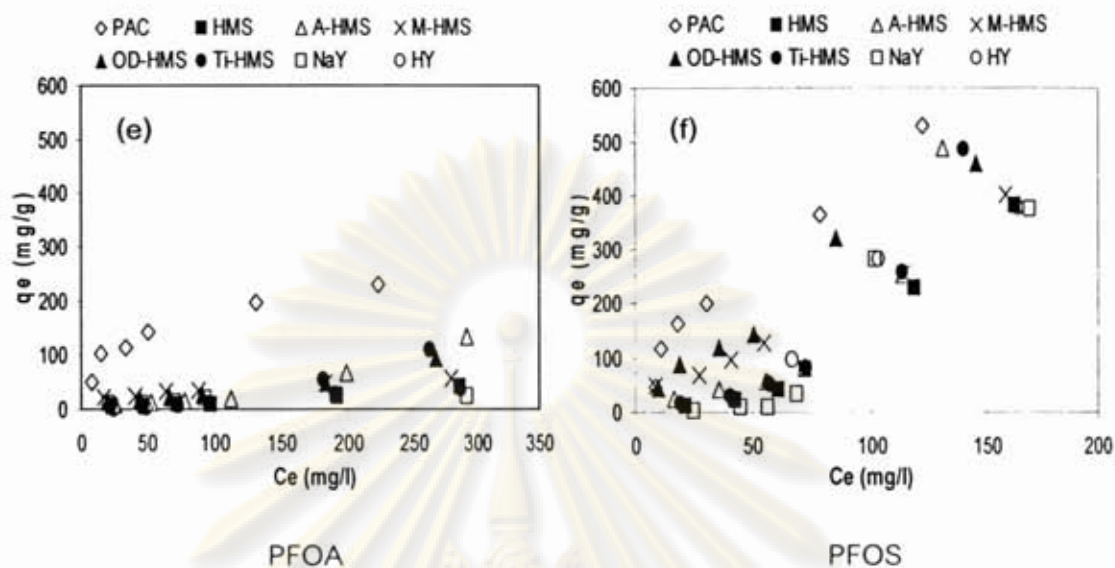
Figure 4.15 (cont.) Adsorption Isotherms of PFOA and PFOS adsorbed onto all adsorbents: (a) and (b), initial pH solution 5; (c) and (d), initial pH solution 7; (e) and (f), initial pH solution 9, ionic strength 0.01 M, temperature 25±2 °C

From obtained results, it was found that adsorption of PFOS was higher than PFOA on all adsorbents as shown in Figure 4.15, although, PFOA and PFOS have equal perfluorocarbon chain length. From the basic properties of PFCs, it was report that PFCs were classify in two groups, Perfluorocarboxylate (PFCA) and Perfluoroalkyl sulfonate (PFAS) molecules consist of one perfluorinated carbon chain and one special functional group. The functional group, such as carboxyl (COOH) and sulfonyl group (SO$_3$H) which have an anionic can affiliate with water and make PFCs hydrophilic. According to these data, it might be reasonable that presence of different kinds of functional groups grafted on hydrophilic part of PFOA and PFOS not only influenced the properties of their pK$_a$ values, but also affected the differentiation of their hydrophilic moiety. PFOA showed higher solubility in water than PFOS. Solubility in water of PFOA and PFOS was 570 mg/l and 3,400 mg/l, respectively. Therefore, it might be also suggested that carboxyl functional group of PFOA molecule had higher solubility than sulfonyl functional group of PFOS. In addition, it was suggested that couple of different functional group and different hydrophilic moiety might be also directly influenced adsorption of these anionic surfactants due to diverse behavior in adsorption

phenomenon of hydrogen bonds between carboxyl or sulfonyl group of adsorbates and silanol group (Si-OH) grafted on the surface of adsorbents. Due to carboxyl group of PFOA had strongly hydrophilic moiety and electronegative atom (oxygen atoms) could have attractive force with water molecules by intermolecular hydrogen bonding easier than sulfonyl group of PFOS. Hence, according to this information, it might be suggested that the competition of attractive force by hydrogen bonds between oxygen atoms on carboxyl group of PFOA and water molecules caused decreasing of hydrogen bonds content by attractive force between oxygen atoms on carboxyl group of PFOA and silanol group grafted on the surface of adsorbents while adsorption interaction occurred. On the other hands, it can be suggested that hydroxyl functional group (OH⁻) in water molecule can be disturbed to adsorption of PFOA adsorbed on silanol group surface of adsorbents easier than adsorption of PFOS by decrease attractive force due to hydrogen bonds between oxygen atoms on carboxyl group of PFOA and silanol group on the surface of adsorbents. From this reason, it is consistent with the weaker adsorption of PFOA, comparing with adsorption of PFOS. Moreover, the presence of functional group on PFCs has strongly affected the degree of PFCs adsorption, including effects of PFCs characteristics itself.

4.3.3 Effect of Crystalline Structure

To study the effect of crystalline structure, microporous materials (NaY and HY zeolite) were applied to compare the adsorption capacities of both PFOA and PFOS with mesoporous materials (HMS). We were analyzed the data by employed the initial pH solution at 7. Figure 4.16 illustrated the adsorption isotherms of PFOA and PFOS on HMS, NaY and HY zeolite.
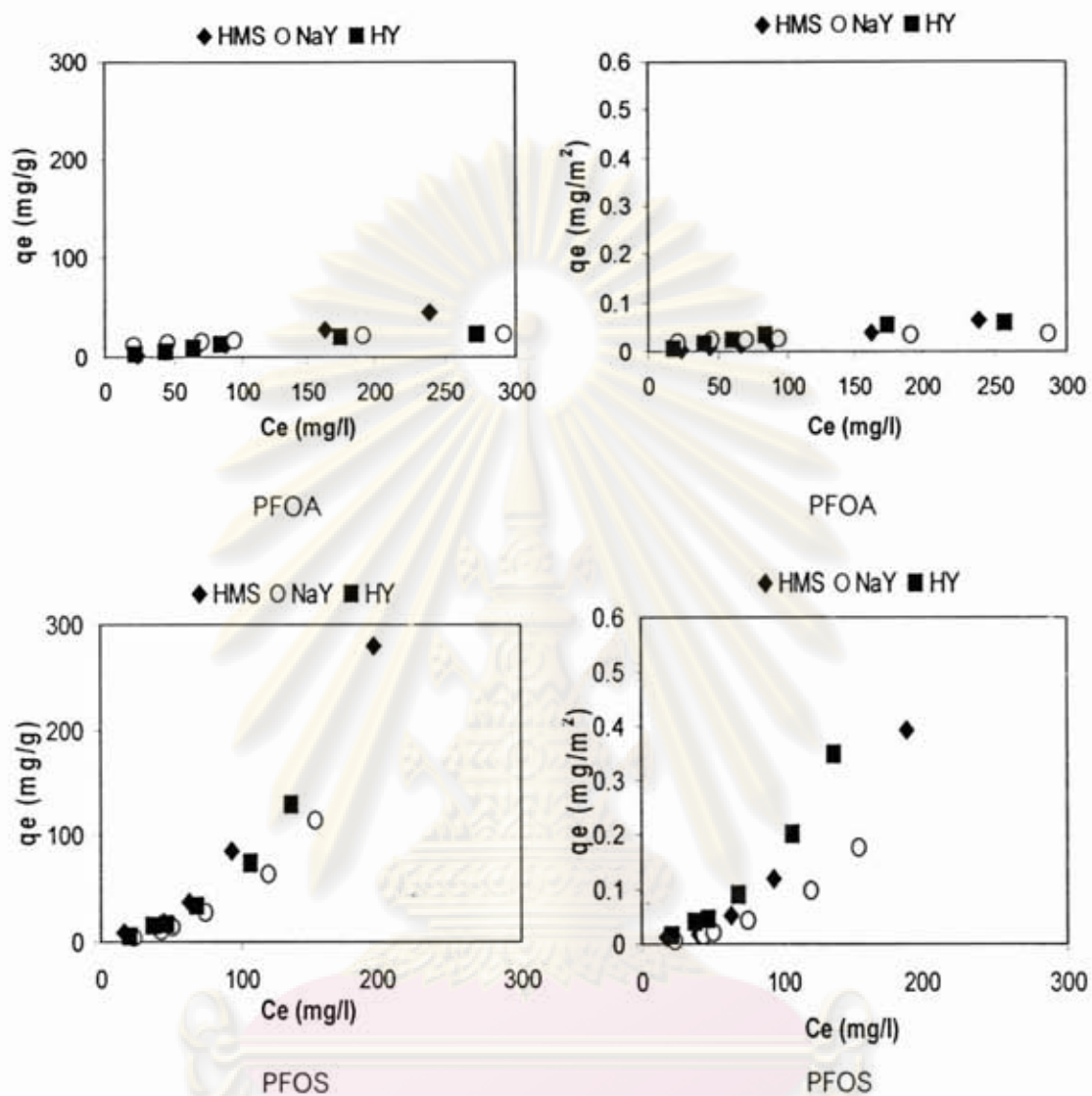
Figure 4.16 Adsorption isotherms of PFOA and PFOS on HMS, NaY

and HY zeolite at initial pH solution 7, ionic strength 0.01 M, temperature 25±2°C

From the above information, molecular size of PFOS molecule was showed as ~1.3 nm and 1 nm in width and length, respectively. And, the width of PFOA molecule was smaller than PFOS molecule by showed value less than 1.3 nm but, the length of PFOA molecule still was the same as PFOS molecule which equal to 1 nm as reported in other research works (Erkoc and Erkoc, 2001; Johnson et al., 2007). Comparing with pore structure of applied adsorbents, it might be indicated that PFOA and PFOS molecule cannot access to internal surface area of NaY and HY zeolite.

However, PFOA and PFOS molecule can access into internal surface of mesopore of synthesized HMSs. Hence, effect of microporous crystalline structure and pore blocking were expected to influence to reduce adsorption of both PFOA and PFOS on these microporous materials (NaY and HY zeolite). However, obtained results found that mesostructure (HMS) and microstructure (NaY and HY zeolite) had adsorption capacity of PFOA not different clearly from each other since, the adsorption capacities of HMS, NaY and HY zeolite were comparable. The adsorption of PFOA on HMS, HY and NaY zeolite was 45.49 mg/g, 23.07 mg/g and 21.89 mg/g, respectively as shown in Figure 4.16. On the contrary, HMS had higher adsorption capacity of PFOS (280.43 mg/g) than microstructure such as HY zeolite (128.67 mg/g) and NaY zeolite (114.01 mg/g) clearly. However, the obtained results found that at low equilibrium PFOS concentration, the adsorption capacities of HMS, HY and NaY zeolite were not different clearly comparing with at high equilibrium concentration as shown in Figure 4.16. From their properties, the CMC values for PFOS and PFOA should be about 4,573 and 15,696 mg/l, respectively (Kissa, 2001). Although, the PFOS or PFOA concentrations used in this study are far below their CMC values almost no micelles can form in solution. However, when the concentration of PFOA or PFOS were raised up, also might be caused PFOA or PFOS molecule can be more form aggregated itself in bulk solution, especially for PFOS molecule which had molecular size bigger than PFOA (Qiang Yu et al., 2009). According to this information, it might be reasonable that adsorption of PFOS on microporous structure (NaY and HY zeolite) had adsorption capacities lower than mesoporous structure HMS clearly while raised up PFOS concentration in bulk solution. On the other hands, it might be suggested that combination effect of low surface accessibility of these microporous materials and large form aggregation itself in bulk solution of PFOS molecule while raised up PFOS concentration in bulk solution can be increased effect of pore blocking in adsorption of PFOS caused to decrease adsorption capacities of microporous materials (NaY and HY zeolite).

Hence, the results as shown in Figure 4.16, it might be indicated that effect of crystalline structure due to high surface accessibility of mesoporous structure (HMS)

can directly enhance adsorption capacities of PFOS clearly, especially at high equilibrium concentration. On the other hands, adsorption of PFOA on mesoporous material (HMS) did not high comparing with microporous material (NaY and HY zeolite) clearly, although raised up the equilibrium PFOA concentration. Hence, it might be suggested that effect of crystalline structure by comparing between adsorption capacities of mesoporous structure (HMS) and microporous structure (NaY and HY zeolite) was just a little affected adsorption capacities of PFOA.

Furthermore, the presence of silanol group (Si-OH) on HMS, NaY and HY could directly interact with carboxylic and sulfonic group on the hydrophilic part of PFOA and PFOS, respectively. However, NaY and HY zeolite had less silanol group on surfaces, comparing with HMS, due to Brönsted acid site. Moreover, aluminum atom inside silicate structure of Faujasite Y, it can exhibit a negative charge on oxygen atoms and might be balanced by counter ions (such as Na^+, H^+ and K^+) and caused lower silanol groups comparing with HMS (as shown in Figure 4.17).
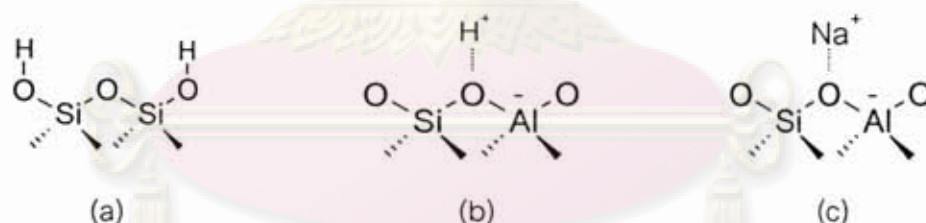
Figure 4.17 Surface structures and functional groups (a) HMS (silanol groups); (b) HY zeolite (Brönsted acid); (c) NaY zeolite

From Figure 4.16, HY zeolite showed a little bit higher adsorption capacity than NaY zeolite although crystalline structures are same. It was noticeable that counter ions on surface of zeolite can be affected to PFCs adsorption capacity. It can be suggested that as protons of HY zeolite having positive charge similar to sodium ions on NaY zeolite, but size of proton was much smaller than sodium ion. It indicated that proton on HY zeolite had higher charge density than sodium ions of NaY zeolite, causing higher adsorption capacity.
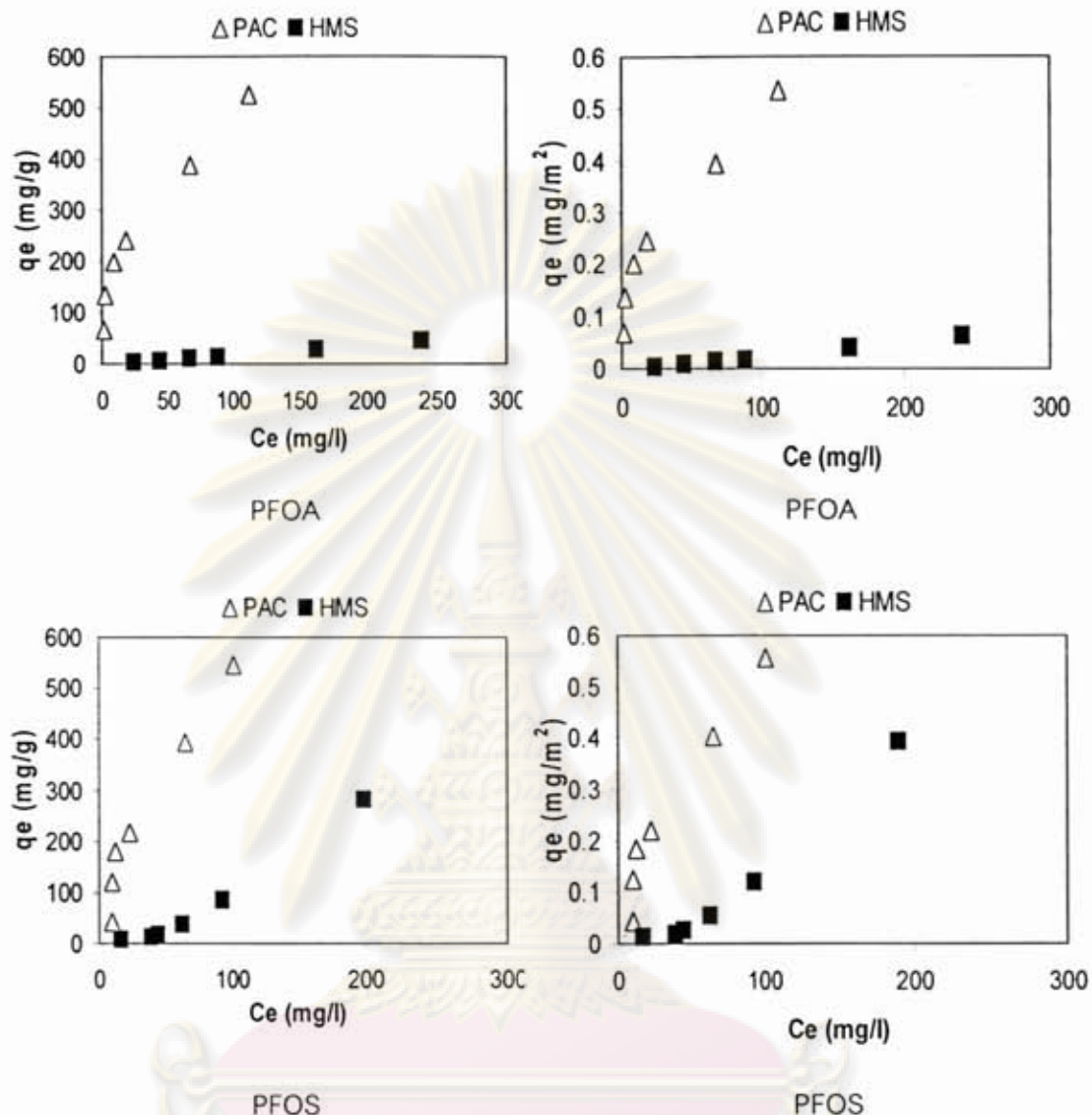
Figure 4.18 Adsorption isotherms of PFOA and PFOS on PAC and HMS at initial pH

solution 7, ionic strength 0.01 M, temperature $25\pm2\,^{\circ}C$

From Figure 4.18, PAC showed much higher adsorption capacity than HMS. It might be caused by large surface area and complexity of surface functional groups on the surface, inducing many interaction forces involved such as electrostatic force, Van Der Waals force and covalent bonding. Furthermore, the parameters and correlation coefficients of Langmuir and Freundlich isotherm model were calculated by using experimental data through linear regression. It was found that obtained data Freundlich isotherm can be fitted to the data with very high correlation coefficients.

Hence, it might be indicated that adsorption phenomenon of PFOA and PFOS on all adsorbents was multi-layer adsorption. From the data as shown in Tables 4.9-4.10, n value indicated the Freundlich constants. If value of 1/n equal to 1, it mean that adsorption isotherm was linear isotherm. If value of 1/n >1, it mean that amount of active site on the surface of adsorbents was much enough for adsorption of adsorbate. In addition, if value of 1/n < 1, it mean that amount of active site on the surface of adsorbents was limited for adsorption of adsorbate (Qiang Yu et al., 2009). Details of calculation method of Langmuir isotherm and Freundlich isotherm are shown in appendix C.
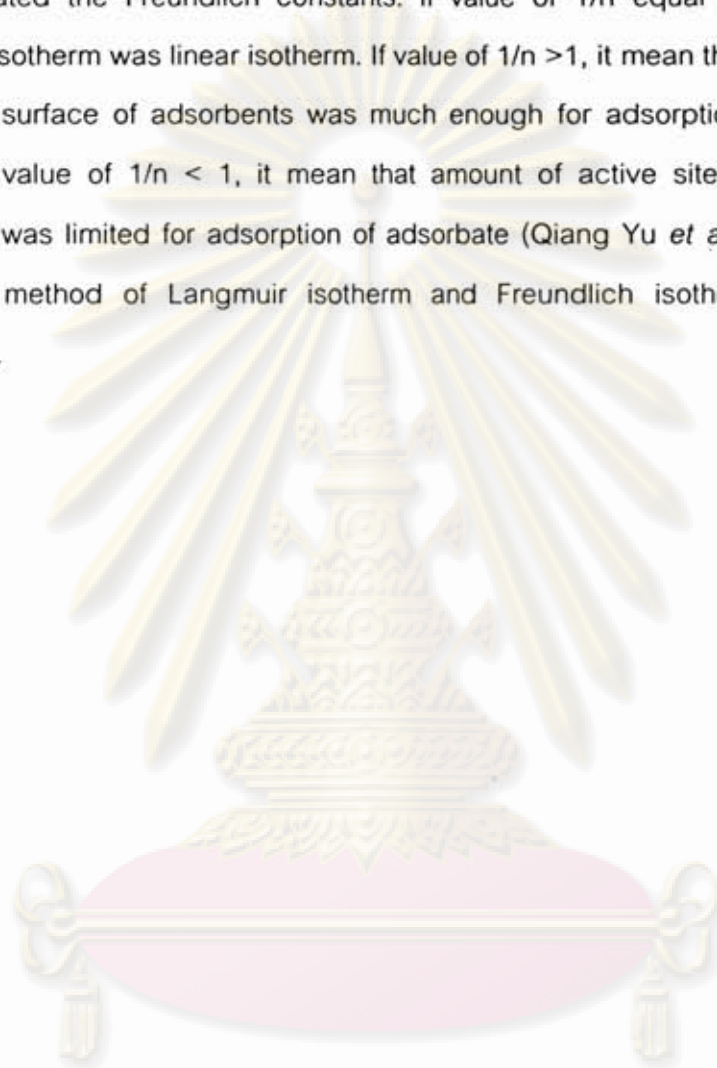
Table 4.9 Parameters of Langmuir and Freundlich isotherm model for PFOA adsorption on PAC, HMS, functionalized HMSs, NaY and HY zeolite at initial pH solution 5, 7 and 9

Adsorbent	Langmuir			Freundlich		
pH	q_m	K_L	R^2	K_f	$1/n$	R^2
PAC						
5	384.615	0.0272	0.9873	29.614	0.4707	0.9147
7	434.783	0.1299	0.9089	54.891	0.4786	0.9944
9	250.000	0.0323	0.9525	14.737	0.5800	0.9995
HMS						
5	9.066	0.0047	0.9709	0.018	1.534	0.9903
7	7.843	0.0064	0.9333	0.033	1.1504	0.9976
9	33.003	0.0052	0.9071	0.058	1.1587	0.9993
A-HMS						
5	80.000	0.0048	0.8697	3.612	4.0883	0.9874
7	69.930	0.0222	0.8984	5.639	0.5470	0.9949
9	21.459	0.0036	0.9606	0.010	1.6302	0.9860
M-HMS						
5	76.923	0.0088	0.9337	1.684	0.6894	0.9591
7	48.077	0.0130	0.8710	1.248	0.6989	0.9944
9	78.125	0.0187	0.8506	1.3546	0.7522	0.9753
OD-HMS						
5	169.492	0.0010	0.9398	10.917	0.4543	0.9855
7	64.516	0.0204	0.8618	2.477	0.6675	0.9878
9	19.342	0.0063	0.8542	0.038	1.2738	0.9839
Ti-HMS						
5	37.313	0.0592	0.8939	0.233	1.0990	0.9431
7	76.923	0.0114	0.8936	0.144	1.4643	0.9998
9	20.704	0.0059	0.87574	0.0506	2.1237	0.9977
NaY						
5	32.258	0.0416	0.832	2.142	0.5579	0.9999
7	24.039	0.0231	0.7703	0.072	1.0871	0.9892
9	20.080	0.0506	0.6228	3.505	0.4170	0.9998
HY						
5	29.674	0.0100	0.9526	0.161	0.9197	0.9792
7	33.333	0.0117	0.9578	0.599	0.7340	0.9946
9	7.698	0.0050	0.9726	0.009	1.5033	0.9925

Table 4.10 Parameters of Langmuir and Freundlich isotherm model for PFOS adsorption on PAC, HMS, functionalized HMSs, NaY and HY zeolite at initial pH solution 5, 7 and 9

Adsorbent	Langmuir			Freundlich		
pH	q_m	K_L	R^2	K_f	$1/n$	R^2
PAC						
5	1428.571	0.0058	0.6191	63.988	0.3672	0.9948
7	50000	0.0002	0.4998	65.418	0.4032	0.9980
9	5000	0.0013	0.8011	25.562	0.6262	0.9940
HMS						
5	24.096	0.0083	0.9780	0.6017	0.2581	0.9860
7	7.9239	0.0064	0.9321	0.0663	1.4331	0.9926
9	33.003	0.0052	0.9071	0.0583	1.4283	0.9993
A-HMS						
5	121.951	0.0043	0.8372	0.0605	1.7676	0.9998
7	18.975	0.0133	0.9910	6.984	3.5979	0.9966
9	74.074	0.0075	0.9479	0.046	1.8736	0.9859
M-HMS						
5	91.743	0.0286	0.5519	2.937	0.8161	0.9801
7	172.414	0.0055	0.9828	0.410	1.3403	0.9922
9	227.273	0.0281	0.8222	1.534	1.1264	0.9953
OD-HMS						
5	277.778	0.0293	0.9444	26.749	0.4383	0.9675
7	196.078	0.0279	0.8137	5.646	1.5210	0.9921
9	45.6621	0.0119	0.8072	0.159	1.6590	0.9921
Ti-HMS						
5	666.667	0.0015	0.8211	0.5156	1.2477	0.9989
7	15.674	0.0090	0.9749	0.007	2.0201	0.9895
9	166.667	0.0041	0.4773	0.0027	2.4079	0.9982
NaY						
5	31.250	0.0201	0.5292	0.026	1.5480	0.9994
7	20.704	0.0519	0.9163	1.159	1.8525	0.9990
9	6.473	0.0100	0.9324	0.032	2.7766	0.9980
HY						
5	73.529	0.0170	0.8177	1.682	0.8250	0.9927
7	33.113	0.0071	0.9811	0.036	1.6387	0.9924
9	51.546	0.0079	0.9793	0.048	1.7746	0.9949

4.4 Adsorption Mechanisms

4.4.1 Effect of pH

To reveal the effect of the electrostatic interaction between adsorbents and negative charge PFOA and PFOS, the effects of pH on the adsorption capacities of all adsorbents were investigated by varying initial pH solution from 5, 7 and 9 controlled by phosphate buffer.
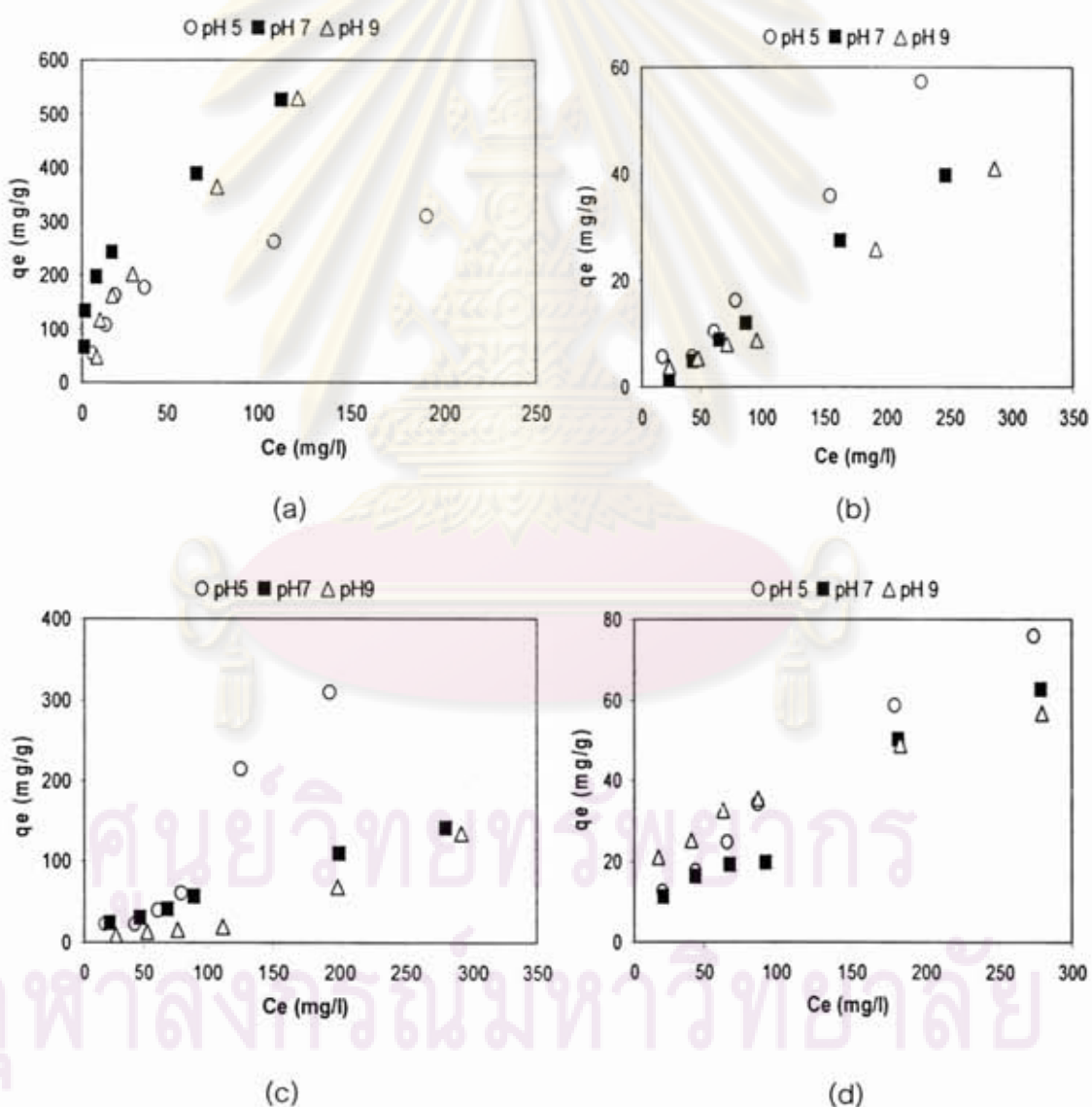
Figure 4.19 Adsorption capacities of PFOA on (a) PAC, (b) HMS, (c) A-HMS, (d) M-HMS, (e) OD-HMS, (f) Ti-HMS, (g) NaY and (h) HY zeolite, ionic strength 0.01 M, temperature 25±2°C
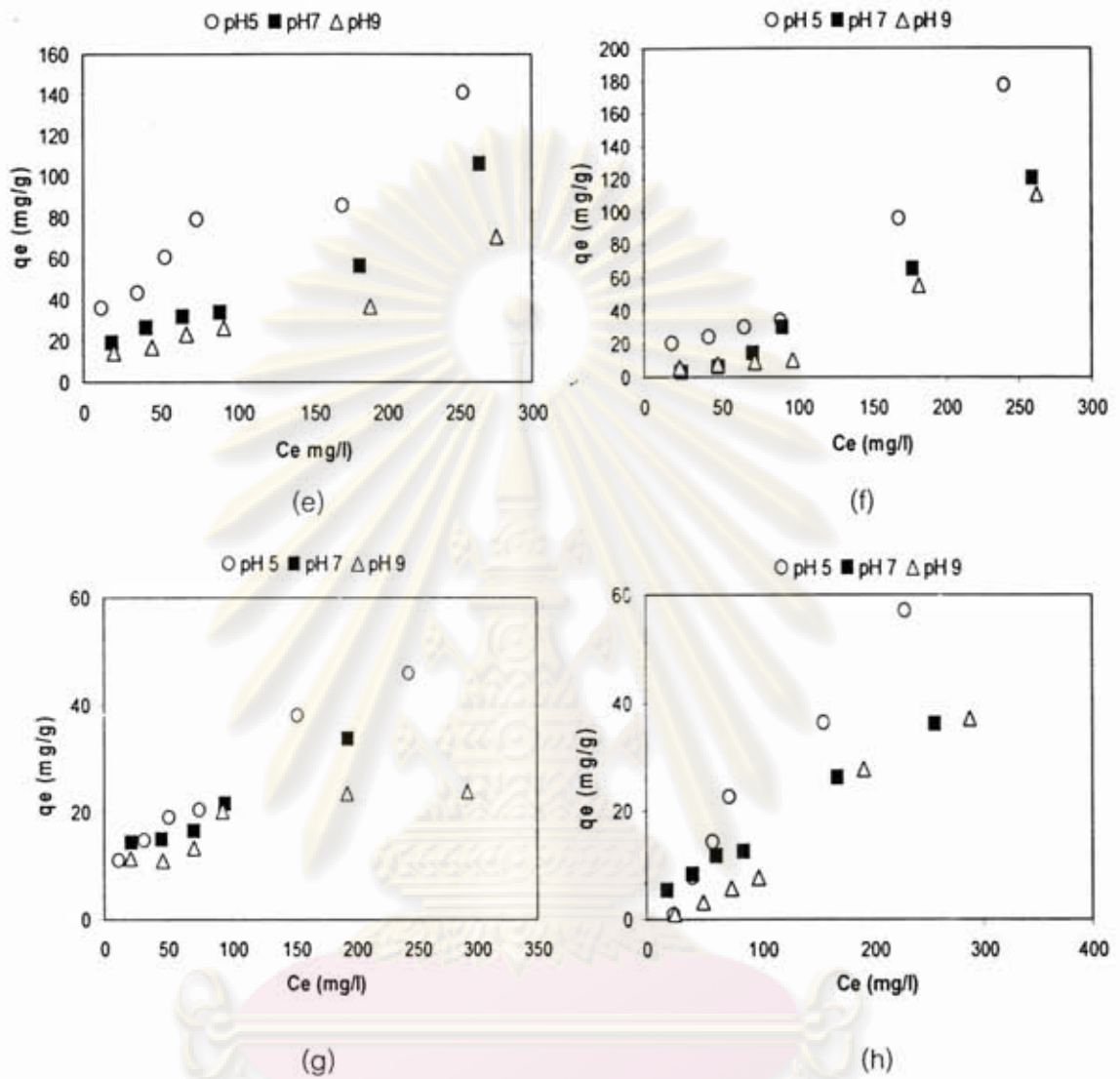
Figure 4.19 (cont.) Adsorption capacities of PFOA on (a) PAC, (b) HMS, (c) A-HMS, (d)
M-HMS, (e) OD-HMS, (f) Ti-HMS, (g) NaY and (h) HY zeolite, ionic strength 0.01 M,
temperature 25±2°C
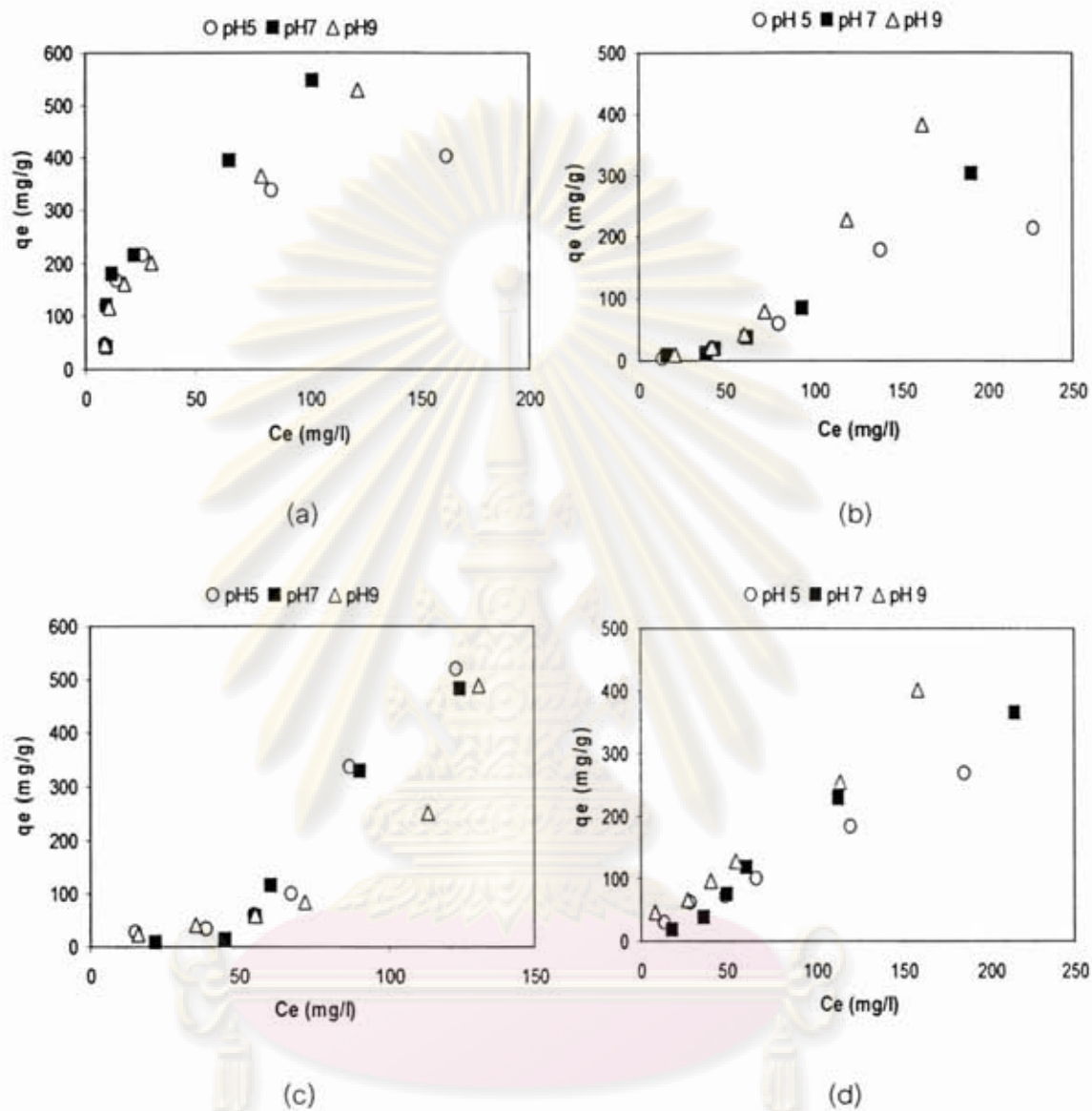
Figure 4.20 Adsorption capacities of PFOS on (a) PAC, (b) HMS, (c) A-HMS, (d) M-HMS, (e) OD-HMS, (f) Ti-HMS, (g) NaY and (h) HY zeolite, ionic strength 0.01 M, temperature 25±2°C
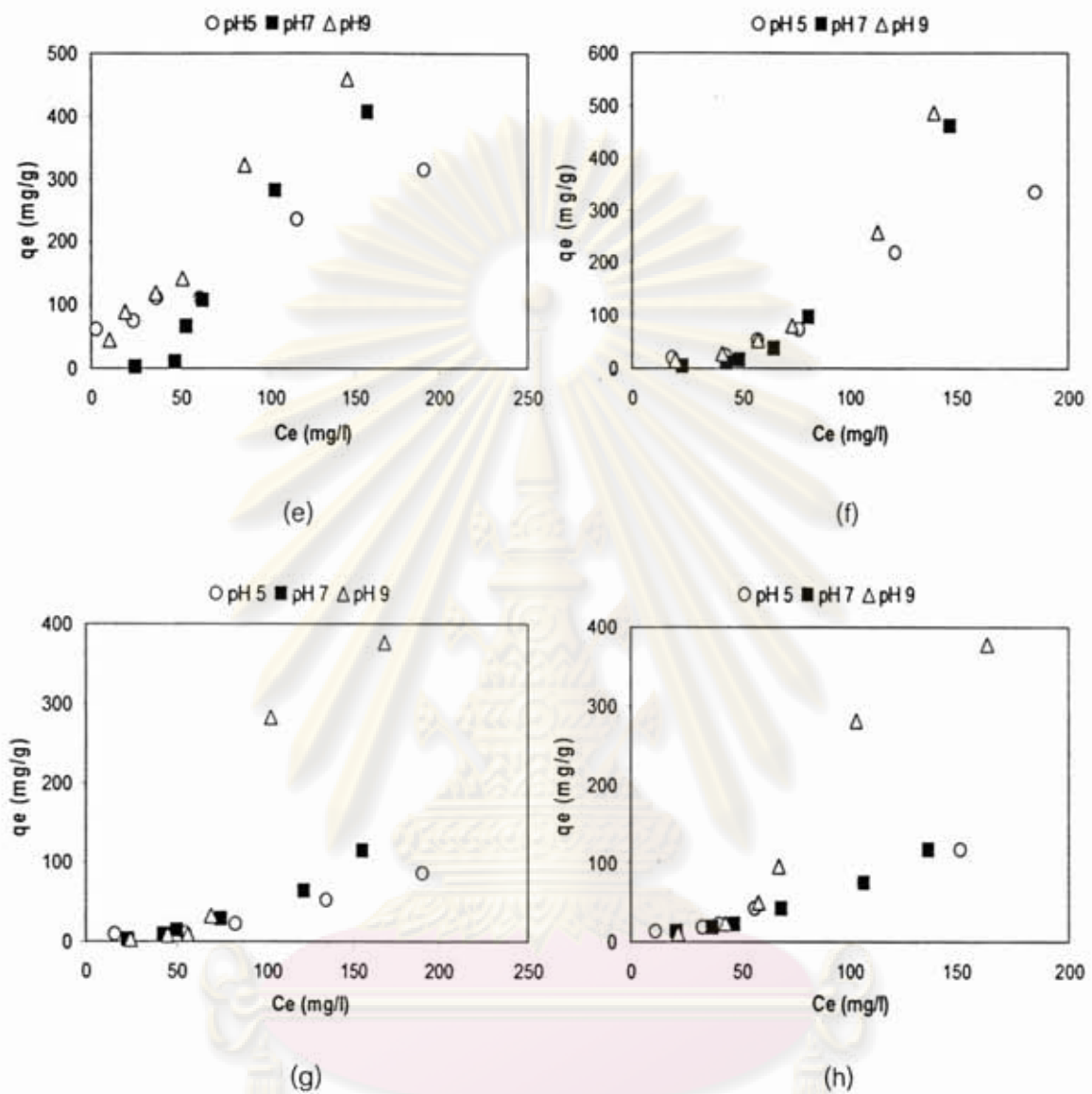
Figure 4.20 (cont.) Adsorption capacities of PFOS on (a) PAC, (b) HMS, (c) A-HMS, (d) M-HMS, (e) OD-HMS, (f) Ti-HMS, (g) NaY and (h) HY zeolite, ionic strength 0.01 M, temperature 25±2°C

At initial pH solution 5, surface of all adsorbents had higher positively charged than initial pH solution 7 which supposed to be enhance adsorption capacity by electrostatic attraction force between positively charged surface of adsorbents and negatively charged of PFOA and PFOS molecule. On contrary, surface of all adsorbents would be deprotonated and change to be negatively charged at initial pH solution 9.

Figures 4.19-4.20, the pH_{zpc} of PAC surface showed around 7. PAC showed highest adsorption of PFOA and PFOS at pH 7 following with pH 9 and pH 5, respectively. However, it might be indicated that adsorption of PFOA and PFOS on PAC was not influenced by decreasing of pH. Effect of electrostatic attraction force could not promoted adsorption capacity of PAC. Van Der Waals force seems to be played an important role in adsorption of PFOA and PFOS on PAC. However, at initial pH 5, adsorption capacity of PAC was lowest. It might be caused by electrostatic interaction between hydronium ion for water molecule and PFOS molecule. Water can be protonated to be hydronium ion, which exhibits stronger positively charged. Hence, interaction between positively charged of hydronium ion and negatively charged of PAC surface might be interfered by stronger electrostatic interacting between hydronium ion and PFOS, especially at low pH solution.

HMS showed highest adsorption of PFOA at initial pH 5 following with pH 7 and pH 9, respectively. Hence, electrostatic attraction can be affected to adsorption of PFOA on HMS. At initial pH 5, adsorption of PFOS on HMS was decreased even neutral charge of HMS surface did not change significantly from pH 4-6. It might be caused by electrostatic interaction between hydronium ion for water molecule and PFOS molecule. Water can be protonated to be hydronium ion, which exhibits stronger positive charge. Hence, interaction between hydronium ion and HMS surface might be interfered by stronger electrostatic interacting between hydronium ion and PFOS, especially at low pH.

A-HMS showed extremely high adsorption of PFOA and PFOS at initial pH 5 following with pH 7 and pH 9, respectively. These obtained result showed consistent with surface charge of A-HMS caused by decreasing of pH solution. Not only hydrogen bonds can be affected to adsorption of PFOA and PFOS on A-HMS, but also electrostatic attraction force.

M-HMS showed highest adsorption of PFOA at initial pH 5 following with pH 7 and pH 9, respectively. Electrostatic attraction can affect to adsorption of PFOA on M-HMS. On the other hands, at initial pH 5, adsorption of PFOS showed lower than pH 7 and pH 9, respectively. Hence, decreasing pH solution can enhance electrostatic interaction between hydrophobic PFOS molecule and hydronium ion in the water, which affect directly to hydrophobic surface of M-HMS.

OD-HMS showed highest adsorption of PFOA at initial pH 5 following with pH 7 and pH 9, respectively. Electrostatic attraction can be affected to adsorption of PFOA on OD-HMS. On the other hands, at initial pH 5, adsorption of PFOS showed lower than pH 7 and pH 9, respectively. Hence, decreasing pH solution can enhance electrostatic interaction between hydrophobic PFOS molecule and hydronium ion in the water, which affect directly to hydrophobic surface of OD-HMS.

Ti-HMS showed highest adsorption of PFOA at pH initial 5 following with pH 7 and pH 9, respectively. Effect of electrostatic attraction might cause increasing of PFOA adsorption on Ti-HMS. On the other hands, at initial pH 5, adsorption of PFOS showed lower than pH 7 and pH 9, respectively. Hence, decreasing pH solution can enhance electrostatic interaction between PFOS molecule and hydronium ion in the water, which affect directly to hydrogen bonding of PFOS on silanol groups of Ti-HMS.

NaY showed highest adsorption of PFOA at pH initial 5 following with pH 7 and pH 9, respectively. Effect of electrostatic attraction can increase adsorption of PFOA on NaY. On the contrary, at initial pH 9 adsorption of PFOS was extremely high

comparing with pH 7 and 5. However, at pH 5 and 7, surface charge of NaY did not change significantly caused a little bit higher adsorption capacity at pH 7 comparing with pH 5. It might be indicated that at high pH, repulsive interaction between negative charged hydroxide ion and PFOS could enhance adsorption capacity of PFOS on NaY.

HY showed highest adsorption of PFOA at pH initial 5 following with pH 7 and pH 9, respectively. Electrostatic attraction might enhance adsorption of PFOA on HY. On the contrary, at initial pH 9 adsorption of PFOS was extremely high comparing with pH 7 and 5 as same as NaY. It might be indicated that at high pH, repulsive interaction between negative charged hydroxide ion and PFOS could enhance adsorption capacity of PFOS on HY.

From above results, it might be suggested that, PFOA adsorption capacity on applied adsorbents such as HMS, A-HMS, M-HMS, OD-HMS, NaY and HY zeolite was highly affected by electrostatic force due to decreasing of pH, except hydrophobic and high complexity adsorbent as PAC. On the contrary, adsorption of PFOS on almost adsorbents was not affected by changing electrostatic force due to decreasing of pH solution, except A-HMS. Some obtained results can be indicated that it was not consistent with other research work (Qiang Yu et al., 2009), due to they found that effect of pH solution by decreasing of pH can be influenced to higher adsorption of PFOA and PFOS.

4.5 Regeneration efficiency of PFOS adsorbed HMS, M-HMS, OD-HMS and PAC by solvent extraction method

To study the regeneration efficiency of PFOS by solvent extraction method, in this study, HMS was chosen for representative of hydrophilic adsorbents. Including of OD-HMS and M-HMS also were chosen for representative of hydrophobic adsorbents. Furthermore, these hydrophilic and hydrophobic surface adsorbents were compared

regeneration efficiency with PAC. The solvent, which selected to extract PFOS from surface of adsorbents, was ethanol.

From Tables 4.11-4.14 reported PFOS recovery efficiencies from HMS, M-HMS, OD-HMS and PAC by solvent extraction method. Mixing time was set for 3 hrs at 25°C, according to time course data of preliminary testing of HMS by mixture of ethanol and water at ratio 5:5 (Punyapalakul and Takizawa, 2004). From Tables 4.11-4.14 recovery efficiency of PFOS from HMS, M-HMS, OD-HMS and PAC increased when ratio between solvent and water was increased. However, PFOS recovery efficiency of HMS and OD-HMS was reached 100% when ratio of mixture was exceeded 5:5. However, recovery efficiencies of M-HMS cannot reach 100%, although, using highest ratio of solvent and water. Furthermore, recovery efficiency of PFOS from PAC also cannot reach 100 %, although, pure solvent was applied. It might be caused by complexity of PAC surface, which causes stronger and more complicate bonding with PFOS molecule than high uniform surface functional group (silanol and octyl groups) of both synthesized HMSs (HMS and OD-HMS). However increasing of ethanol ratios could enhance extraction of PFOS from both M-HMS and PAC adsorbents. Hydroxyl group of alcohol molecule is expected to play an important role in hydrogen bonding competition with HMS surface. Hydrogen bonding of hydrophilic part (sulfonyl functional group) of PFOS and silanol groups of HMS was suggested to be broken and replaced by alcohol molecule in the mixtures. On contrary, competition of Van Der Waals interaction with perfluoroalkyl chain of PFOS is suggested for PAC and hydrophobic synthesized HMSs (OD-HMS and M-HMS).

Table 4.11 Recovery ratio of PFOS for HMS

Solvent : Water	Recovery ratio % (100 mg/50 ml of mixture)
10:0	108.272
7:3	105.136
5:5	114.157
4:6	74.744
3:7	71.504
2:8	68.472
1:9	58.689

Table 4.12 Recovery ratio of PFOS for M-HMS

Solvent : Water	Recovery ratio % (100 mg/50 ml of mixture)
10:0	87.190
7:3	86.947
5:5	87.985
4:6	47.250
3:7	41.861
2:8	35.236
1:9	30.774

Table 4.13 Recovery ratio of PFOS for OD-HMS

Solvent : Water	Recovery ratio % (100 mg/50 ml of mixture)
10:0	103.119
7:3	100.717
5:5	107.319
4:6	61.701
3:7	66.066
2:8	60.977
1:9	57.898

Table 4.14 Recovery ratio of PFOS for PAC

Solvent : Water	Recovery ratio % (100 mg/50 ml of mixture)
10:0	75.409
7:3	87.410
5:5	94.578
4:6	81.459
3:7	80.959
2:8	55.155
1:9	45.222

4.5.1 Effect of ratios of extract mixture volume and amount of adsorbents on PFOS recovery efficiency

For all adsorbents, the mixture of ethanol and water at 5:5 v/v was selected to study the effect of extractant-adsorbent ratio on PFOS recovery efficiency. Mixture and adsorbent ratios were varied from 250 to 8000 v/w and stirred in water bath at 25±2°C for 3 hrs. Figure 4.21 show recovery efficiencies of each adsorbent at various extractant-adsorbent ratios.
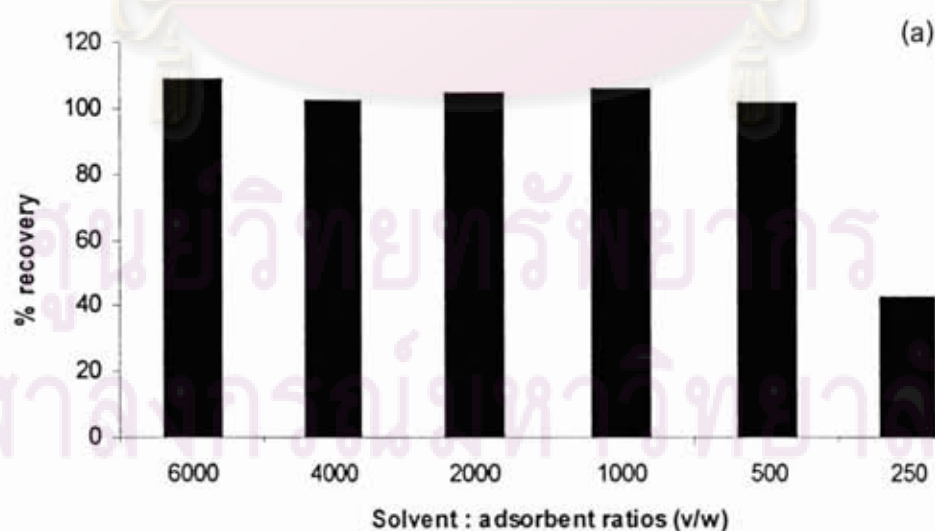
Figure 4.21 Effect of ratios between solvent mixture and PFOS adsorbed adsorbents (ml/g) on recovery efficiencies of PFOS: (a), HMS; (b), M-HMS; (c), OD-HMS; (d) PAC
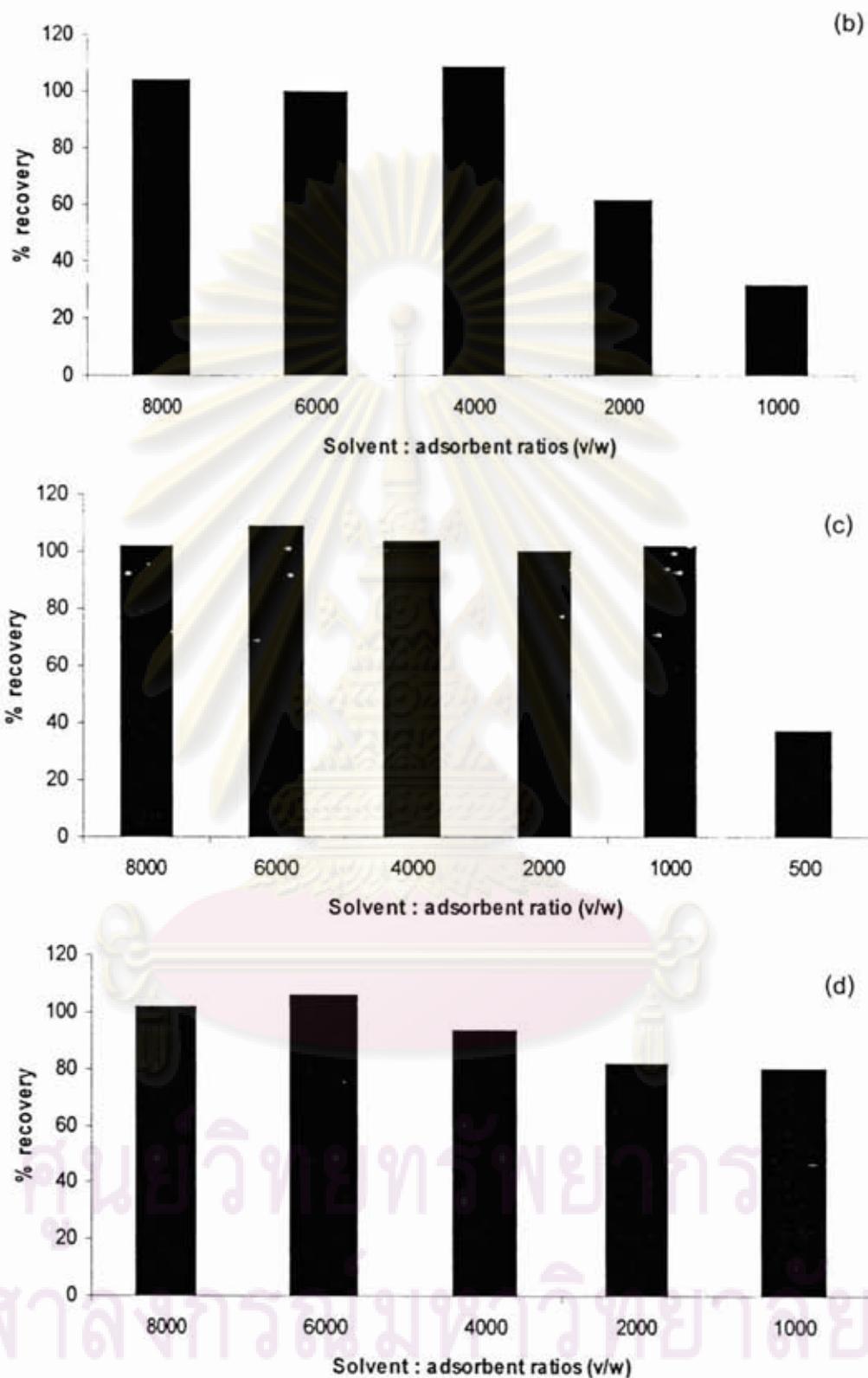
Figure 4.21 (cont.) Effect of ratios between solvent mixture and PFOS adsorbed adsorbents (ml/g) on recovery efficiencies of PFOS: (a), HMS; (b), M-HMS; (c), OD-HMS; (d) PAC

From the results in Figures 4.21 (a) and (c), recovery rates of HMS and OD-HMS were reached 100% at extractant-adsorbent ratios higher than 500 v/w% and 1,000 v/w%, respectively. At a ratio of 250 ml/g and 500 ml/g, PFOS recovery efficiencies of HMS and OD-HMS were 42 and 37 percent, respectively. Recovery efficiencies of M-HMS were reached 100% at extractant-adsorbent ratios higher than 4,000 v/w%. At a ratio of 1,000 ml/g and 2,000 ml/g, PFOS recovery efficiencies of M-HMS were 32 and 62 percent, respectively. However, PFOS recovery efficiencies of PAC (Figure 4.21(d)) decreased when the extractant-adsorbent ratios were reduced to less than 6,000 ml/g. From these results, it can be concluded that PFOS on HMS, OD-HMS and M-HMS surface can be recovered easier than on PAC surface, which might be caused by more complex surface of PAC. It can also be suggested that because of uniform surface functional groups, HMS, M-HMS and OD-HMS required less extract solution than PAC for the same recovery efficiency of PFOS.

4.5.2 Reused HMS and PAC efficiencies

PFOS adsorption isotherms of virgin adsorbents, extraction-regenerated adsorbents (Re-et-adsorbents) are shown in Figure 4.22. Solvent extraction of HMS, M-HMS, OD-HMS and PAC were repeated 3 times. From Figure 4.22, it was clearly showed that slightly decrease of HMS and PAC adsorption capacities were detected. But, repeating of extraction regeneration up to 3 times did not change adsorption capacities of HMS and PAC significantly. However, adsorption capacities of PFOS on regenerated functional grafted HMS (M-HMS and OD-HMS) did not change significantly, comparing with virgin one. Hydrophobic grafted surface functional groups can be protected collapse of silicate crystalline structure by capping hydrophilic silanol group protect Si-O-Si bonds from hydrolysis reaction, resulting in an increase in stability.

Hydrolysis reaction was suggested to cause residual of ethanol adsorbed on surface and collapse of HMS crystalline structure, which might relate to decrease of adsorption capacity up to 30%. Due to ethanol was adsorbed on the

surfaces of HMS by hydrogen bonding between silanol groups and hydroxyl part of molecule, caused decrease of adsorption capacity. Ethanol in the extraction mixture brings about hydrolysis reaction, which causes leaching of Si from crystalline structure by the following equation:

$$4Si-O-Si \ + \ 4H_2O \longrightarrow 4Si-OH + Si(OH)_4 \qquad ...(4.5)$$
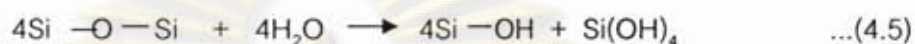
Shylesh and coworker (2008) reported that the structural collapse of mesoporous silicates in the presence of water is due to OH⁻ catalyzed silica hydrolysis, which subsequently decomposes order of materials. Hence, the increased quantity of hydroxide ion in both neutral and basic conditions causes of loss of mesopore order.

Furthermore, residual of ethanol on PAC surface might cause reduction of adsorption capacity of PAC up to 21%. Therefore, it might be suggested that adsorption capacities after solvent extraction of regenerated adsorbents are considered to be decreased by adsorption of solvent on the surfaces and collapse of crystalline structures.
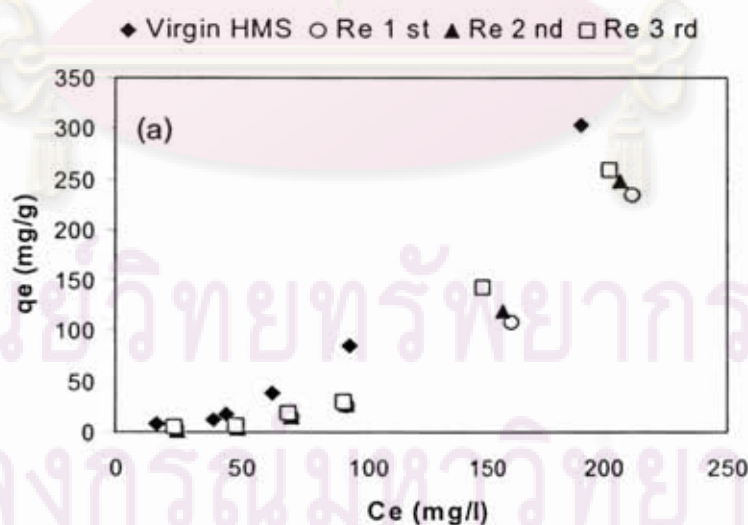
Figure 4.22 Comparison of PFOS adsorption isotherms of virgin adsorbents and Re-et-adsorbents (1ˢᵗ-3ʳᵈ), (a), HMS; (b), M-HMS; (c), OD-HMS, (d), PAC at initial pH solution 7, ionic strength 0.01 M, temperature 25±2°C
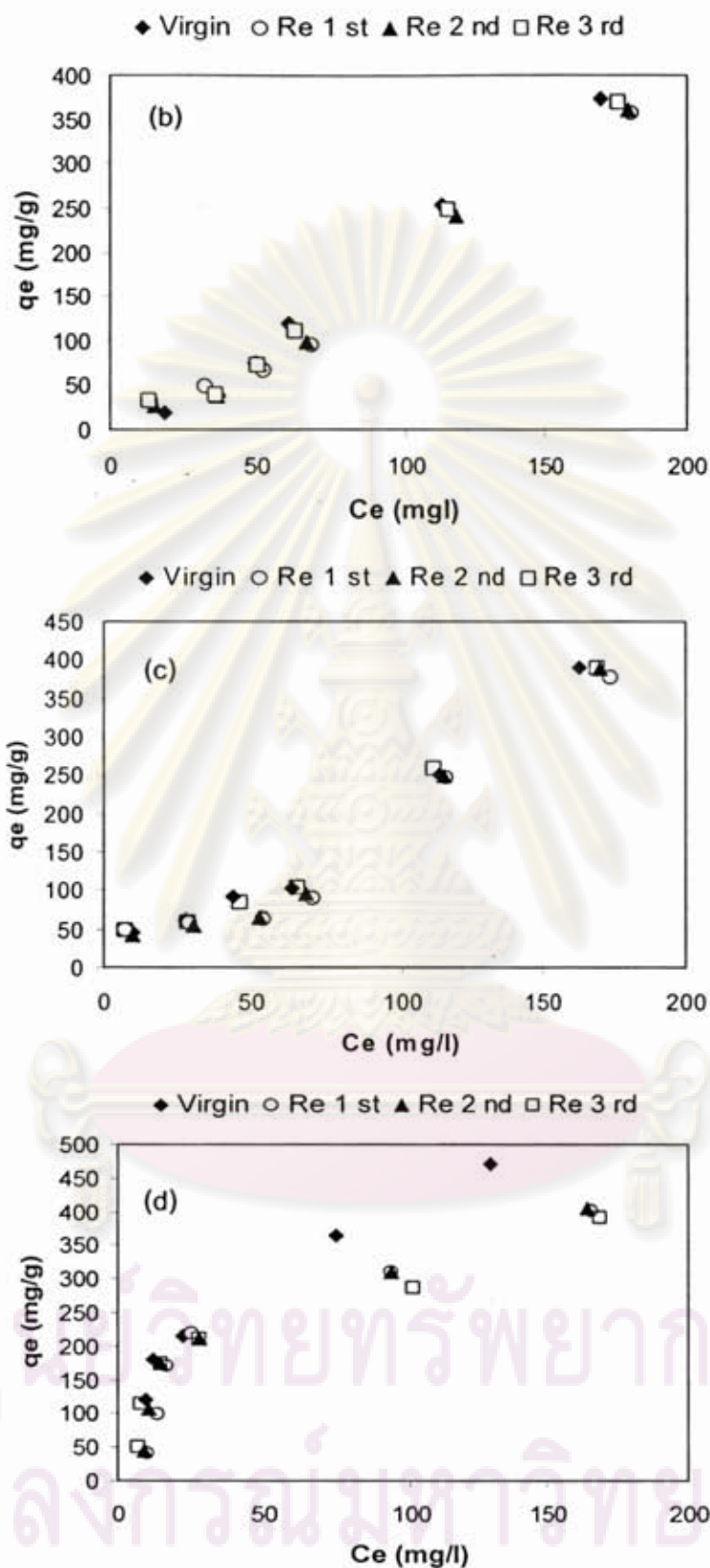
Figure 4.22 (cont.) Comparison of PFOS adsorption isotherms of virgin adsorbents and Re-et-adsorbents (1st-3rd), (a), HMS; (b), M-HMS; (c), OD-HMS, (d), PAC at initial pH solution 7, ionic strength 0.01 M, temperature 25±2°C

4.5.3 Physical characteristics of regenerated HMS, M-HMS and OD-HMS and their effects on adsorption capacities.

The adsorption capacities of HMS decreased after solvent extraction. However, effect of remained PFOS on adsorbent surfaces can be neglected, since; nearly 100% of adsorbed PFOS was recovered. Hence, effect of crystalline structures and pore characteristics of regenerated HMS, M-HMS and OD-HMS on adsorption capacities were investigated.

4.5.3.1 X-ray powdered diffraction patterns

XRD patterns of HMS, M-HMS and OD-HMS in series of virgin and Re-et of adsorbents were shown in Figures 4.23-4.25. XRD pattern of Re-et-HMS showed slight decreasing of two peak intensity at $2\theta = 2.31°$, consisting of (100) diffraction and $2\theta = 4.34°$, consisting of (200) diffraction. On the contrary, Re-et-M-HMS, and Re-et-OD-HMS showed slight decreasing of one peak intensity at $2\theta = 2.4°$ and 2.24°, consisting of (100) diffraction, suggesting a decline in the order of hexagonal structure (Peter *et al.*, 1994; Bagshaw *et al.*, 1995; Tanev and Pinnavaia, 1996; Liu *et al.*, 2006). However, crystalline structures of regenerated OD-HMS seem to be affected a little bit as same as regenerated HMS, since shifting and broader peaks of OD-HMS could not be detected.
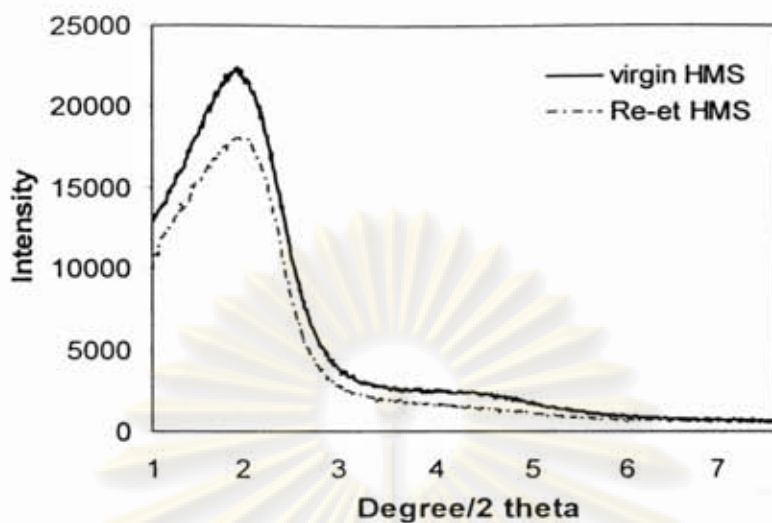
Figure 4.23 XRD powdered diffraction patterns of virgin HMS and Re-et-HMS
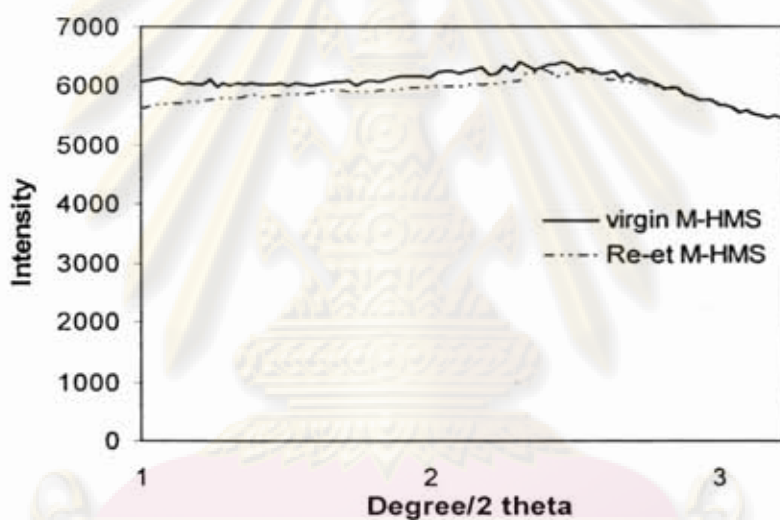
Figure 4.24 XRD powdered diffraction patterns of virgin M-HMS and Re-et-M-HMS
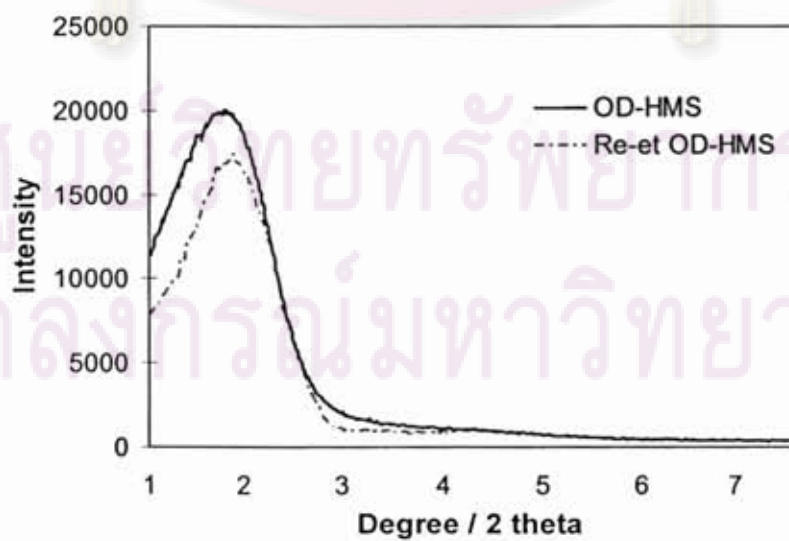
Figure 4.25 XRD powdered diffraction patterns of virgin OD-HMS and Re-et-OD-HMS

4.5.3.2 Surface areas and pore structure measurement by nitrogen adsorption isotherms

Surface structure parameters of each adsorbent were calculated and reported in Table 4.15. Surface areas and pore volumes of Re-et-HMS and Re-et-M-HMS were decreased, comparing with virgin HMS and M-HMS, respectively. But, pore volume of Re-et-M-HMS was not different from virgin M-HMS significantly. Increasing of pore size of Re-et-HMS and Re-et-M-HMS also was detected due to declining of crystalline structure and decreasing of surface areas. On the other hands, the obtained results of Re-et-OD-HMS indicated clearly increasing of surface areas, pore sizes and pore volumes comparing with virgin OD-HMS. However, the reason of this increasing is still unclear.

Table 4.15 Surface structure parameters of virgin and regenerated HMS, M-HMS and OD-HMS

Sample	BET surface area (m^2/g)	Average Pore Size (nm)	Pore Volume (mm^3/g)
Virgin HMS	712.24	2.60	773.42
Re-et-HMS	628.2	3.82	696.00
Virgin M-HMS	912.68	2.48	433.47
Re-et-M-HMS	688.3	2.56	439.80
Virgin OD-HMS	723.0	4.87	879.5
Re-et-OD-HMS	941.3	5.20	1,223.00

Decreasing of surface areas of HMS series are in consistent with decreasing of PFOS adsorption capacity, which shown in Figure 4.22. Adsorption capacity of Re-et-HMS showed a little reduction of the capacity. Although, surface areas of Re-et-M-HMS were decreased significantly, the effect on PFOS adsorption capacity still cannot be detected clearly. Moreover, Re-et-OD-HMS adsorbed capacity was not

decreased after regenerated. However, XRD patterns of Re-et-OD-HMS can prove a little collapse of hexagonal structure. Adsorption of PFOS on Re-et-OD-HMS did not change comparing with virgin OD-HMS significantly. It can be suggested that mixture of water and ethanol caused hydrolysis reaction between silicate structure and water, especially for Si-O-Si, causing the increase of collapse of the ordered mesoporous structure, consistent with detected physical characteristics.

4.5.3.3 Scanning Electron Microscope (SEM)

Figure 4.26 illustrate SEM micrographs of virgin and Re-et HMS, M-HMS and OD-HMS. From SEM pictures, collapse of Re-et-HMS particles were found a little bit after three time regeneration, consistent with XRD and nitrogen adsorption isotherm results. However, collapse of the particles shape or structures of regenerated OD-HMS and M-HMS cannot be detected clearly via SEM picture.
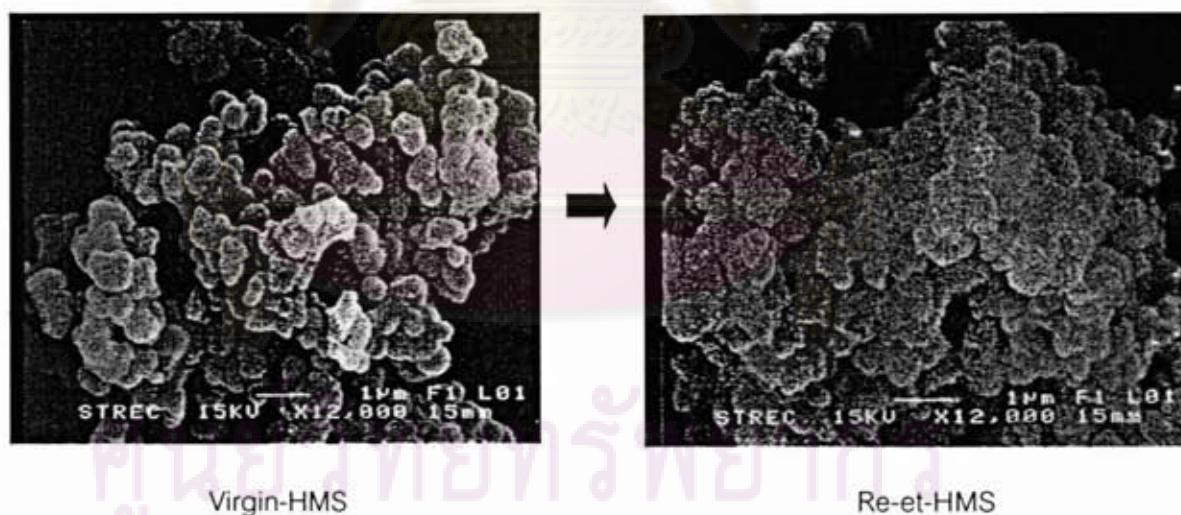
Virgin-HMS   Re-et-HMS

Figure 4.26 Comparison of SEM picture of virgin HMSs and Re-et-HMSs

Virgin-M-HMS

Re-et-M-HMS

Virgin-OD-HMS

Re-et-OD-HMS
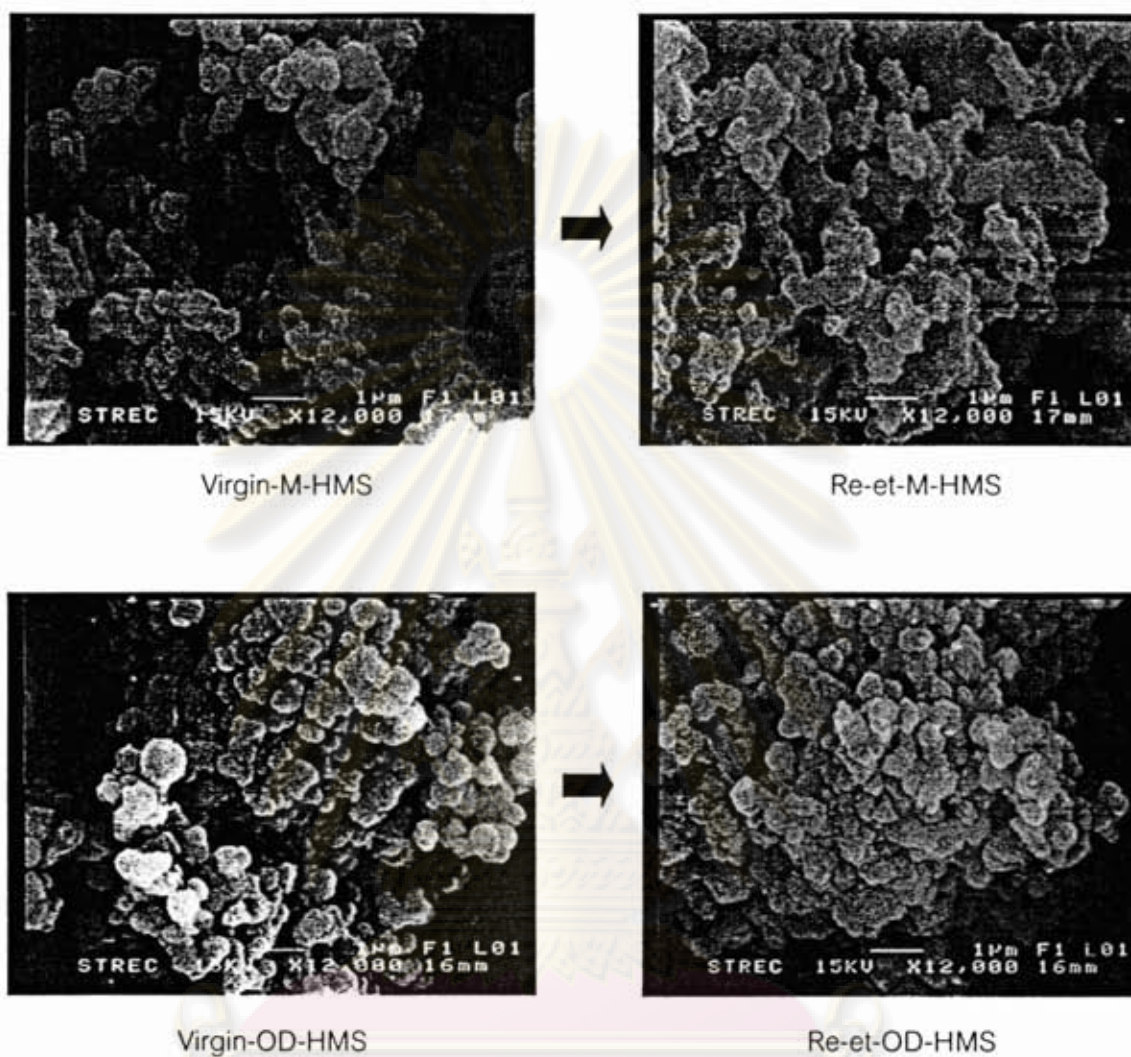
Figure 4.26 (cont.) Comparison of SEM pictures of virgin HMSs and Re-et-HMSs

CHAPTER V
CONCLUSIONS AND RECOMMENDATIONS

1. Conclusion

The ultimate goal of this study was to determine PFCs adsorption capacities of mesoporous synthesized HMSs and microporous zeolite in aqueous solution, compared with PAC. Effects of physico-chemical characteristics of these adsorbents and effects of molecular structures of PFCs were discussed base on adsorption kinetic and isotherm data.

The XRD patterns of functionalized HMSs exhibit very broad peak, indicating that the mesostructure of functionalized HMSs was less order. The specific surface areas of functionalized HMSs were decreased due to grafting of organic functional group, especially the presence of amino functional group. HMS and functionalized HMSs have average pore sizes in the range of mesopore scale (2-50 nm). Elemental analysis and FT-IR spectra can confirm the presence of amino and mercapto functional groups on the surface of functionalized HMSs. The presence of amino-functional groups on HMS gave the highest pH_{zpc}. Grafted organic functional groups by post grafting method can be prevented the collapse of crystalline comparing with direct co-condensation method.

Adsorption kinetic follows the pseudo-second-order model for PFCs adsorption on all adsorbents at initial pH 5, 7 and 9, indicating that the adsorption step may involve chemisorptions. The calculated q_e values agree well with the experimental q_e values. Effect of pH did not affect to equilibrium time for PFCs.

In this study, adsorption of PFCs on mesostructure (synthesized HMSs) and microstructure (PAC, NaY and HY zeolite) can be described as followed:

- PAC had highest adsorption capacity comparing with other adsorbents due to high surface area and complexity of function group on its surface.

- Combined effect of hydrogen bonds and electrostatic attraction force of hydrophilic adsorbents was the major force, which could enhance adsorption capacity of PFCs.

- Hydrophobic interaction or Van Der Waals force on hydrophobic adsorbents was an important force, which affect to adsorption of PFCs.

- In this study, surface area, pore volume and pore size of synthesized HMSs (A-HMS, M-HMS, OD-HMS, Ti-HMS and HMS) did not directly influence to adsorption capacities of PFCs.

- Grafted organic functional groups on adsorbents can directly affect adsorption of PFCs.

- Crystalline structure might affect to PFCs adsorption capacity, especially for PFOS at high equilibrium concentration.

- PFCs adsorption capacity was also affected by pH depending on pH_{zpc} of each adsorbent especially for PFOA.

- PFOS had higher adsorption capacity than PFOA, due to, different kinds of functional groups on molecular structure and solubility of PFOA and PFOS.

- Adsorption phenomenon of PFCs on all adsorbents can be fitted to Freundlich isotherm

For regeneration study, it can be concluded that HMS, M-HMS, OD-HMS can be regenerated by solvent extraction methods. Because of uniform surface functional groups, PFOS adsorbed on HMS, M-HMS and OD-HMS can be extracted nearly 100 percent. HMS, OD-HMS and M-HMS required lower amount of mixture of extract solution than PAC. Repeating of regeneration by solvent extraction did not affect the PFOS adsorption capacities of reused M-HMS and OD-HMS, significantly. Effect of hydrolysis by solvent-extraction process might decrease PFOS adsorption capacities of HMS up to 30%. Hydrophobicity caused by grafted functional groups can protect silicate crystalline

structure from hydrolysis reaction. Reused PAC had lower adsorption capacity than the virgin one about 21 %.

2. Application in engineering field

Nowadays, synthesis cost of synthesized HMSs as adsorbent is still high (approximately 20 bath/g) comparing with PAC commercial. However, in application of using synthesized HMSs as adsorbents in order to remove PFCs in real wastewater released from the industrial plant was recommended to use these materials as adsorbents. Due to synthesized HMSs which have specific properties as high uniform surface functional groups caused it have regenerated easily by solvent extraction method. Furthermore, these materials can easy to recover pollutant from the surface of adsorbates. According to this reason, the benefit of using these materials was performed by reduction amount of pollutants released to the environment. On the other hands, it also might be reduce the cost of substrate that used in an industrialized production process.

3. Recommendations

1. Effects of molecular structure of other kind of PFCs, for example, chain length, structure of hydrophilic part, etc, are still needed to evaluate the possibility to use silicate adsorbents for PFCs removal.

2. Selective adsorption of designable surface functional groups of silicate functional groups should be studied for increase the possibility to recover PFCs from wastewater and reuse.

3. Cost analysis have to be investigated comparing with other treatment method and worldwide commercial adsorbents such as PAC.

REFERENCES

3M Company. 1999. The science of organic fluorochemistry. USEPA docket: EPA-HQ-OPPT-2002-0043-0006. New York,

Ahn M.; Schaffner C.; and Giger W. 1999. Behavior of Alkylphenol polyethoxylate surfactants in the aquatic environment-III. Occurrence and elimination of their persistent metabolites during infiltration of river water to groundwater. Water Research 30 (1) : 37-46.

Al-Ghouti M.; Khraishes M.A.M.; Ahmad M.N.; and Allen S.J. 2003. The removal of dyes from textile wastewater : a study of the physical characteristics and adsorption mechanisms of diatomaceous earth. Journal of Environmental Management 69 : 229-238.

Anonymous. 2002. Environmental Protection Agency tentatively OKs PFOS for semiconductor industry. Solid State Technol. 45 : 32.

Aprile C.; Abad A.; Corma A.; and Garcia H. 2005. Synthesis and catalytic activity of periodic mesoporous materials incorporating gold nanoparticles. Journal of Materials Chemistry 15 : 4408-4413.

Armitage J. I. T.; Cousins K.; Prevedouros M.; MacLeod; Russell M. H.; Buck R. C.; and Korzeniowski S. H. 2006. Modeling global-scale fate and transport of perfluorooctanoate emitted from direct sources. Environ. Sci. Technol. 40 (22) : 6969-6975.

Bagshaw S A; Prouzet Ea; and Pinnavaia T J. 1995. Templating of mesoporous molecular sieves by nonionic polyethylene oxide surfactants. Science. 269 (5228) : 1242–1244.

Beck J. S.; Chu C. T-W.; Higgins J. B.; Kresge C. T.; Leonowicz M. E.; McCullen S. B.; Olson D. H.; Roth W. J.; Schlenker, J. L.; Schmitt K. D.; Sheppard E. W.; and Vartuli C. 1992. A New Family of Mesoporous Molecular Sieves Prepared with Liquid Crystal Templates. J. Am. Chem. Soc. 114 : 10834-10843.

Beck J.S.; Kresge C.T.; Kennedy G.J.; Vartuli J.C.; Schramm S.E.; and Roth W.J. 1994. Molecular or Supramolecular Templating: Defining the Role of Surfactant Chemistry in the Formation of Microporous and Mesoporous Molecular Sieves. Chem. Mater. 6 : 1816-1821.

Blasco T.; Corma A.; Navarro T.; and Pariente J.P. 1995. Synthesis, Characterization and Catalytic Activity of Ti-MCM-41 Structures. Journal of Cataysis 156 : 65-74.

Brunel D.; Cauvel A.; Fajula F.; and Direnzo F. 1995. MCM-41 Type Silicas asSupports for Immobilized Catalysts, Zeolites: A Refined Tool for Designing Catalytic Sites. Elsevier Science : 173-180.

Carrado K.A. 2000. Synthetic Organo- and Polymer-clays: Preparation, Characterization, and Materials Applications. Applied Clay Science 17 : 1-23.

Decottignies M.; Phalippou J.; and Zarzycki J. 1978. Synthesis of Glasses by Hot-pressing of Gels. Journal of Materials Science 13 : 2605-2615.

Dillert R.; Bahnemann D.; and Hidaka H. 2007. Light-induced degradation of perfluorocarboxylic acids in the presence of titanium dioxide. Chemosphere 67 (4) : 785-79.

Dimitrov S.; Walker J.D.; Lewis M.; Purdy R.; Kamenska V.; and Windle W. 2004. Predicting the biodegradation products of perfluorinated chemicals using CATABOL, SAR QSAR. Environ. Res. 15 : 69.

Ellis D.A.; Muir D.C.G.; Martin J.W.; and Mabury S.A. 2001. Thermolysis offluoropolymers as a potential source of halogenated organic acids in the environment. Nature 412 : 321–324.

Erkoc S.; and Erkoc F. 2001. Structural and electronic properties of PFOS and LiPFOS. J. Mol. Struct. (Theochem) 549 : 289–293.

Feng X.; Kim A.Y.; Fryxell G.E.; Liu J.; Kemner K.M.; and Wang L. Q. 1997. Functionalized Monolayers on Ordered Mesoporous Supports. Science 276 : 923–926.

Footitt A.; Brooke D.; and Nwaogu T. A. 2004. Perfluorooctane sulphonate: risk reduction strategy and analysis of advantages and drawbacks. RPA in association with BRE Environment. Norfolk, UK,

Giesy J.P.; and Kannan K. 2002. Perfluorochemical surfactants in the environment. Environ. Sci. Technol. 36 : 146A–152A.

Goss K-U. 2007. The pK$_a$ values of PFOA and other highly fluorinated carboxylic acids. Environ. Sci. Technol. 42 : 456-458.

Hansen K.; Johnson J. H. O.; Butenhoff J. L.; Eldridge J. S.; and Dick L. A. 2002. Quantitative characterization of trace levels of PFOS and PFOA in the Tennessee River. Environ. Sci. Technol. 36 (8) : 1681-1685.

Harada K.; Koizumi A.; Inoue K.; Saito N.; Kamiyama S.; Sasaki S.; Watanabe T.; and Yoshinaga T. 2004. The influence of time, sex and geographic factors on levels of perfluorooctane sulfonate and perfluorooctanoate in human serum over the last 25 years. J. Occup. Health 46 (2) : 141-147.

Hatfield T. L. 2001a. Hydrolysis reactions of perfluorooctanoic acid (PFOA). USEPA docket: EPA-HQ-OPPT-2002-0051-0013. 3M Environmental Laboratory,

Hatfield T. L. 2001b. Screening studies on the aqueous photolytic degradation of perfluorooctanoic acid (PFOA). USEPA docket: EPA-HQ-OPPT-2002-0051-0023. 3M Environmental Laboratory,

Higgins C.P.; and Luthy R.G. 2006. Sorption of perfluorinated surfactants on sediments. Environ. Sci. Technol. 40 : 7251–7256.

Hill A.J. 1999. Surfactant solubilization of polycyclic aromatic hydrocarbons from nonaqueous phase liquids. Master's Thesis, Department of Civil Engineering and Applied Mechanics McGill University.

Ho Yuh-Shan. 2003. Removal of copper ions from aqueous solution by tree fern. Water Research 37 (10) : 2323-2330.

Ho L. S. W. 2004. The removal of cyanobacterial metabolites from drinking water using ozone and 118 granular activated carbon. University of South Australia,

Holmström K. E.; Bignert A.; and Järnberg U. 2005. Temporal Trends of PFOS and PFOA in Guillemot Eggs from the Baltic Sea, 1968-2003. Environ. Sci. Technol. 39 (1) : 80-84.

Hori H.; Hayakawa E.; Einaga H.; Kiatagawa H.; Koike K.; Arakawa R.; Kutsuna S.; and Ibusuki T. 2004a. Decomposition of environmentally persistent perfluorooctanoic acid in water by photochemical approaches. Environ. Sci. Technol. 38 (22) : 6118-6124.

Hori H.; Nagaoka Y.; Yamamoto A.; Sano T.; Yamashita N.; Taniyasu S.; Kutsuna S.; Osaka I.; and Arakawa R. 2006. Efficient decomposition of environmentally persistent perfluorooctanesulfonate and related fluorochemicals using zerovalent iron in subcritical water. Environ. Sci. Technol. 40 (3) :1049-1054.

Hsien C.T.; and Teng H. 1999. Influence of mesopore volume and adsorbate size on adsorption capacities of activated carbons in aqueous solutions. Carbon 38 : 863-869.

Hudson S.; Hodnett B.K.; Magner E.; and Cooney J. 2005. Methodology for the Immobilization of Enzymes onto Mesoporous Materials. J. Phys. Chem. B 109 : 19496-19506.

Inagaki S.; Kuroda K.; and Fukushima Y. 1993. Synthesis of Highly Ordered Mesoporous Materials from a Layered Polysilicate. J. Chemical Society.Chemical communications : 680.

Janos P.; Buchtova H.; and Ryznarova M. 2003. Sorption of dyes from aqueous solutions onto fly ash. Water Res. 37 : 4938–4944.

Jiansheng Li; Jiangyan Zhao; Lianjun Wang; Xiaoyu Miao; Xiuyun Sun; and Yanxia Hao. 2007. Synthesis amino-functionalization of mesoporous silica and its adsorption of Cr(VI). J. Colloid Interface Sci.

Johnson R.L.; Anschutz A.J.; Smolen J.M.; Simcik M.F.; and Penn R.L. 2007. The adsorption of perfluorooctane sulfonate onto sand, clay, and iron oxide surfaces. J. Chem. Eng. 52 : 1165–1170.

Kannan K.; Jones E.; Gorzelany J.F.; Koistinen J.; Geisey J.P.; Beckman K.; Hansen K.J.; Nyman M.; Helle P.D.; and Evans T. 2001. Accumulation of perflurooctane sulfonate in marine mammals. Environ. Sci. Technol. 35 : 1593.

Kannan K.; Oehme G.; Falandysz J.; Giesy J.P.; Corsolini S.; and Focardi S. 2002a. Perfluorooctanesulfonate and related fluorinated hydrocarbons in marine mammals, fishes, and birds from coasts of the Baltic and the Mediterranean Seas. Environ. Sci. Technol. 36 : 3210.

Kannan K.; Giesy J.P.; Hansen K.J.; and Wade T.L. 2002b. Perfluorooctane sulfonate in oyster, Crassostrea virginica, from the Gulf of Mexico and the Chesapeake Bay, USA, Arch. Environ. Contam. Toxicol. 42 : 313.

Kei Inumaru; Junichi Kiyoto; and Shoji Yamanaka, Royal Society of Chemistry. 2000. Molecular selective adsorption of nonylphenol in aqueous solution by organo-functionalized mesoporous silica[Online]. Available from: http://www.rsc.org/ej/CC/2000/b002301i.pdf[2008, November 23]

Kissa E. 2001. Fluorinated Surfactants and Repellents, second ed. Marcel Dekker. New York,

Koon Fung Lam; Gordon McKay; Ka Yee Ho; and King Lun Yeung. 2004. Selective Ordered Mesoporous Silica Adsorbents. J. Phys. Chem. 110.

Kruk M.; Sayari A.; and Jaronice M. 1997. Structure and Surface Properties of Siliceous and Titanium-modified HMS Molecular Sieves. Microporous Materials 9 : 173-182.

Lee B.H.; Lee H.J.; Yi J.H.; and Kim Y.H. 2001. Synthesis of functionalized porous silicas via templating method as heavy metal ion adsorbents: the introduction of surface hydrophilicity onto the surface of adsorbents. Microporous and Mesoporous Materials 50 (1) : 77-90.

Liu J.; Kim A. Y.; Fryxell G. E.; Wang L. Q.; Gong M.; and Feng X. 1998. Hybrid mesoporous materials with functionalized monolayers. Adv. Mater. 10 : 1-5.

Liu Hong; Guanzhong Lu; Yanglong Guo; Yun Guo; and Junsong Wang. 2006. Synthesis of framework-substituted Fe-HMS and its catalytic performance for phenol hydroxylation. Nanotechnology 17 : 997-1003.

Maria Chong A.S.; and X.S. Zhao. 2004. Design of large-pore mesoporous materials for immobilization of penicillin G acylase biocatalyst. Catalyst Today 93-95 : 293-299.

Martin J. W.; Muir D. C. G.; Solomon K. R.; and Mabury S. A. 2003a. Bioconcentration and tissue distribution of perfluorinated acids in rainbow trout (*oncorhynchus mykiss*). Environ. Toxicol. Chem. 22 (1) : 196-204.

Martin J. W.; Muir D. C. G.; Solomon K. R.; and Mabury S. A. 2003b. Dietary accumulation of perfluorinated acids in juvenile rainbow trout (*oncorhynchus mykiss*). Environ. Toxicol. Chem. 22 (1) : 189-195.

Martin J. W.; Braune B. M.; Muir D. C. G.; Hoekstra P. F.; Smithwick M. M.; and Mabury S. A. 2004b. Identification of Long-Chain Perfluorinated Acids in Biota from the Canadian Arctic. Environ. Sci. Technol. 38 (2) : 373-380.

Mercier L.; and Pinnavaia T. J. 1997. Access in mesoporous materials: Advantages of a uniform pore structure in the design of a heavy metal ion adsorbent for environmental remediation. Adv. Mater. 9 : 500-503.

Mercier L.; and Pinnavaia T.J. 2000. Direct synthesis of hybrid organic-inorganic nanoporous silica by a neutral amine assembly route: structure-function control by stoichiometric incorporation of organosiloxane molecules. Chem Mater. 12 : 188-196.

Messina P.V.; and Schulz P.C. 2006. Adsorption of reactive dyes on titania-silica mesoporous materials. Journal of Colloid and Interface Science 299 : 305-320.

Minnesota Department of Health. 2007. Environmental Health Information - Perfluorochemicals and Health, Minnesota. US,

Newalkar B.L.; Choudary N.V.; Vijayalakshmi R.P.; Kumar O.; Bhat T.S.G.; Komarneni S.; and Turaga U.T. 2003. Adsorption of light hydrocarbons on HMS type mesoporous silica. Microporous and Mesoporous Materials 65 : 267-276.

OECD. 2002. Co-operation on existing chemicals hazard assessment perfluorooctane sulfonate (PFOS) and its salts. ENV/JM/RD(2002)17/FINAL. New York,

Partiff G.D.; and Rochester C.H. 1983. Adsorption of Small Molecules, Adsorption from Solution at the Solid/Liquid Interface. Academic Press,

Peter T.; Tanev Malama Chibwe; and Thomas Pinnavaia J. 1994. Titanium-containing mesoporous molecular sieves for catalytic oxidation of aromatic compounds. Nature 368 : 321-323.

Poulsen P.B.; Jensen A.A.; and Wallstrom E. 2005. More environmentally friendly alternatives to PFOS-compounds and PFOA. Environmental Protection Agency, Danish Ministry of the Environment,

Prevedouros K.; Cousins I.T.; Buck R.C.; and Korzeniowski S.H. 2006. Sources, fate and transport of perfluorocarboxylates. Environ. Sci. Technol. 40 : 32–44.

Punyapalakul P.; and Takizawa S. 2004. Effect of Organic Grafting Modification of Hexagonal Mesoporous Silicate on Haloacetic Acid Removal. Environmental Engineering Forum 44 : 247-256.

Punyapalakul P.; and Takizawa S. 2004. Removal of Alkylphenol Polyethoxylates Using Hexagonal Mesoporous Silicate. Degree of Doctor of Philosophy Department of Urban Engineering Graduate School of Engineering The university of Tokyo Japan.

Punyapalakul P.; and Takizawa S. 2006. Selective Adsorption of Nonionic Surfactant on Hexagonal Mesoporous Silicate (HMSs) in the present of Ionic Dyes. Water research 40 : 3177-3184.

Qiang Yu; Ruiqi Zhang; Shubo Deng; Jun Huang; and Gang Yu. 2009. Sorption of perfluorooctane sulfonate and perfluorooctanoate on activated carbons and resin: Kinetic and isotherm study. water research : 1 – 9.

Remde A.; and Debus R. 1996. Biodegradability of fluorinated surfactants under aerobic and anaerobic conditions. Chemosphere 52 : 1563.

Renner R. 2001. Growing concern over perfluorinated chemicals. Environ. Sci. Technol. 35 (7) : 154-160.

Robert I.; Gordon Kennedy J.; Edward; Maginn; Mohan Kalyanaraman; and Nooney. 2000. Heavy Metal Remediation Using Functionalized Mesoporous Silicas with Controlled Macrostructure. Langmuir 17 : 528-533.

Rosen M. J. 1989. Surfactant and interfacial phenomena. 2 nd. John Wiley & Sons : New Jersey,

Rouse J.D.; Furukawa K.; and Hirata O.S. 2001. Influence of diphenyloxide disulfonate surfactants on biodegradation of hydrocarbons. The International Journal 3 : 23-36.

Roy S.; Bandyopadhyay S.; and Chakravorty D. 1996. Sol-gel Synthesis of Colloidal Silica Using Cyclohexane. Journal of Materials Science Letter 15 : 1872-1874.

Saito N.; Koizumi A.; Harada K.; Nakatome K.; Sasaki K.; and Yoshinaga T. 2003. Perfluorooctane sulfonate concentrations in surface water in Japan. Arch. Environ. Contam. Toxicol. 45 (2) : 149-158.

Santanu Paria; and Khilar Kartic C. 2004. A review on experimental studies of surfactant adsorption at the Hydrophilic solid–water interface. Advances in Colloid and Interface Science 110 : 75–95.

Schaefer A., American Chemistry Society. 2006. Perfluorinated surfactants contaminate German waters[Online]. Available from: http://pubs.acs.org/doi/abs/10.1021/es062811u[2008, November 1]

Schröder H. F. 2003. Determination of fluorinated surfactants and their metabolites in sewage sludge samples by liquid chromatography with mass spectrometry and tandem mass spectrometry after pressurised liquid extraction and separation on fluorine-modified reversed-phase sorbents. J. Chromatogr. A 1020 (1) : 131-151.

Schröder H. F.; and Meesters R. J. W. 2005. Stability of fluorinated surfactants in advanced oxidation processes - A follow up of degradation products using flow injection-mass spectrometry, liquid chromatography-mass spectrometry and liquid chromatography-multiple stage mass spectrometry. J. Chromatogr. A 1082 (1) : 110-119.

Schulthess C.P.; and Sparks D.L. 1986. Back titration technique for proton isotherm modeling of oxide surfaces. Soil Sci. Soc. Am. J. 50 : 1406-1411.

Shylesh S.; Prinson P.; Samuel; Sheetal Sisodiya; and Singh A. P. 2008. Periodic Mesoporous Silicas and Organosilicas: An Overview Towards Catalysis. Catal Surv Asia 12 : 266–282.

Sindia M.; Rivera-Jimnez; and Arturo Hernandez-Maldonado J. 2008. Nickel(II) grafted MCM-41: A novel sorbent for the removal of Naproxen from water. Microporous and Mesoporous Materials.

Skutlarek D. M.; Exner; and Faerber H. 2006. Perfluorinated surfactants in surface and drinking water. Environ. Sci. Pollut. Res. 13 : 299–307.

Smithwick M.; Derocher A. E.; Sonne C.; Muir D. C. G.; Born E. W.; Gabrielsen G. W.; Stirling I.; Nagy J.; Martin J. W.; Solomon K. R.; Taylor M. K.; Dietz R.; Letcher R. J.; Mabury S. A.; and Evans T. J. 2005. Circumpolar study of perfluoroalkyl contaminants in polar bears (Ursus maritimus). Environ. Sci. Technol. 39 (15) : 5517-5523.

So M. K.; Zheng J.; Giesy N. J. P.; Lam P. K. S.; Taniyasu S.; Im S. H.; Yamashita; and Fang Z. 2004. Perfluorinated compounds in coastal waters of Hong Kong, South China, and Korea. Environ. Sci. Technol. 38 (15) : 4056-4063.

Soonglerdsongpha. 2006. Removal of Haloacetic acid by adsorption on mesoporous silicates. Degree of Master of Science Program in Environmental Management Graduate School Chulalongkorn University.

Tanev P.T.; and Pinnavaia T.J. 1994. Titanium-containing mesoporous molecular sieves for catalytic oxidation of aromatic compounds. Letter to Nature 368 : 321-323.

Tanev P.T.; and Pinnavaia T.J. 1995 A neutral templating route to mesoporous molecular sieves. Science 267 : 865-867.

Tanev P.T.; and Pinnavaia T.J. 1996. Mesoporous Silica Molecular Sieves Prepared by Ionic and Neutral Surfactant Templating: A Comparison of Physical Properties. Chem. Mater. 8 : 2068-2079.

Tang C.Y.Y.; Robertson A.P.; Criddle C.S.; Leckie J.O.; and Fu Q.S. 2006. Use of reverse osmosis membranes to remove perfluorooctane sulfonate (PFOS) from semiconductor wastewater. Environ. Sci. Technol. 40 : 7343–7349.

Thieme M.; and Schüth F. 1999. Preparation of a mesoporous high surface area titanium oxo phosphate via a non-ionic surfactant route. Microporous and Mesoporous Materials 27 : 193-200.

Tuel A. 1999. Modification of Mesoporous Silicas by Incorporation of heteroelements in the Framework. Microporous and Mesoporous Materials 27 : 151-169.

US EPA. 2002. Revised draft hazard assessment of perfluorooctanoic acid and its salts. U.S. EPA Administrative Record AR226-1136: Environmental Protection Agency,

Valeria Ochoa-Herrera; and Reyes Sierra-Alvarez. 2008. Removal of perfluorinated surfactants by sorption onto granular activated carbon, zeolite and sludge. Chemosphere.

Wang L.; Wang Z.; Zhao J.; Yuan Z.; Yang H.; and Zhao. 1999. Preparation of Mesoporous Silica by Co-precipitation in the Presence of Non-ionic Surfactant. Materials Chemistry and Physics 59 : 171-174.

Wang N.; Szostek B.; Gannon J.T.; Sulkecki L.M.; Folsom P.W.; Buck R.C.; Capka V.; and Berti W.R. 2005. Fluorotelomer alcohol biodegradation – direct evidence that perfluorinated carbon chains breakdown. Environ. Sci. Technol. 39 : 7516–7528.

Yamada T.; Kaiser M. A.; Taylor P. H.; Buck R. C.; and Giraud R. J. 2005. Thermal degradation of fluorotelomer treated articles and related materials. Chemosphere 61 (7) : 974-984.

Yamashita G.; Petrick K.; Kannan S.; Taniyasu T.; Gamo; and Horii Y. 2005. A global survey of perfluorinated acids in oceans. Mar. Pollut. Bull. 51 : 658.

Yiu H.H.P.; and Wright P.A. 2005. Enzymes supported on ordered mesoporous solids: a special case of an inorganic-organic hybrid. Journal of Materials Chemistry 15 : 3690-3700.

Yoshitake H.; Koiso E.; Horie H.; and Yoshimaru H. 2005. Polyamine-functionalized mesoporous silicas: Preparation, structural analysis and oxyanion adsorption. Microporous and Mesoporous materials 85 : 183-194.

Yue Y.H.; Tu. Sun Y.; Xu; and Gao Z. 1998. Catalytic Activities and properties of AlHMS Mesoporous Molecular Sieve. Applied Catalysis A: General 175 : 131-137.

Zhang P.; Yu G.; Chen J.; Zhang L.; and Chang X. 2005b. Method for defluorinating and degrading complete fluorine substituted compounds. No.CN1680219-A CN10011126 07. Univ Qinghua (Uyqi),

APPENDICES
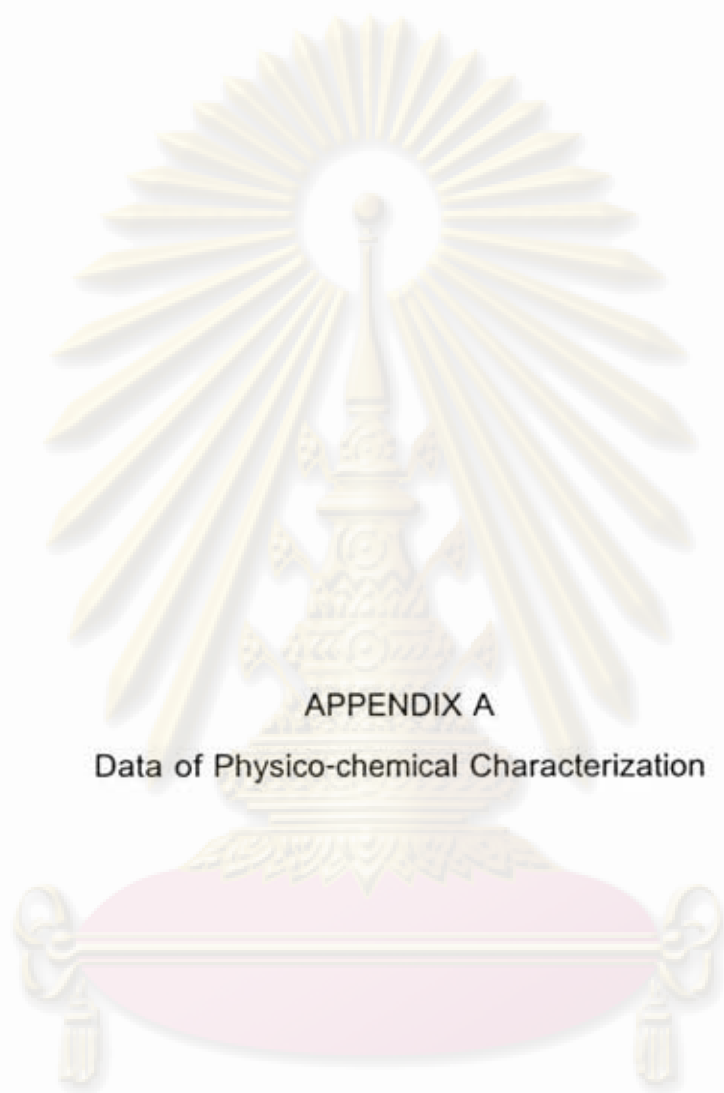
APPENDIX A

Data of Physico-chemical Characterization

ศูนย์วิทยทรัพยากร
จุฬาลงกรณ์มหาวิทยาลัย

Table A1 Data from elemental analysis for total nitrogen and sulfur content

Total Nitrogen content

Name	TN (mg)	Weight (g)	TN (g/g)	%N
A-HMS	0.8865	0.06	0.01477	1.477498

Total Sulfur content

Name	Mass of S (g)	Weight (g)	TS (g/g)	%S
M-HMS	0.0105	0.1057	0.0992	9.9243

Table A2 Data from calculation of surface charge of HMS

Sample	pH	Surface charge (C/g)
1	3.39	20.6894
2	3.6	8.8539
3	3.78	7.3326
4	4.06	2.1769
5	4.37	1.5538
6	4.99	-0.0495
7	5.42	-0.8257
8	5.97	-2.0218
9	6.7	-8.4018
10	7.24	-20.5957
11	8.23	-33.4557
12	8.56	-54.58
13	8.94	-115.0719

Table A3 Data from calculation of surface charge of A-HMS

Sample	pH	Surface charge (C/g)
1	8.37	47.683
2	8.68	22.519
3	8.7	10.64
4	8.73	1.095
5	8.79	-3.612
6	8.81	-13.353
7	8.84	-25.043
8	8.9	-48.706
9	8.8	-1.464

Table A4 Data from calculation of surface charge of M-HMS

Sample	pH	Surface charge (C/g)
1	8.63	-24.0164
2	7.56	-9.5771
3	7.01	-4.7963
4	6.62	-2.3749
5	6.14	-0.0338
6	4.96	1.4146
7	4.4	1.9738
8	3.97	2.5858
9	3.45	2.3544

Table A5 Data from calculation of surface charge of OD-HMS

Sample	pH	Surface charge (C/g)
1	3.89	-24.0164
2	4.12	-9.5771
3	4.36	-4.7963
4	4.66	-2.3749
5	5.09	-0.0338
6	5.66	1.4146
7	6.17	1.9738
8	7.42	2.5858

Table A6 Data from calculation of surface charge of Ti-HMS

Sample	pH	Surface charge (C/g)
1	6.79	47.251
2	7.4	23.583
3	7.42	11.755
4	7.63	2.259
5	7.71	-2.541
6	7.8	-12.219
7	8.02	-23.902
8	8.24	-47.253

Table A7 Data from calculation of surface charge of NAY zeolite

Sample	pH	Surface charge (C/g)
1	4.81	42.801
2	5.08	21.474
3	5.2	10.135
4	5.49	1.51
5	5.88	-2.012
6	6.68	-11.539
7	6.96	-22.501
8	7	-47.725

Table A8 Data from calculation of surface charge of HY zeolite

Sample	pH	Surface charge (C/g)
1	3.88	16.125
2	4.08	3.865
3	4.18	-3.657
4	4.22	-11.658
5	4.26	-15.363
6	4.32	-23.61
7	4.41	-31.319
8	4.65	-53.651

Table A9 Data from calculation of surface charge of PAC

Sample	pH	Surface charge (C/g)
1	6.62	23.605
2	6.73	11.911
3	6.75	2.292
4	6.81	-2.434
5	6.94	-12.07
6	7.01	-23.885
7	7.07	-46.387
8	6.87	-0.014

ศูนย์วิทยทรัพยากร
จุฬาลงกรณ์มหาวิทยาลัย
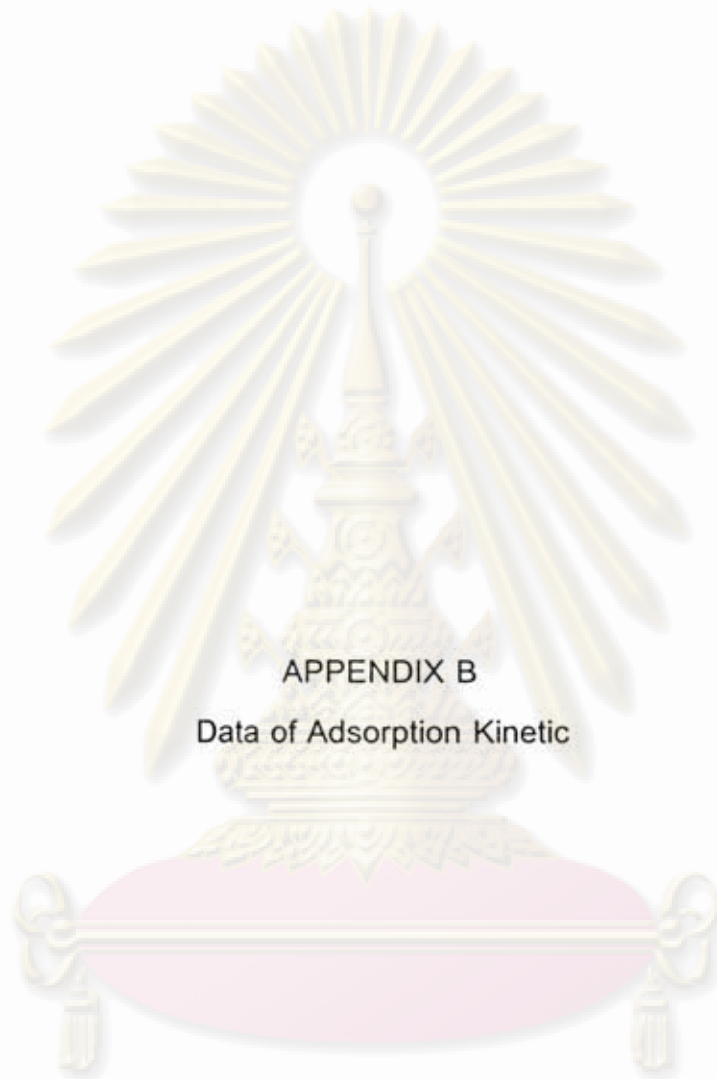
APPENDIX B

Data of Adsorption Kinetic

ศูนย์วิทยทรัพยากร
จุฬาลงกรณ์มหาวิทยาลัย

1. Method of prepared blank in adsorption experiments

1. The amount ratio of adsorbent to Milli-Q water, which fixed initial pH solution and ionic strength at 0.01 M by phosphate buffer were set at 0.01 g: 30 ml same as condition of prepared sample.

2. Blank solution was shaken in shaking water bath at 25±2°C, 150 rpm until equilibrium. The condition and equilibrium time of experiment process used as same as sample.

3. After that it was filtered by filter paper no.42.

4. Then the concentration of organic species dissociate in solution were analyzed by using Total Organic Carbon (TOC) Analyzer (TOC-VCPH), which used standard curve as same as sample and analyzed blank together with sample.

Table B1 sample of value of TOC value of PFOS adsorbed on OD-HMS at initial pH solution 7

Total TOC value (mg/l)	TOC value of blank water (mg/l)	TOC value of blank OD-HMS (mg/l)	weight (g)	Volume (l)	TOC value of rest PFOS (mg/l)	C_e (mg/l)	Adsorption Capacity (mg/g)
8.802	0.2545	4.14	0.0102	0.03	4.4075	24.48	1.53
15.21	0.2545	4.14	0.0108	0.03	10.8155	46.20	10.55
17.08	0.2545	4.14	0.0102	0.03	12.6855	52.54	66.05
19.76	0.2545	4.14	0.0108	0.03	15.3655	61.63	106.59
31.85	0.2545	4.14	0.0104	0.03	27.4555	102.62	280.92
48.09	0.2545	4.14	0.0105	0.03	43.6955	157.67	406.66

TOC value of rest PFOS (mg/l) = Total TOC value (mg/l) - TOC value of blank water (mg/l) - TOC value of blank OD-HMS (mg/l)

Table B2 Data from Adsorption kinetic of PAC, HMS, A-HMS, M-HMS, OD-HMS, Ti-HMS, NAY and HY zeolite at initial pH 5

Time (hr)	Concentration of PFOA after adsorption (mg/l)							
	PAC	HMS	A-HMS	M-HMS	OD-HMS	Ti-HMS	NaY	HY
0	300.00	100.00	100.00	100.00	100.00	100.00	100.00	100.00
0.003	239.66	99.13	99.36	95.10	98.42	96.25	96.24	97.14
0.083	233.14	98.52	89.80	95.76	89.28	95.70	96.95	96.63
0.167	232.87	98.14	88.65	93.02	85.61	89.78	95.35	98.23
0.5	228.61	98.13	86.46	96.43	84.78	90.43	91.85	95.93
1	226.11	97.57	83.34	93.25	80.94	89.54	93.69	96.87
3	223.54	96.40	84.37	96.53	85.52	90.05	94.41	94.06
5	222.76	95.88	82.37	92.14	81.99	90.23	91.44	96.70
10	222.21	94.16	81.29	89.22	74.14	88.29	93.05	92.61
24	221.86	94.19	81.37	88.99	74.48	87.90	92.85	91.91
30	221.08	93.96	80.71	89.28	74.05	87.18	93.11	91.95
48	220.83	93.99	80.67	89.15	73.99	87.08	93.03	91.35

Table B3 Data from Adsorption kinetic of PAC, HMS, A-HMS, M-HMS, OD-HMS, Ti-HMS, NAY and HY zeolite at initial pH 5

Time (hr)	Concentration of PFOS after adsorption (mg/l)							
	PAC	HMS	A-HMS	M-HMS	OD-HMS	Ti-HMS	NaY	HY
0	300.00	100.00	100.00	100.00	100.00	100.00	100.00	100.00
0.003	128.38	93.73	92.02	93.18	80.83	94.60	96.08	92.91
0.083	128.28	92.14	79.64	92.90	75.82	93.05	94.81	94.13
0.167	126.97	95.60	72.44	89.55	74.11	90.97	93.20	89.89
0.5	126.77	90.79	71.42	74.69	76.34	88.43	93.87	87.69
1	123.89	76.72	73.22	73.53	75.55	82.25	93.04	88.77
3	121.80	80.03	72.34	72.95	72.89	78.66	96.03	86.04
5	121.06	81.66	69.33	67.21	63.63	82.41	94.62	89.94
10	120.19	80.94	67.21	69.75	60.41	76.54	92.19	85.30
24	119.70	80.76	67.17	69.71	60.32	76.27	92.91	84.57
30	119.02	80.28	67.26	69.28	60.57	76.33	92.46	85.69
48	118.93	80.32	67.13	69.10	60.29	76.09	92.31	85.05

ศูนย์วิทยทรัพยากร
จุฬาลงกรณ์มหาวิทยาลัย

Table B4 Data from Adsorption kinetic of PAC, HMS, A-HMS, M-HMS, OD-HMS, Ti-HMS, NAY and HY zeolite at initial pH 7

Time	Concentration of PFOA after adsorption (mg/l)							
(hr)	PAC	HMS	A-HMS	M-HMS	OD-HMS	Ti-HMS	NaY	HY
0	299.57	100.00	100.00	100.00	100.00	100.00	100.00	100.00
0.003	152.13	92.30	89.80	94.22	84.26	94.37	87.95	82.12
0.083	139.35	92.96	88.94	96.28	88.95	91.15	90.36	86.86
0.167	120.87	97.30	74.13	93.28	84.06	91.71	93.01	87.03
0.5	84.74	83.54	87.66	90.38	77.84	92.10	85.05	80.47
1	78.67	89.16	84.92	92.93	-	91.58	90.12	88.72
3	72.78	85.82	78.87	90.86	75.75	89.66	83.60	80.63
5	67.29	85.27	80.75	89.40	79.47	88.88	87.33	87.64
10	67.66	84.94	79.33	91.43	76.56	88.73	87.50	83.29
24	67.99	83.49	83.73	87.93	76.01	89.35	87.45	85.38
30	72.57	84.37	81.36	86.72	77.75	89.30	86.73	81.55
48	72.68	82.71	81.44	89.15	77.19	89.15	86.03	86.14

ศูนย์วิทยทรัพยากร
จุฬาลงกรณ์มหาวิทยาลัย

Table B5 Data from Adsorption kinetic of PAC, HMS, A-HMS, M-HMS, OD-HMS, Ti-HMS, NAY and HY zeolite at initial pH 7

Time (hr)	Concentration of PFOS after adsorption (mg/l)							
	PAC	HMS	A-HMS	M-HMS	OD-HMS	Ti-HMS	NaY	HY
0	299.57	109.47	100.00	100.00	100.00	100.00	109.47	109.47
0.003	47.80	92.52	82.36	71.26	70.03	86.96	74.15	70.00
0.083	60.42	83.43	76.99	65.23	69.38	83.24	76.32	71.80
0.167	55.00	85.31	73.04	70.86	61.58	81.34	73.71	73.65
0.5	36.10	84.61	72.35	65.32	67.08	80.91	72.34	66.40
1	27.35	56.61	50.88	68.82	64.34	84.64	74.37	72.66
3	26.87	62.26	49.49	64.76	71.47	86.37	81.89	60.09
5	23.28	57.75	48.16	67.09	68.41	83.70	77.78	59.24
10	22.37	58.67	48.24	62.87	61.31	85.81	74.87	59.47
24	16.90	57.47	45.57	65.23	60.53	84.14	75.05	59.78
30	17.72	58.91	48.59	62.00	-	84.44	76.17	58.15
48	17.49	55.13	46.65	61.60	62.62	84.36	73.21	60.77

ศูนย์วิทยทรัพยากร
จุฬาลงกรณ์มหาวิทยาลัย

Table B6 Data from Adsorption kinetic of PAC, HMS, A-HMS, M-HMS, OD-HMS, Ti-HMS, NAY and HY zeolite at initial pH 9

Time (hr)	Concentration of PFOA after adsorption (mg/l)							
	PAC	HMS	A-HMS	M-HMS	OD-HMS	Ti-HMS	NaY	HY
0	300.00	100.00	100.00	100.00	100.00	100.00	100.00	100.00
0.003	254.20	98.90	90.98	90.39	96.66	99.65	89.89	98.21
0.083	252.24	97.79	94.79	83.35	95.64	97.01	92.10	98.56
0.167	238.48	98.35	92.29	88.42	94.88	97.45	92.17	90.26
0.5	231.29	98.00	92.96	86.69	96.01	96.85	90.80	91.61
1	228.48	96.80	97.48	86.74	94.13	96.73	92.75	90.85
3	226.25	97.70	96.04	87.72	92.49	92.69	90.35	91.97
5	221.00	95.86	94.76	84.77	90.32	95.21	88.04	91.97
10	220.07	96.03	94.04	85.26	93.28	95.02	92.60	94.41
24	220.32	94.38	94.37	83.29	93.40	94.91	91.68	93.09
30	220.14	93.87	93.08	83.84	90.82	94.73	91.95	94.60
48	220.06	96.41	93.71	85.26	92.81	94.65	91.36	93.19

Table B7 Data from Adsorption kinetic of PAC, HMS, A-HMS, M-HMS, OD-HMS, Ti-HMS, NAY and HY zeolite at initial pH 9

Time (hr)	Concentration of PFOS after adsorption (mg/l)							
	PAC	HMS	A-HMS	M-HMS	OD-HMS	Ti-HMS	NaY	HY
0	300.00	100.00	100.00	100.00	100.00	100.00	100.00	100.00
0.003	141.05	92.84	82.30	78.41	80.97	94.80	94.62	83.43
0.083	136.74	87.17	72.33	71.00	79.48	89.91	92.89	82.12
0.167	132.24	87.32	69.80	66.61	71.07	85.01	92.73	78.55
0.5	131.51	79.48	79.03	63.99	69.04	78.26	82.19	71.37
1	128.96	75.73	72.25	54.15	70.55	74.71	84.53	69.92
3	126.83	75.49	75.43	55.61	61.31	74.11	81.53	67.58
5	124.27	78.08	74.89	51.75	56.78	75.11	81.53	64.87
10	123.41	73.84	71.99	54.88	58.57	72.50	85.13	65.15
24	123.50	73.75	72.53	53.85	57.38	72.27	86.07	65.49
30	123.58	73.79	74.28	53.09	57.87	71.73	86.12	64.71
48	123.48	73.19	72.11	54.46	57.08	71.78	85.38	64.22

ศูนย์วิทยทรัพยากร
จุฬาลงกรณ์มหาวิทยาลัย

1. Method of calculation of Pseudo first order model

1) Calculated these data by using the data from adsorption kinetic profile in each adsorbates and adsorbents at different pH as shown in these sample tables below:

Table B8 Sample of data calculated from adsorption kinetic profile of adsorption of PFOS on HMS at initial pH 7

Time (min)	C_e (mg/l)	q_e (mg/g)	q_t (mg/g)	q_e-q_t (mg/g)	Log (q_e-q_t)
2880	55.13	43.47	43.47	0	
1800	58.91	43.47	40.45	3.02	0.48
1440	57.47	43.47	41.60	1.87	0.27
600	58.67	43.47	40.64	2.83	0.45
300	57.75	43.47	41.37	2.09	0.32
180	62.26	43.47	37.77	5.70	0.76
60	56.61	43.47	42.28	1.19	0.07
30	84.61	43.47	19.89	23.58	1.37
10	85.31	43.47	19.32	24.15	1.38
5	83.43	43.47	20.83	22.64	1.35
2	92.52	43.47	13.56	29.91	1.48

ศูนย์วิทยทรัพยากร
จุฬาลงกรณ์มหาวิทยาลัย

2) Plotted graph against between Time (min) and $\log(q_e-q_t)$

Figure B1 Pseudo first order model calculated from adsorption kinetic profile of adsorption of PFOS on HMS at initial pH 7.

3) Calculated adsorption rate k_1 (1/min) and calculated q_e (mg/g) by using the data from obtained plotting graph

$$y = mx + c \qquad \qquad ...(1)$$

From graph $\qquad \qquad y = 0.0005(x) + 1.0738 \qquad ...(2)$

- k_1 (1/min) $= 2.303^*(m)$

$$= 2.303^*(0.0005)$$

$$= 0.0012$$

k_1 (1/hr) $= 0.0012^*60$

$$= 0.069$$

- calculated q_e (mg/g) $= \log(c)$

$$= \log(1.0738)$$

$$= 11.852$$

2. Method of calculation of Pseudo second order model

1) Calculated these data by using the data from adsorption kinetic profile in each adsorbates and adsorbents at different pH as shown in these sample tables below:

Table B9 Sample of data calculated from adsorption kinetic profile of adsorption of PFOS on HMS at initial pH 7

Time (min)	C_e (mg/l)	q_e (mg/g)	q_t (mg/g)	t/q_t
2880	55.13	43.47	43.47	0
1800	58.91	43.47	40.45	44.50
1440	57.47	43.47	41.60	34.62
600	58.67	43.47	40.64	14.76
300	57.75	43.47	41.37	7.25
180	62.26	43.47	37.77	4.77
60	56.61	43.47	42.28	1.42
30	84.61	43.47	19.89	1.51
10	85.31	43.47	19.32	0.52
5	83.43	43.47	20.83	0.24
2	92.52	43.47	13.56	0.15

ศูนย์วิทยทรัพยากร

จุฬาลงกรณ์มหาวิทยาลัย

2) Plotted graph against between Time (min) and t/q_t
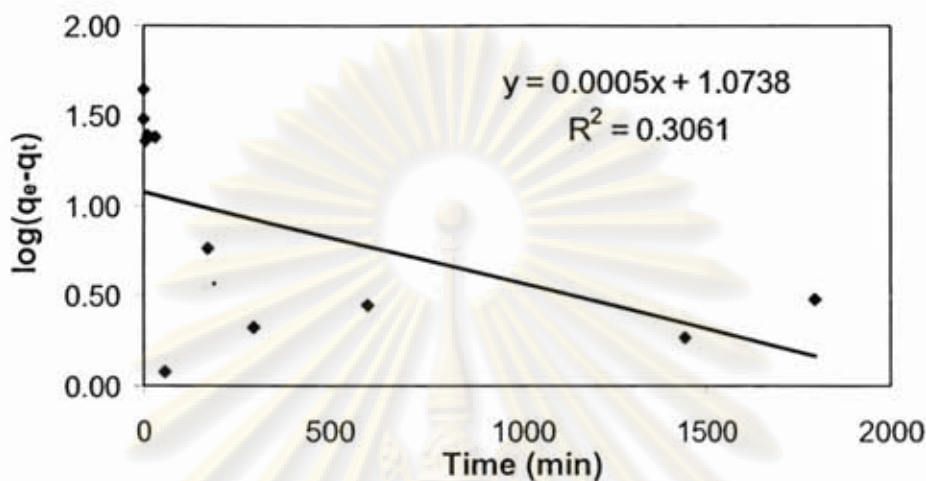

$$y = 41.103x + 8.3131$$
$$R^2 = 0.9995$$
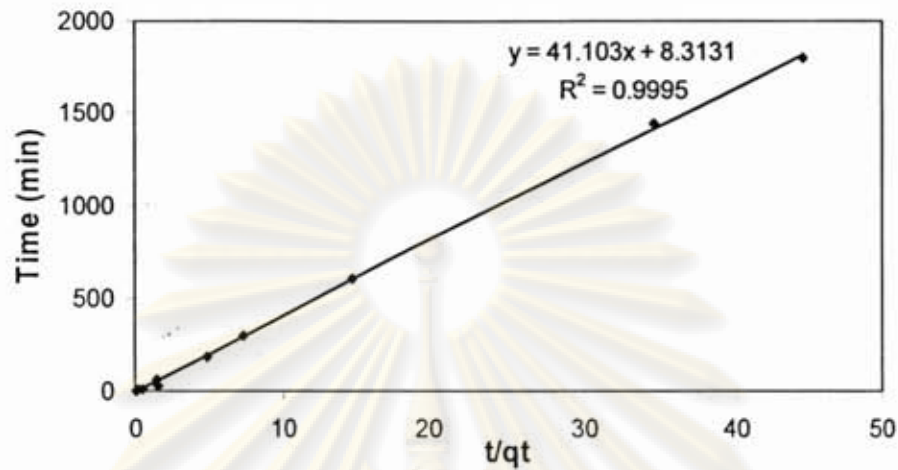
Figure B2 Pseudo second order model calculated from adsorption kinetic profile of

adsorption of PFOS on HMS at initial pH 7.

3) Calculated adsorption rate k_2 (1/min) and calculated q_e (mg/g) by using the
data from obtained plotting graph

$$y = mx + c \qquad \ldots(1)$$

From graph $\qquad y = 41.103(x) + 8.3131 \qquad \ldots(2)$

- calculated q_e (mg/g) $\quad = 41.103$

- $\dfrac{1}{k_2 q_e^2} \quad = c$

- $k_2 \quad = \dfrac{1}{8.3131(41.103)^2}$

- k_2 (1/min) $= 7.1 \times 10^{-5}$

k_1 (1/hr) $= 7.1 \times 10^{-5}(60) = 0.00427$

$$h = k_2 q_e^2 \qquad \ldots(3)$$

$$= 0.00427(41.103)^2$$

$$= 7.21752 \text{ mg/g h}$$

APPENDIX C

Data of Adsorption Isotherms

ศูนย์วิทยทรัพยากร
จุฬาลงกรณ์มหาวิทยาลัย

Table C1 Data from Adsorption isotherms of PAC, HMS, A-HMS, M-HMS, OD-HMS, Ti-HMS, NAY and HY zeolite at initial pH 5

Initial conc. (mg/l)	Adsorption capacity of PFOA (mg/g)							
	PAC	HMS	A-HMS	M-HMS	OD-HMS	Ti-HMS	NaY	HY
25	54.38	5.64	22.85	12.52	35.47	19.92	10.99	0.88
50	106.14	5.66	22.25	17.42	42.82	23.83	14.73	7.70
75	162.19	10.38	·39.08	24.65	60.14	30.12	19.12	14.40
100	176.31	16.21	60.91	34.27	78.90	34.13	20.41	22.71
200	262.13	35.82	213.45	58.63	85.26	95.46	37.98	36.44
300	309.24	57.14	309.12	75.79	141.32	177.13	45.89	56.96

Table C2 Data from Adsorption isotherms of PAC, HMS, A-HMS, M-HMS, OD-HMS, Ti-HMS, NAY and HY zeolite at initial pH 5

Initial conc. (mg/l)	Adsorption capacity of PFOS (mg/g)							
	PAC	HMS	A-HMS	M-HMS	OD-HMS	Ti-HMS	NaY	HY
25	46.50	3.08	27.65	29.10	56.90	19.24	8.97	12.83
50	120.80	20.70	32.74	44.35	81.96	23.25	8.93	17.87
75	167.16	37.63	60.39	67.09	109.89	53.08	10.32	21.90
100	215.39	59.45	99.33	86.26	109.58	71.89	21.95	42.80
200	336.85	178.34	260.01	182.64	198.87	217.57	52.59	75.07
300	402.31	214.23	355.53	229.41	299.83	333.58	85.93	116.95

Table C3 Data from Adsorption isotherms of PAC, HMS, A-HMS, M-HMS, OD-HMS, Ti-HMS, NAY and HY zeolite at initial pH 7

Initial conc. (mg/l)	Adsorption capacity of PFOA (mg/g)							
	PAC	HMS	A-HMS	M-HMS	OD-HMS	Ti-HMS	NaY	HY
25	65.70	1.26	23.53	11.03	18.70	2.42	11.08	5.37
50	132.61	4.70	30.89	16.29	26.41	6.00	14.24	8.32
75	196.57	8.84	41.05	19.14	31.24	14.12	14.97	11.81
100	241.21	12.06	56.63	19.58	33.74	29.94	16.48	12.56
200	387.18	27.50	109.58	49.97	56.21	65.44	21.61	26.26
300	524.92	39.68	141.55	62.48	106.01	120.69	33.82	36.11

Table C4 Data from Adsorption isotherms of PAC, HMS, A-HMS, M-HMS, OD-HMS, Ti-HMS, NAY and HY zeolite at initial pH 7

Initial conc. (mg/l)	Adsorption capacity of PFOS (mg/g)							
	PAC	HMS	A-HMS	M-HMS	OD-HMS	Ti-HMS	NaY	HY
25	42.21	8.63	7.94	19.19	45.13	3.85	3.23	5.44
50	120.48	12.70	13.88	37.94	61.56	9.83	9.74	14.45
75	179.69	18.56	56.04	74.75	91.76	15.14	13.69	16.70
100	215.39	37.92	115.33	118.06	102.48	36.52	28.11	33.51
200	364.83	85.43	394.41	253.37	251.02	96.18	63.44	74.40
300	471.34	303.13	627.26	373.63	390.08	460.88	114.01	128.67

Table C5 Data from Adsorption isotherms of PAC, HMS, A-HMS, M-HMS, OD-HMS, Ti-HMS, NAY and HY zeolite at initial pH 9

Initial conc. (mg/l)	Adsorption capacity of PFOA (mg/g)							
	PAC	HMS	A-HMS	M-HMS	OD-HMS	Ti-HMS	NaY	HY
25	49.32	3.89	8.80	20.99	14.13	5.98	11.31	1.02
50	103.71	5.32	12.90	25.05	16.80	7.64	11.04	3.10
75	114.86	8.02	16.34	32.62	22.84	9.37	13.33	5.81
100	142.14	8.80	20.19	35.47	26.05	10.14	20.24	7.73
200	197.83	25.85	68.26	59.58	36.55	55.18	23.56	27.74
300	230.61	41.00	134.28	88.67	70.06	110.52	23.92	37.20

Table C6 Data from Adsorption isotherms of PAC, HMS, A-HMS, M-HMS, OD-HMS, Ti-HMS, NAY and HY zeolite at initial pH 9

Initial conc. (mg/l)	Adsorption capacity of PFOS (mg/g)							
	PAC	HMS	A-HMS	M-HMS	OD-HMS	Ti-HMS	NaY	HY
25	46.94	10.92	24.29	47.41	31.77	15.86	1.96	10.30
50	115.93	21.65	41.50	67.60	61.68	27.79	8.12	23.14
75	162.70	42.65	58.08	97.26	90.51	53.80	9.00	50.48
100	201.01	79.63	83.99	128.52	121.21	81.41	32.70	95.78
200	364.77	228.30	252.53	290.26	279.96	257.29	282.27	281.85
300	529.29	382.72	497.77	429.63	425.63	485.00	376.36	377.50

Table C7 Data from adsorption isotherms of virgin adsorbents (PAC, HMS, M-HMS and OD-HMS) at initial pH solution 7

Initial conc. (mg/l)	Adsorption capacity of PFOS (mg/g) on virgin adsorbents			
	PAC	HMS	M-HMS	OD-HMS
25	42.21	8.63	19.19	45.13
50	120.48	12.70	37.94	61.56
75	179.69	18.56	74.75	91.76
100	215.39	37.92	118.06	102.48
200	364.83	85.43	253.37	251.02
300	471.34	303.13	373.63	390.08

Table C8 Data from adsorption isotherms of regenerated adsorbents (PAC, HMS, M-HMS and OD-HMS) at initial pH solution 7

Initial conc. (mg/l)	Adsorption capacity of PFOS (mg/g) on regenerated adsorbents											
	PAC			HMS			M-HMS			OD-HMS		
25	Re 1st	Re 2nd	Re rd	Re 1st	Re 2nd	Re 3rd	Re 1st	Re 2nd	Re 3rd	Re 1st	Re 2nd	Re 3rd
50	13.31	30.51	50.57	4.19	1.19	5.15	31.55	27.31	33.37	49.27	42.73	49.27
75	63.81	79.60	90.67	5.16	3.59	6.74	48.68	37.96	39.26	58.26	54.02	59.32
100	113.40	125.61	141.09	13.74	14.23	19.67	66.80	72.21	72.72	62.81	65.20	84.58
200	162.00	151.84	170.39	33.86	37.96	42.98	94.36	98.68	110.11	89.19	95.16	103.80
300	260.57	247.48	269.12	140.64	138.03	155.39	247.43	239.63	247.93	246.59	249.23	258.79

1. Method of calculation of Langmuir model

1) Calculated these data by using the data from adsorption isotherms in each adsorbates and adsorbents at different pH as shown in these sample tables below:

Table C9 Sample of data calculated from adsorption isotherms of adsorption of PFOS on HMS at initial pH 7

C_e (mg/l)	q_e (mg/g)	$1/C_e$	$1/q_e$
39.06	8.63	0.06	0.12
44.03	12.70	0.03	0.08
62.07	18.56	0.02	0.05
92.90	37.92	0.02	0.03
190.44	85.43	0.01	0.01

2) Plotted graph against between $1/c_e$ and $1/q_e$
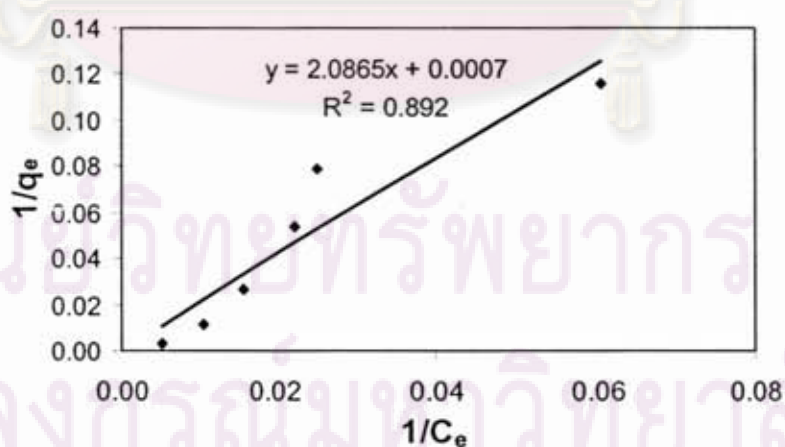
Figure C1 Langmuir model calculated from adsorption isotherms of adsorption of PFOS on HMS at initial pH 7

3) Calculated q_m (mg/g) and b by using the data from obtained plotting graph

$$y = mx + c \qquad \qquad \text{...(1)}$$

From graph
$$y = 2.0865(x) + 0.0007 \qquad \qquad \text{...(2)}$$

$$q_m \text{ (mg/g)} = 1/c$$
$$= 1/0.0007$$
$$= 1428.571$$
$$b = (1/(q_m \cdot m))$$
$$= (1/(1428.571 \cdot 2.0865))$$
$$= 0.0003$$

2. Method of calculation of Freundlich model

1) Calculated these data by using the data from adsorption isotherms in each adsorbates and adsorbents at different pH as shown in these sample tables below:

Table C10 Sample of data calculated from adsorption isotherms of adsorption of PFOS on HY at initial pH 7

C_e (mg/l)	q_e (mg/g)	log C_e	log q_e
20.56	5.44	1.31	0.74
36.66	14.45	1.56	1.16
46.23	16.70	1.66	1.22
67.59	33.51	1.83	1.53
106.79	74.40	2.03	1.87

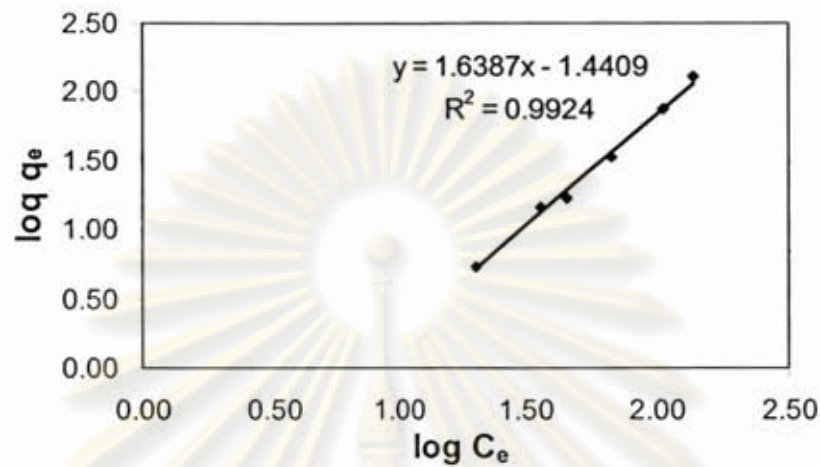2) Plotted graph against between $\log(c_e)$ and $\log(q_e)$

Figure C2 Pseudo second order model calculated from adsorption isotherms of

adsorption of PFOS on HY at initial pH 7

3) Calculated k_f and $1/n$ by using the data from obtained plotting graph

$$y = mx + c \qquad \ldots(1)$$

From graph $\qquad y = 1.6387(x) - 1.4409 \qquad \ldots(2)$

- $k_f = \ln(c)$

$\quad = \ln(-1.4409)$

$\quad = 0.0362$

- $1/n = m$

$\quad = 1.6387$

APPENDIX D

Method of TOC Anayzer

ศูนย์วิทยทรัพยากร

จุฬาลงกรณ์มหาวิทยาลัย

1. Total Organic Carbon (TOC)

Total organic carbon (TOC) is the amount of carbon bound in an organic compound and is often used as a non-specific indicator of water quality or cleanliness of pharmaceutical manufacturing equipment.
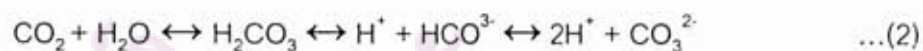
2. Method of TOC Analyzer

TOC analyzers usually works by measuring the carbon dioxide (CO_2) released during the oxidization of organic carbon and/or acidifying of inorganic carbon. Subtracting the inorganic carbon from the total carbon yields TOC. Another common variant of TOC analysis involves removing the IC portion first and then measuring the leftover carbon. The TOC analyzer then draws the relationship between the amounts of CO_2 to the amount of organic/in-organic carbon to decide the total organic carbon level.

$$\text{Total Carbon} \quad = \quad \text{Total Organic Carbon} - \text{Inorganic Carbon} \qquad \text{...(1)}$$

Or

$$TC \quad = \quad TOC - IC$$

In combustion, analyzer was using the established 680°C.

$$CO_2 + H_2O \leftrightarrow H_2CO_3 \leftrightarrow H^+ + HCO_3^- \leftrightarrow 2H^+ + CO_3^{2-} \qquad \text{...(2)}$$

TC Standard

$y = 1.9156x - 1.0974$
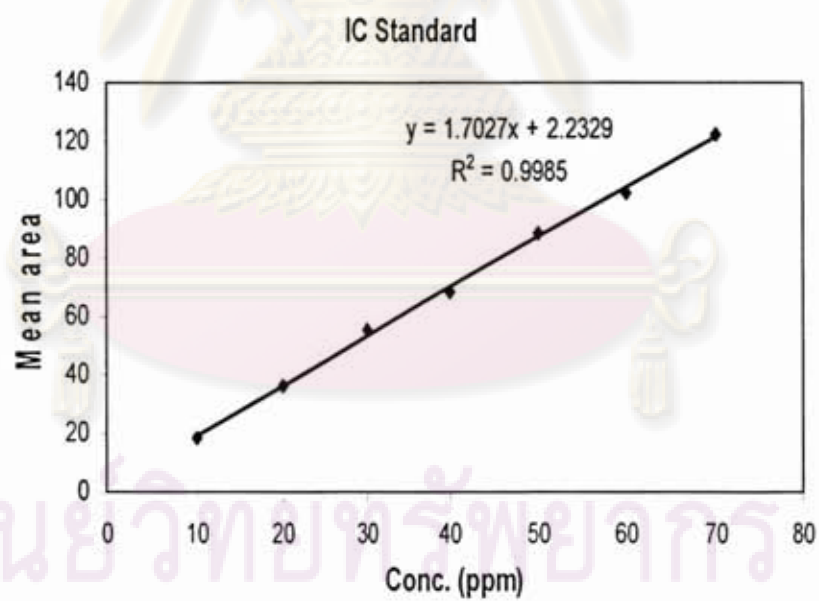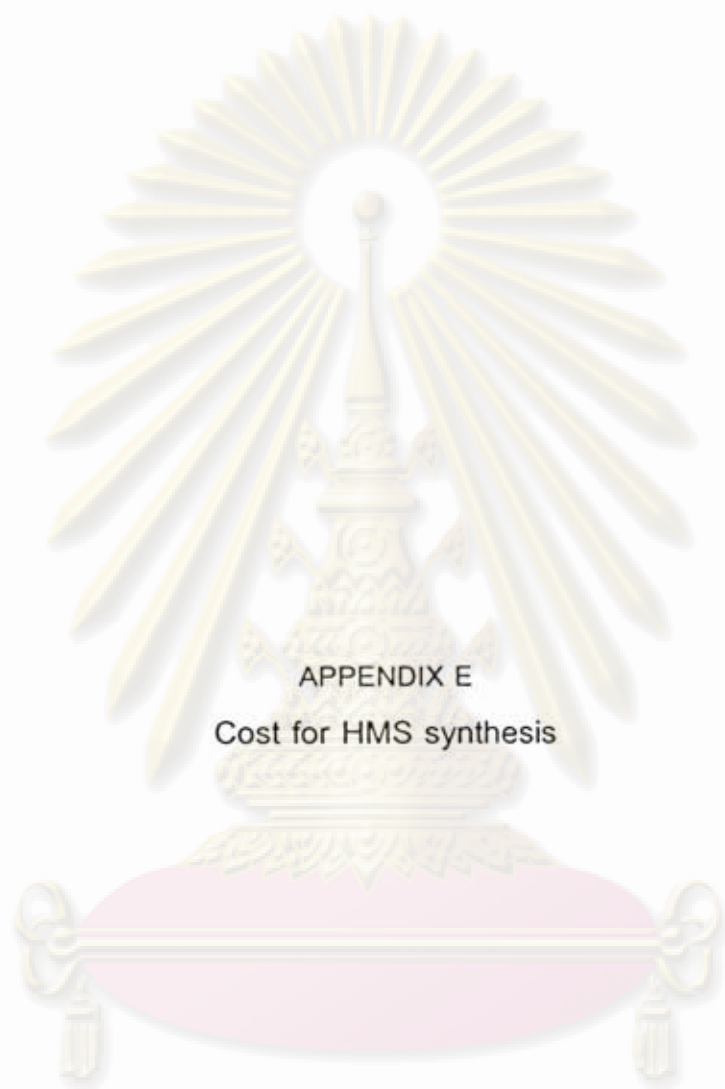$R^2 = 0.9998$
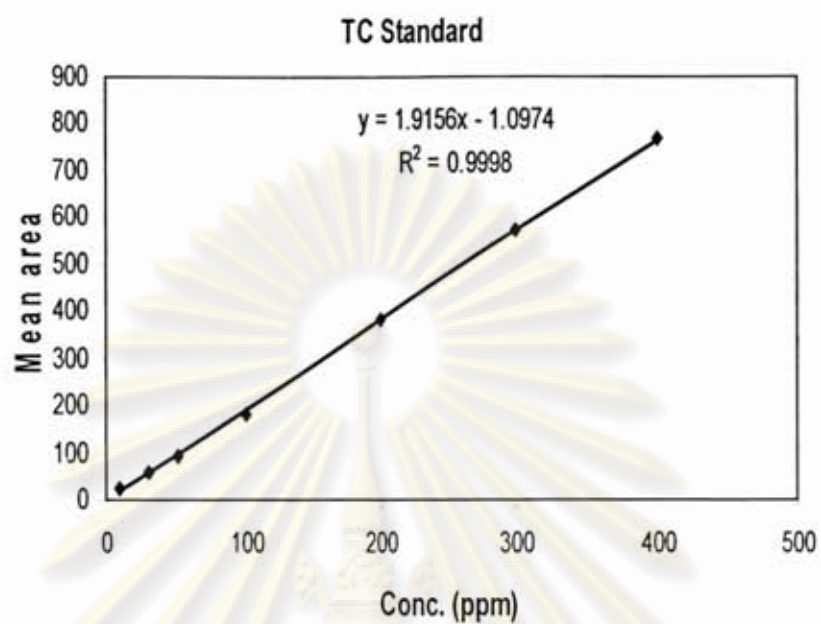
Figure D1 TC Standard

IC Standard

$y = 1.7027x + 2.2329$
$R^2 = 0.9985$

Figure D2 IC Standard

APPENDIX E

Cost for HMS synthesis

ศูนย์วิทยทรัพยากร
จุฬาลงกรณ์มหาวิทยาลัย

Table E1 Estimated calculation of cost for HMS synthesis

Materials and Energy	Cost (baht)
1. Incinerator	59
2. Magnetic stirrer	39
3. TEOS	23
4. Dodecylamine	20
5. Ethanol	16
Total	157

*Total amount of HMS per one batch = 7.5 g

Biography

Miss Kuntida Suksomboon was born on February 18, 1985 in Bangkok province. After she graduated high school in Benjamarachalai, Bangkok, she went to study in Faculty of environmental and resources studies at Mahidol University. She graduated Bachelor's degree of science of environmental resource studies in 2006. After that, she continued his study for a Master's degree of science in Environmental management, Chulalongkorn University.